USE OF VASCULAR ENDOTHELIUM METABOLIC PROPERTIES TO STUDY THE PULMONARY VASCULATURE DURING EXERCISE

by

Jocelyn Dupuis

A thesis submitted to the Faculty of Graduate Studies and
Research in partial fulfillment of the requirements
for the degree of
Doctor of Philosophy

Department of Medicine
Division of Experimental Medicine
McGill University
Montreal, Quebec

If I have seen farther than others, it has been by standing on the shoulders of giants.

Sir Isaac Newton

This work is dedicated to my giants: Dr Carl A. Goresky, Dr Jean-Lucien Rouleau and my family. Thank you for your strong and comforting shoulders.

ABSTRACT

The exercise induced reduction in the heterogeneity of perfusion of the lung may result from vascular distension or recruitment or a combination of both. We studied the accommodation of the increased pulmonary blood flow in the transition from rest through two successive levels of exercise in 19 awake mongrel dogs. To do so, we used the single bolus multiple indicator dilution technique with markers of the pulmonary vascular surface area and studied their behaviour at exercise. In a first set of experiments (n=9) [3H]norepinephrine served as the vascular surface area tracer while [3H]benzoyl-Phe-Gly-Pro ([3H]BPGP), an inactive angiotensin-converting enzyme substrate was utilized in another (n=10). Three other tracers were also injected with the surface markers: two vascular space markers, [51Cr]erythrocytes and [125I]albumin, and a water space tracer, [14C]1,8-octanediol. The mixture was injected into the pulmonary circulation and timed outflow samples were collected in the ascending aorta to obtain dilution curves. With exercise, the increase in pulmonary blood flow was accompanied by a linear increase in oxygen consumption. The range of blood flow achieved varied from 41 ml/s to 457 ml/s. The central blood volume as measured from the intravascular references increased linearly with flow. The tracer accessible extravascular lung water increased with flow and rapidly approached a maximal asymptotic proportion representing 75% of the postmortem lung weight. The ratio of the dilutional estimates of the extravascular lung water to that measured gravimetrically also increased in a similar fashion to reach an asymptotic proportion of close to 100%. These values were attained for moderate values of blood flow and did not increase further with higher blood flows. Tracer norepinephrine extractions at rest and at the two levels of exercise were 17% ± 1.2, 14% ± 0.8 and 15% ± 0.8 (SE) respectively Using the Crone approximation we computed the permeability surface area product (PS) for norepinephrine. The PS product increased linearly with flow. Similarly, the

proportional [3H]BPGP hydrolysis did not vary with flow, and averaged 55%. The first order kinetic parameter A_{max}/K_m for [3H]BPGP hydrolysis (equivalent to the PS product) also increased linearly over all ranges of blood flow. We conclude that with exercise there is a linear increase in pulmonary vascular volume. In the transition from low to moderate levels of blood flow there is lung tissue recruitment which can only be the result of lung vascular recruitment. Assuming no variation with flow of the lung permeability to norepinephrine or of the pulmonary angiotensin-converting enzyme function, there is a linear increase with blood flow of the pulmonary vascular surface area that can interact with a vascular substrate. This suggests that when all of the lung tissue is being perfused, there is nevertheless further recruitment, with increases in flow, of vascular surface that can modify vascular substrates. We found that as pulmonary blood flow is tripled, the lung vascular surface area is also tripled and that capillary recruitment contributes to the process over the whole range of flows.

RESUME

Lors de l'exercice il y a réduction de l'hétérogénéité de perfusion des poumons résultant soit d'une distention vasculaire, soit d'un recrutement, ou encore d'une combinaison des deux. Pour mieux comprendre ce phénomène, nous avons étudié 19 chiens au repos et à deux niveaux croissant d'effort en utilisant des marqueurs de la surface vasculaire pulmonaire à l'aide de la technique de dilution avec indicateurs multiples. Dans une première série d'expériences , la [3H]norépinéphrine servi de traceur de la surface vasculaire (n=9) alors que le [3H]benzoyl-Phé-Gly-Pro ([3H]BPGP), un substrat inerte de l'enzyme de conversion de l'angiotensine, fut utilisé dans une autre série (n=10). Trois autres traceurs furent injectés simultanément avec les marqueurs de surface: deux marqueurs de l'espace intravasculaire, des érythrocytes (marqués au [^{51}Cr]) et de l'albumine ([^{125}I]), et un marqueur de l'espace en eau du poumon, le [^{14}C]1,8-octanediol. Les courbes de dilution furent obtenues par injection de la mixture dans la circulation pulmonaire et recueil d'échantillons dans l'aorte ascendante. Lors de l'exercice, l'augmentation du débit sanquin pulmonaire s'accompagna d'une augmentation linéaire de la consommation en oxygène. Les débits sanguin pulmonaire mésurés variaient de 41 ml/s au repos à 457 ml/sec à l'effort. L'eau extravasculaire pulmonaire accessilble au traceur augmenta rapidement avec le débit pour se rapprocher d'une valeur asymptotique maximale représentant 75% des poids pulmonaire post-mortem. Le rapport entre l'eau extravasculaire pulmonaire mesurée par dilution et celle mesurée gravimétriquement augmenta de facon similaire pour atteindre une valeur asymptotique maximale de près de 100%. Ces valeurs furent obtenues à des niveaux modérés de débit pulmonaire et n'augmentairent pas avec des niveaux plus élevés. L'extraction de la norépinéphrine au repos, et aux deux niveaux d'exercise était de 17% ± 1.2, 14% ± 0.8 et 15% ± 0.8 (ds) respectivement. En utilisant le model de Crone nous avons calculé le produit perméabilite-surface (PS) pour la norépinéphrine et avons trouvé qu'il augmente de facon linéaire avec le débit sanquin

pulmonaire. De facon similaire, la fraction d'hydrolyze du [3H]BPGP ne varia pas avec l'effort avec une moyenne de 55%. Le paramètre cinétique de premier ordre A_{max}/K_m (equivalent au produit PS) calculé pour le [3H]BPGP augmenta aussi de facon linéaire avec le débit pulmonaire. Nous concluons que l'exercice résulte en une augmentation linéaire du volume sanquin pulmonaire. A mesure que le débit cardiaque augmente il y a recrutement tissulaire pulmonaire qui devient rapidement maximal à des niveaux modérés de débit. Ce recrutement tissulaire ne peut être le fruit que d'un recrutement vasculaire pulmonaire. Assumant aucun changement, avec l'exercice, de la perméabilite pulmonaire à la norépinephrine et de l'activité de l'enzyme de conversion, il y a une augmentation linéaire avec l'exercice de la surface vasculaire pulmonaire pouvant interagir avec ces substrats circulants. Ceci suggère que même lorsque tout le tissus pulmonaire est perfusé, il y a néanmoins un recrutement capillaire qui se poursuit pour des niveaux plus élevés de débit. Nous avons démontré que lorsque le débit pulmonaire triple avec l'exercice, la surface vasculaire pulmonaire triple aussi, le recrutement capillaire pulmonaire participant à ce phénomène à tous les niveaux de débit cardiaque.

PREFACE

This thesis is submitted to the McGill Faculty of Graduate Studies and Research which gives candidates the choice of two options in the submission of their thesis. Option A is the conventional format known to all universities while option B is in the form of published or publishable papers. This work is submitted in the form of option B according to the thesis guidelines of the Faculty of Graduate Studies and Research:

"The candidate has the option, subject to the approval of the Department, of including as part of the thesis the text, or duplicated published text, of an original paper, or papers. In this case the thesis must still conform to all other requirements explained in Guidelines Concerning Thesis Preparation. Additional material (procedural and design data as well as descriptions of equipment) must be provided in sufficient detail (e.g. in appendices) to allow a clear and precise judgement to be made of the importance and originality of the research reported. The thesis should be more than a mere collection of manuscripts published or to be published. It must include a general abstract, a full introduction and literature review and a final overall conclusion. Connecting texts which provide logical bridges between different manuscripts are usually desirable in the interests of cohesion."

"It is acceptable for theses to include as chapters authentic copies of papers already published, provided these are duplicated clearly on regulation thesis stationary and bound as an integral part of the thesis. Photographs or other materials which do not duplicate well must be included in their original form. In such instances, connecting texts are mandatory and supplementary explanatory material is almost always necessary."

"The inclusion of manuscripts co-authored by the candidate and others is acceptable but the candidate is required to make an explicit statement on who contributed to such work and to what extent, and supervisors must attest to the accuracy of the claims, e.g. before the Oral Committee. Since the taks of the Examiners is made more difficult in these cases, it is in the candidate's interest to make the responsibilities of authors perfectly clear. Candidates following this option must inform the Department before it submits the thesis for review."

Two papers will be presented in chapters 2 and 3 respectively. The paper presented in chapter 2 is entitled "Use of norepinephrine uptake to measure lung capillary recruitment with exercise" by J.Dupuis, C.A. Goresky, C. Juneau, A. Calderone, J.L. Rouleau, C.P. Rose, and S. Goresky, and was published in the Journal of Applied Physiology, 68(2):700-713,1990. The second paper, in chapter 3, is entitled "Pulmonary angiotensin-converting enzyme substrate hydrolysis during exercise " by J. Dupuis, C.A. Goresky, J.W. Ryan, J.L. Rouleau, and G.G. Bach, and is submitted for consideration for publication in the same journal.

I would like to acknowledge the work of the co-authors of these papers. C. Juneau contributed to the developement of the experimental model used in these studies and did some of the pilot experiments, A. Calderone is a biochemist who taught me how to separate catecholamine metabolites using cation exchange resins, C.P. Rose and S. Goresky measured arterial and venous catecholamines by HPLC. J. W. Ryan, from the university of Miami, spent a week in Montreal to teach me the techniques of product separation for the angiotensin-converting enzyme substrate [3H]benzoyl-Phe-Gly-Pro and kindly provided this substrate for our experiments. G. G Bach is a mechanical engineer who contributed to the development of the mathematical modeling of the enzyme catalysed conversion of tracer

substrate to product at the inner surface of endothelial cells which is detailed in appendix 1 of chapter 3. C.A. Goresky and J.L Rouleau were the thesis co-supervisors.

Chapter 1 is a general introduction to the thesis. Chapters 2 and 3 each contain its own abstract, introduction, materials and methods, discussion and references. The thesis ends with the claims to original research and a general conclusion.

TABLE OF CONTENTS

LIST OF FIGURES

LIST OF TABLES

CHAPTER 1

THE PULMONARY CIRCULATION AND THE METABOLIC FUNCTIONS OF THE LUNG

INTRODUCTION

" He who really understands what is involved in the breathing of man has sensed the breath of god and thereby saved his soul "

(Michael Servetus, c1511-1553)

It is believed that the first account of the pulmonary circulation was by Michael Servetus (13) in a rather theological publication entitled "Christianismi Restitutio". His description challenged the accepted Galenic dogma which stated that the blood was formed in the liver and then passed from the right to the left cavity of the heart by flowing through pits distributed in the interventricular septum. In the left cavity, the "vital spirit" was mixed with the "pneuma" coming from the lung, and was then distributed to the tissues. Servetus, who practised vivisection, noticed that there were no pores in the septum separating the two cavities and concluded that the blood must pass through the lungs before returning to the left ventricle. This brief historical note emphasizes the many controversies surrounding the pulmonary circulation; the concept of the pulmonary circulation itself remained controversial until the discovery of the circulation by Harvey in the 17th century. Interestingly, Servetus' convictions (especially those regarding the doctrine of the Trinity!) brought him to the stake were he was burnt as an heretic with all but three copies of his book.

One of the presently most debated and controversial subjects in pulmonary physiology still pertains to the pulmonary circulation. With increasing pulmonary blood flow (as seen with exercise) there is a simultaneous increase in the pulmonary vascular volume (7). Based on physical principles alone there are only two ways by which this phenomenon can occur. First, an increase in the diameters of the pulmonary vessels will

raise their volume by a factor corresponding to the squared increments of their radius. We will refer to this first mechanism as "vascular distension". Alternatively, with increasing pulmonary blood flow there could be flow in new vascular channels which were not previously perfused thus adding to the overall vascular volume. We will refer to this latter mechanism as representing "vascular recruitment". The accommodation of increased pulmonary blood flow with exercise could be the result of either distension or recruitment, or a combination of both.

There have, thus far, been no experimental tools that could clearly distinguish between vascular distension and recruitment. In the present studies we took advantage of the metabolic properties of the pulmonary vascular endothelium which can extract, metabolize and store various circulating substances. To some extent, the kinetic characteristics of these substances will depend on the vascular surface area that is available for interaction. We used two such markers of the pulmonary vascular surface area and studied their metabolism at rest and through two successive levels of exercise in the awake dog by the use of the multiple indicator dilution technique. Tritiated norepinephrine was used in one set of experiments while the tritiated angiotensin-converting enzyme substrate benzoyl-Phe-Gly-Pro (BPGP) served in another. This chapter will review basic concepts in pulmonary vascular physiology and will describe some endothelial cell-vascular substrate interactions .

PULMONARY CIRCULATION

DISTRIBUTION AT REST

The pulmonary circulation is a high compliance low resistance system distributed along a certain vertical height (25 cm in the normal upright human) which creates a vascular pressure gradient decreasing from the bottom to the apex of the lung (7). The uniqueness of the pulmonary capillaries reside in their close proximity to the alveolar spaces, thus facilitating gas exchange. The distribution of pulmonary blood flow will therefore be influenced not only by the arterial and venous pressures but also by the complex interplay between the gravitational field and the intra-alveolar pressure. At rest, these interactions are responsible for a perfusion gradient that decreases from the bottom to the apex of the lung. This phenomenon has been well studied using hemodynamic, morphometric and gas exchange studies (the reader is referred to the introductions of chapter 2 and 3 for details). Four lung zones have been described by West in an effort to delineate this finding. These zones do not represent true anatomical borders but represent resting physiological conditions which gradually progress from one to the other along the vertical height of the lung. This work will frequently refer to lung zones so that we consider it important to briefly review their description.

ZONE 1. In this zone, the alveolar pressure exceeds the pulmonary arterial pressure ($P_A > P_{pa}$). The capillaries are therefore attenuated or collapsed and offer the greatest resistance to blood flow. In the upright subject this condition is encountered at the apex of the lung where minimal flow is achieved.

ZONE 2. In this condition, the pulmonary arterial pressure exceeds the alveolar pressure which in turn exceeds the pulmonary venous pressure ($P_{pa} > P_A > P_{pv}$). This is thought to result in a cusplike narrowing at the venous end of the capillary which acts as a Starling resistor. Unlike the flow in systemic capillaries which is determined

by the arterial-venous pressure difference, the flow in zone 2 is governed by the the arterial-alveolar pressure difference. As we descend vertically along this zone, the arterial pressure and blood flow both increase. It is the zone where the greatest variation of blood flow occurs along the vertical height; it ordinarily represents the middle portion of the lung.

ZONE 3. At the base of the lung the pulmonary arterial and venous pressures both exceed the alveolar pressure ($P_{pa}>P_{pv}>P_A$) so that the capillaries are fully distended and offer minimal resistance to blood flow. This is the zone where the best tissue perfusion is achieved.

ZONE 4. This zone is situated in the most dependent portion of the lung where we find a paradoxical decrease in perfusion despite the highest arterial pressures. It is believed that distortion of the extra-alveolar vessels in this zone at functional residual capacity is responsible for the mild decrease observed.

DISTRIBUTION AT EXERCISE

Numerous physiologic as well as pathologic conditions will modify the factors responsible for the pulmonary blood flow distribution seen in resting conditions. The most common of these conditions is surely exercise. With exercise there is an increase in pulmonary blood flow (or by definition the cardiac output) which is matched to the increased metabolic demand (O_2 uptake). Compared to the important increase in blood flow (it may be multiplied by a factor of 20 in extreme conditions!) there is relatively very little increase in the pulmonary vascular pressures with exercise, so that there is an important decrease in resistance. This accommodation to the increased pulmonary blood flow with exercise appears linked to an increase in the pulmonary vascular volume. At rest the

pulmonary blood volume represents 10% to 12% of the total blood volume (about 200 ml in a 20 kg dog) and it can virtually double with high levels of exercise (7,10). The blood volume is distributed about equally in the arteries, the capillaries and the veins (7) (about 56, 68 and 76 ml respectively in a 20 kg dog). The cross sectional area of the pulmonary vascular tree increases exponentially from the main pulmonary artery to the capillaries so that the increase in blood volume seen with exercise occurs mostly in the capillary bed (7).

With exercise there is also a reduction in the heterogeneity of perfusion of the lungs, the upper parts becoming better perfused. Because of the increase in pulmonary arterial pressure, the capillaries in zone 2 condition may have distended giving rise to a zone 3 condition, while zone 1 capillaries may have become recruited (reopened) to behave as a zone 2. The increase in capillary blood volume with exercise has been well documented by various morphometric techniques (9,16) and by studying the pulmonary diffusing capacity for some gases (oxygen or carbon monoxide) (3,8), the latter being partly dependent on the capillary volume. However these methods do not readily distinguish between vascular distension and recruitment and although most investigators believe in the presence of distension, some are reluctant to accept the recruitment theory in normal physiologic conditions. There is consequently a need to devise new methods which will undoubtedly confirm or refute the presence of vascular recruitment and which may help to quantify the roles of distension versus recruitment. One possible avenue is to use the metabolic properties of the pulmonary vascular endothelium to obtain information on the capillary surface area that is accessible to an appropriate vascular substrate.

METABOLIC FUNCTIONS OF THE LUNG

The primary function of the lungs is the exchange of gases, so that we often overlook its important metabolic role. The vascular surface area of the lung is greater than that of any

other internal organ and its privileged position between the right and the left heart chambers enables the lung to receive the whole cardiac output. The pulmonary vascular endothelial cells possess enzymes, receptors and transduction mechanisms which enable them to change the biological activity of numerous substances presented to them via the pulmonary circulation.

Many vasoactive substance are removed or inactivated by the lungs. These substances are generally released locally, so that their action is thought to be restricted at or near the site of release. The lung then acts as a protective mechanism, by inactivating blood spillover of these substances before they reach the systemic circulation. Norepinephrine and 5-hydroxytryptamine are two examples of vasoactive amines belonging to this category.

Alternately, the lung may act as a modulator that can modify a circulating substance to produce a new vasoactive moiety. The best known example of the latter is the conversion of angiotensin I to angiotensin II by the pulmonary angiotensin-converting enzyme. A review of all the metabolic properties of the lung is beyond the scope of the present work and we shall concentrate on the description of the pulmonary handling of norepinephrine and angiotensin-converting enzyme substrates which are the substances of interest in our studies.

NOREPINEPHRINE

In 1964, Eiseman et all reported that the half life of norepinephrine was markedly reduced when perfused through an isolated lung lobe (6). Since then, numerous publications have established that norepinephrine is removed from the circulation and metabolised by the pulmonary vascular endothelium (11).

The limiting factor in norepinephrine removal by the lung is the rate of transport into the endothelial cells. It is a saturable transport mechanism with an estimated K_m value between 1.1 and 2.4 μM and V_{max} between 2.2 and 5.6 $nmol \cdot sec^{-1} \cdot gm^{-1}$ and it is inhibited by imipramine and cocaine. The uptake is temperature sensitive and sodium dependent while it is inhibited by potassium. It is not affected by the presence of inhibitors of monoamine oxidase (MAO) or of catechol O-methyltransferase (COMT). There is no storage of norepinephrine in the endothelial cells and the extracted amine is rapidly metabolised by MAO and COMT (both enzymes are present in the endothelial cells). The average extraction of norepinephrine in the dog using continuous infusion methods or single bolus infusions is close to 20%. The rate limiting step in the norepinephrine extraction is the carrier mediated transport process which is itself dependent on the vascular surface area that comes into contact with the circulating norepinephrine. One can therefore use norepinephrine as a marker of the pulmonary vascular surface area.

ANGIOTENSIN-CONVERTING ENZYME

The angiotensin-converting enzyme (ACE) is a peptidase located at the luminal surface of the pulmonary vascular endothelium (15). Although ACE can be found in blood and various other tissues, its major reservoir resides in the lungs. Pulmonary ACE is responsible for the conversion (or more appropriately hydrolysis) of angiotensin 1 to angiotensin 2. The observation of this activity first became possible when intrinsically labeled angiotensin 1 became available. Because of the location of the enzyme (on the endothelial luminal surface), there is no endothelial uptake process associated with the hydrolysis, and the pulmonary outflow profile for the sum of the ACE substrate plus product has ordinarily been found to be indentical to that of a reference intravascular tracer. Thus, the pulmonary ACE is often referred to as an ectoenzyme.

In the past ten years, following the discovery of the most potent and specific ACE inhibitors in peptides isolated from snake venom (Bothrops jararaca, Ferreira 1965), numerous ACE inhibitors (captopril, enalapril, lisinopril, pirindopril, etc.) as well as ACE substrates have been developed for clinical or research purposes. The ACE substrates form a class of compounds that are biologically inactive although they are metabolised at various rates by the converting enzyme. The most widely used of these substrates is [3H]benzoyl-Phe-Ala-Pro ([3H]BPAP) which has a single pass hydrolysis of approximately 80% in the dog lung to yield one radioactive product, [3H]Benzoyl-Phe. At such a high fractional hydrolysis however, kinetic computations may become less accurate, so that it seemed appropriate to develop and test other substrates. Two such substrates have been developed, [3H]benzoyl-Phe-Gly-Pro ([3H]BPGP) and [3H]benzoyl-Ala-Gly-Pro ([3H]BAGP). The experiments depicted in chapter three were done with the use of [3H]BPGP which has a high affinity for the angiotensin-converting enzyme, while it is pharmacologically inactive. The fractional hydrolysis for [3H]BPGP in a single lung passage in the dog is approximately 55%, which should yield more sensitive-to-change estimates of ACE kinetic parameters.

Because of its luminal surface distribution, the pulmonary angiotensin-converting enzyme kinetics will be dependent on the vascular surface area that is accessible to a vascular substrate. ACE substrates have therefore been used as markers of the pulmonary vascular surface or integrity in numerous physiologic and pathologic conditions. Tritiated BPGP therefore seemed to be a good candidate to serve as a pulmonary vascular surface tracer marker in the exercising dog, one whose metabolism is greater than that of labeled norepinephrine, and so may be more accurately evaluated.

PROBLEMS ARISING FROM THE USE OF TRITIATED NOREPINEPHRINE AND BPGP

The aim of the present work is to use the multiple indicator dilution technique with [3H]norepinephrine and [3H]BPGP as markers of the pulmonary vascular surface area at rest and with exercise. The use of these substances at rest and at exercise in awake, chronically instrumented dogs, raises some methodological difficulties which are inherent to the unavoidable contact with whole blood during its passage through the pulmonary circulation. We will briefly discuss this topic here, so that the reader may appreciate the techniques that were utilized (materials and methods, chapter 2 and 3) to overcome these difficulties.

When measuring plasma catecholamine concentrations, one has to handle the drawn samples with special care. If they are left at room temperature without preservatives, there will be a rapid decay in the measured concentration over the first 30 minutes (2). This decay is caused partly by the presence of MAO and COMT in plasma, but more importantly by the the interaction of the red blood cells with plasma catecholamines. Norepinephrine in found in the red blood cells in concentrations equal to that of plasma. There exists an active transport mechanism for norepinephrine across the erythrocytic membrane and the red blood cells also possess the enzymes required for catecholamine metabolism (especially COMT). If norepinephrine is added to red blood cells, there will be an active transport into the cells which will be maximal after two hours, with the intra-erythrocytic norepinephrine concentration being twice that in plasma (4). This transport is temperature sensitive and is inhibited at 4 degrees Celsius. It has been shown to be modified in certain pathologic conditions, so that it is postulated that this intra-erythrocytic pool of catecholamines may play a role in the manifestation of diseases. In the DOCA-salt hypertensive rat, for example, Bouvier et al. (1) demonstrated that the increased plasma norepinephrine

concentration in the hypertensive animal was accompanied by an increased measured concentration in the red blood cells.

The red blood cell uptake of norepinephrine poses a special problem if one is to measure the pulmonary uptake of norepinephrine with the multiple indicator dilution technique in "in vivo" conditions. If no special precautions are taken, the extraction data may be falsely elevated since part of the uptake may be attributable to the red blood cells. Measures taken to avoid this problem are to minimize the time of contact between the blood and norepinephrine, to keep all blood samples on ice, and to add competitive inhibitors of the uptake process to the collected samples.

A different problem arises in the study of pulmonary angiotensin-converting enzyme kinetics "in vivo". One has to take into account the presence of ACE in plasma itself, that may hydrolyze the substrate to be studied, resulting in a falsely elevated estimation of the fractional hydrolysis. This problem has never been addressed before and investigators have avoided it by making plasma free injection mixtures and by perfusing the lungs with physiologic solutions instead of blood. However, the issue becomes quite problematic if one wishes to study awake dogs at rest and during exercise. In chapter 3, it became necessary to validate the technique by demonstrating that the plasma hydrolysis of [^{3}H]BPGP within a single pulmonary transit time was negligible when compared to pulmonary hydrolysis. It was already known that there is greater than one order of magnitude difference (120 sec versus 4 to 8 sec) in the time required for equivalent degrees of conversion of angiotensin 1 to angiotensin 2 in the peripheral blood, as compared to that through the pulmonary circulation (12). This is not surprising if one considers the much greater concentration of ACE in the lungs together with the presence of natural ACE inhibitors in plasma (14). Nevertheless, extreme care was needed in the preparation of the

injection mixture of the [3H]BPGP studies to assure plasma free (that is, ACE free) injectates.

The best known ACE substrate, BPAP, has been recently demonstrated to bind to bovine serum albumin in a way which affects its pulmonary hydrolysis, but even in albumin free isolated lung preparations, it has been suggested that BPAP hydrolysis is always complete, even at low flows, suggesting the existence of two conformers of BPAP. This appeared to be verified by the finding that there is a slow second component in BPAP hydrolysis by commercially available ACE, corresponding in magnitude more or less to the component not hydrolyzed during a single passage (5). In chapter 3, two "in vitro" experiments were carried out to study BPGP hydrolysis by dog lung ACE and its hydrolysis by the ACE present in dog serum; in both cases, BPGP hydrolysis proceeds according to a single rate constant. Therefore BPGP, unlike BPAP, does not appear to possess a second slowly hydrolysable conformer, and BPGP-protein binding, if it exists, does not noticeably interfere with this substrate hydrolysis.

REFERENCES

1. Bouvier, M. L., L. Farley, and J. De Champlain. Red cell catecholamine levels in normotensive and DOCA-salt hypertensive rats. *Am. J. Physiol.* 253 (*Heart Circ. Physiol. 22)*: H270-H275, 1987.
2. Carruthers, M., P. Taggart, N. Conway, and D. Bates. Validity of plasma catecholamines estimations. *The Lancet.* 2: 62-67, 1970.
3. Cerretelli, P., and P. E. Di Prampero. Gas Exchange in exercise. In: *Handbook of physiology. The Respiratory System. Gas Exchange.* Bethesda, MD: Am. Physiol. Soc., 1987, Sect. 3, Vol IV, Chapt. 16, p. 297-339.
4. Danon, A., and J. D. Sapira. Uptake and metabolism of catecholamines by the human red blood cell. *Clinical pharmacology and therapeutics.* 13(5): 916-922, 1972.
5. Dawson, C. A., R.D. Bongard, D. A. Rickaby, J. H. Linehan, and D.L. Roerig. Effect of transit time on metabolism of a pulmonary endothelial substrate. *Am. J. Physiol.* 257 *(Heart Circ. Physiol. 26)*: H853-H865, 1989.
6. Eiseman, B., L. Bryant, and T. Waltuch. Metabolism of vasomotor agents by the isolated perfused lung. *J. Thorac. Cardiovasc. Surg.* 48:798-806, 1964.
7. Fishman, A. P. Pulmonary Circulation. In: *Handbook of Physiology. The Respiratory system,* Edited by A. P. Fishman. Bethesda, MD: Am. Physiol. Soc., 1985, sect 3, vol 1, Chapt. 3, p93-165.
8. Foster, R. E., Diffusion of gases across the alveolar membrane. In: *Handbook of physiology. The Respiratory System. Gas Exchange.* Bethesda, MD: Am. Physiol. Soc., 1987, Sect. 3, Vol IV, Chapt. 5, p. 71-88.
9. Glazier, J. B., J. M. B. Hughes, J. E. Maloney, and J. B. West. Measurements of capillary dimensions and blood volume in rapidly frozen lungs. *J. Appl. Physiol.* 26: 65-590, 1977.

10. Goresky, C. A., J. W. Warnica, J. H. Burgess, and B. E. Nadeau. Effect of exercise on dilution estimates of extravascular lung water and on the carbon monoxide diffusing capacity in normal adults. *Circ. Res.* 37: 379-389, 1975.

11. Junod. A. F. 5-Hydroxytryptamine and other amines in the lungs. In: *Handbook of physiology. The Respiratory System. Circulation and Nonrespiratory Functions.* Bethesda, MD: Am. Physiol. Soc., 1985, Sect. 3, Vol I, Chapt. 9, pp. 337-350.

12. Longenecker, G. L., and C. G. Huggins. Biochemistry of the pulmonary angiotensin-converting enzyme. In: *Lung biology in health and disease. Metabolic functions of the lung.* Ed: Y. S. Bakhle and J. R. Vane. Dekker, New York, Vol 4, Chapt. 3, pp. 55-76, 1977.

13. Persaud, T. V. N. Historical Developement of the concept of a pulmonary circulation. *Can. J. Cardiol.* 5(1):12-16, 1989.

14.. Ryan, J. W. Angiotensin converting enzyme, dipeptidyl carboxypeptidase I, and its inhibitors. In, *Methods in Enzymology. Ed: G.* DiSabato, Academic Press, London, Vol. 163, ch. 18, pp. 194-210, 1988.

15. Ryan, U. S., Processing of angiotensin and other peptides by the lungs. In: *Handbook of physiology. The Respiratory System. Circulation and Nonrespiratory Functions.* Bethesda, MD: Am. Physiol. Soc., 1985, Sect. 3, Vol I, Chapt. 10, p. 351-364.

16. Warrel, D. A., J. W. Evans, R. O. Clarke, G. P. Kingaby, and J. B. West., Pattern of filling in the pulmonary capillary bed. *J. Appl. Physiol.* 32:346-356, 1972.

CHAPTER 2

Use of norepinephrine uptake to measure lung capillary recruitment with exercise.

ABSTRACT

We used the multiple indicator dilution technique with norepinephrine, a vascular endothelium surface marker, to study the pulmonary vascular changes in awake exercising dogs. The vascular space tracers, labeled red blood cells and albumin, and a water space tracer, 1,8-octanediol, were injected with the norepinephrine, and dilution curves were obtained in nine dogs, at rest and at two increasing levels of exercise. Extravascular lung water dilutional estimates increased with flow and rapidly approached a maximal asymptotic value representing 75% of the perfused lung weight. The ratio of the extravascular lung water measured by dilution to that measured gravimetrically also increased, to reach an asymptotic proportion of close to 100%. The transit time defined vascular space increased linearly with flow; the ratio of lung tissue space to lung vascular space therefore decreased with increasing flow. The mean tracer upslope norepinephrine extractions at rest and at the two levels of exercise were $17 \pm 6.8\%$, $14 \pm 4.1\%$, and $15 \pm 4.0\%$. Using the Crone approximation, we computed the permeability surface area products for norepinephrine; These increased linearly with flow. If permeability does not change, the increase in the permeability surface area product with flow can be attributed to capillary recruitment. We conclude that when all of the lung tissue has become accessible to 1,8-octanediol delivered via the perfused vascular space, there is nevertheless further vascular recruitment, with increase in flow, of vascular surface that can extract norepinephrine.

INTRODUCTION

The pulmonary vasculature is influenced by the gravitational field as well as intraalveolar pressure. At rest, the interaction of these create a perfusion gradient that decreases from the base to the apex of the lung (33). Exercise results in a reduction of this heterogeneity of perfusion, the upper parts of the lung becoming better perfused. The change with exercise could result from either recruitment of capillaries in the upper parts of the lung, or distension, or a combination of both. Investigators studying this have often previously focused their efforts on alveolar vessel behaviour in zone 2 of the lungs, where alveolar pressure (PA) exceeds intraluminal hydrostatic pressure at the venous end of the segment, and hence has been considered to exert a kind of backpressure retarding blood flow. Mathematical models of zone 2 conditions, based on the Starling resistor, postulate cusplike flow-limiting segments at the venous end of the alveolar vessels, resulting in reduced flow with virtually no blood volume displacement (5,6). A more realistic three-dimensional model (13) predicts that portions of the alveolar sheet will become unstable and collapse as the alveolar pressure-venous pressure (Pv) difference increases, with a resulting reduction in perfusion of the region as a whole. Microscopic studies have revealed narrowing or collapse of capillary segments as alveolar pressure-venous pressure difference increases (15,32), and Dawson et al. (11), in isolated dog lung lobe preparations under zone 2 conditions, have reported hemodynamic data consistent with the concept that alveolar vascular volume is responsive to changes in the alveolar pressure-venous pressure difference. The same investigators, in similar preparations, demonstrated a reduced rate of uptake for serotonin despite recording a similar extravascular lung water space in the segment, in the transition from zone 3 ($Pv > PA$) to zone 2 conditions ($Pv < PA$) (28). They attributed their observations to collapse of some alveolar vessels in a fashion which maintained access of tracer water to the extravascular space, as opposed to a simple narrowing.

In the present study, we have utilized an uptake process in the pulmonary vascular endothelium, examined by use of the multiple indicator dilution technique, to explore the pulmonary vascular changes which occur in awake dogs in the transition from rest through two successively increasing levels of exercise. We have simultaneously estimated the extravascular lung water accessible from the vascular space, and have compared these dilution estimates with postmortem gravimetric measurements of the extravascular water. Norepinephrine is extracted by a specific carrier mediated process localized to the pulmonary vascular endothelium (22,26) and otherwise is not expected to diffuse readily out of the blood vessels. The endothelium metabolizes the vasoactive amine and the products are returned to the circulation later in time. The pulmonary extraction of norepinephrine depends on the endothelial permeability coefficient, the vascular surface area available for exchange, the conversion process within the cells, and the vascular exposure time within the region. We have utilized [^{3}H]norepinephrine as a pulmonary vascular surface marker and have estimated its permeability-surface area product (PS) at rest and during two increasing levels of exercise in these animals. The water space tracer used was [^{14}C]1,8-octanediol, which has an identical transit time to that for labeled water (9); the use of the ^{14}C-label is particularly convenient, from an experimental point of view. Previous gravimetric measurements of extravascular water were carried out with the whole lung, and have included main stem bronchi (17,18). Since the tracheobronchial tree is perfused by the bronchial artery, this part of the lung is not accessible to a water space tracer injected into the pulmonary circulation. Hence tracer dilution estimates of lung water would be expected to give a lesser value than gravimetric estimates including the tracheobronchial tree. To adjust for this, we measured the gravimetric extravascular water contents in the post mortem lungs both including and excluding the extrapulmonary bronchial tree, and compared these to dilutional estimates of the extravascular lung water. Vascular space tracers for the cellular and plasma phases of blood, [^{51}Cr]erythrocytes and [^{125}I]albumin, were injected simultaneously with the other tracers. With the use of this set

of tracers, it became possible to measure simultaneously the effect of the change in cardiac output on: the central blood volume, which includes the pulmonary vascular volume; the proportion of extravascular lung water that is accessible from the vascular space and which reflects the proportion of lung tissue perfused; and the extraction and calculated permeability-surface area (PS) product for norepinephrine.

MATERIALS AND METHODS

Animal preparation. Nine healthy mongrel dogs (mean weight 28.8 ± 3.4 kg) were studied. After being trained to perform on the treadmill, they were prepared under general anesthesia. Induction was carried out by the use of 6 mg/kg pentobarbital (Abbot Laboratories, Montreal, Canada), and anesthesia was maintained with halothane (Ayerst Laboratories, Montreal, Canada) while the animal was mechanically ventilated by use of a respiratory pump (Harvard Apparatus, Milis, MS, U.S.A.) with a gas mixture containing oxygen and nitrous oxide. A right paramedial cervical incision was performed and the right internal jugular vein as well as the right internal carotid artery were dissected and isolated. Permanent cannulas (modified stomach tubes, Argyle, St. Louis, MD, U.S.A.) were then inserted through a small incision in both vessels and, under fluoroscopic guidance with the help of vascular contrast medium (MD-76, Mallinckrodt, Pointe Claire, QC, Canada), the tip of the arterial cannula was positioned 2 cm above the aortic valve, while the venous cannula was secured in the right atrium. Subcutaneous tunnels were then constructed from the incision to the back of the neck, where two small incisions permitted the exit of the cannulae. The dogs were allowed a minimum of one week to recover from surgery, while patency of the cannulae was assessed every day. To prevent clotting and thromboembolism, the animals received subcutaneous injections of heparin (Leo Laboratories, Pickering, Ontario, Canada), 8000 units twice a day, and the cannulae were flushed with heparin every day.

On the day of the experiment, the animal was positioned on the treadmill and a balloon tipped catheter (Edwards Laboratories, Santa Anna, CA, U.S.A.) was introduced through the venous cannula and advanced to the pulmonary artery, its final position being guided by pressure tracings (Gould Recorder 2400S, Cleveland, OH, U.S.A.). The arterial cannula was connected to a peristaltic pump (Cole Palmer, Chicago, IL, U.S.A.), which in turn led to a circular sample collector containing borosilicate tubes. Blood samples were withdrawn from the arterial cannula and from the pulmonary artery for blood gas analysis. A first multiple indicator dilution study was then carried out. With the dog at rest, a radioactive bolus containing the tracers to be studied was introduced into the venous cannula and rapidly flushed into the circulation with 10 ml of blood. Simultaneously, the sampling pump (3 ml/sec) and collecting rack (3 tubes/sec) were started, and samples were collected over a period of 15 to 20 seconds. The protocol was then repeated, for the two studies carried out during exercise. The treadmill was started at a speed of two miles per hour and every 3 minutes the slope was increased by 10°. The experimental run was repeated at the completion of six minutes (Level A) and of 15 minutes (Level B) of exercise.

Injection mixture. We prepared 8 ml of injection mixture for each animal. It contained [^{51}Cr]labeled erythrocytes and 60 μCi of [^{125}I]albumin (NEN, Boston, MA, U.S.A.), two tracers that remain in the intravascular space and do not cross the capillary barrier. Additionally, 100 μCi of [^{14}C]1,8-octanediol (2.94 mCi/mMol, NEN, Boston, MA, U.S.A.) was added to serve as a water space tracer (its mean transit time is identical to that of labeled water [9]). The octanediol, because of its essentially nonvolatile nature, is virtually excluded from the alveolar space. Cua et al. (9) have interpreted differences in the outflow curves for labeled water and octanediol to indicate the presence of a diffusional shunt of the labeled water through the vapor phase in the alveolar space (its mass is tiny, of course, in comparison with tissue water), leading to a small early precession and delayed downslope of the labeled water with respect to the octanediol. The injection mixture was

adjusted to match the venous hematocrit of the dog, and was separated into three parts, for later injection. Just prior to injection, 10 nmol of [^{3}H]norepinephrine (40-60 Ci/nmol, NEN, Boston, MA, U.S.A.) was added to the injection mixture; with this, no significant erythrocytic uptake of labeled norepinephrine occurred. Aliquots of 50 µl of the injection mixture were diluted with 950 µl of blood, to be counted later and serve as a standard of reference for the determination of the quantity of tracers injected. The radioactivity retained in the venous cannula was determined after each bolus injection by aspirating the cannula and assaying an aliquot, and this was subtracted from the total injected.

Sample collection and preparation. The sample collector was filled with ice, to cool the collecting tubes and samples, and each collecting tube contained 20 µl of catecholamine preservatives (0.25 M EGTA and 0.2 M glutathione). To prevent erythrocytic [^{3}H]norepinephrine uptake (3) in the samples, 1.0 nmol of unlabeled norepinephrine (Aldrich Chemical Co., Milwaukee, Wisconsin, U.S.A.) was added to each sample tube prior to blood collection. Immediately after each experiment, a 100 µl aliquot was taken from each sample and placed in a new tube for processing; 300 µl of normal NaCl, 400 µl of 0.25M zinc sulfate and 400 µl of 0.2M barium hydroxide were added, and the tubes were centrifuged at 1000g for 10 minutes. An aliquot of 300 µl of supernatant was added to 10 ml of a scintillation cocktail, and the samples and standards were assayed in a beta counter. Another aliquot of 200 µl was removed and passed through a column of Bio Rex 70 cation exchange resin (Bio Rad Laboratories, Richmond, CA, U.S.A.), which resolves norepinephrine and its metabolites (16). Deaminated product was eluted from the columns with 3 ml of water, unchanged norepinephrine with 3 ml of 2% borate, and O-methylated products were removed with 3 ml of 0.2 M HCl solution. A 1 ml aliquot from each elution was added to 10 ml of a scintillation cocktail, for assay of beta activity. The tubes with the precipitated pellets were then assayed for gamma activity.

Plasma catecholamines. Prior to injection of the radioactive mixture, 5 ml aliquots of blood were simultaneously drawn from the pulmonary artery (Swan Ganz catheter) and

the arterial cannula, and were collected in precooled glass tubes containing 120 µL of EGTA /reduced glutathione solution (Upjohn). The tubes were immediately centrifuged at 1000 g for 5 min, and the plasma was removed and stored at -20°C. The samples were later thawed and analyzed for plasma norepinephrine and epinephrine levels, using liquid chromatography with electrochemical detection (16). The liquid chromatographic apparatus consisted of a Waters plasma catecholamine column (C18, 5µ, 15 cm), a Waters high performance liquid chromatographic pump, a Waters 460 electrochemical detector with a glassy carbon electrode, a 100 ml pressure-lock syringe (Precision Sampling Corp.), and a Waters 740 data module. The chromatographic mobile phase was prepared as follows: 50 mmol sodium acetate, 20 mmol citric acid, 3.75 mmol sodium 1-octane-sulfonate, 1.0 mmol di-n-butylamine and 0.135 mmol sodium EDTA were dissolved in 1.0 liter of distilled water/methanol (95:5, v/v), with a final pH of 4.3. To 1.5 ml of thawed plasma was added 50 µl of internal standard (10 mg/ml dihydroxybutylamine), 10 mg of alumina, and 400 µl of 2M Tris/EDTA (20 g/l, pH 8.7). The samples were shaken, to promote contact of the solution with the alumina, and to facilitate absorption of the catecholamines by the alumina. The plasma was then removed and the alumina was washed (with 0.2% Tris/EDTA, pH 8.1), to remove unwanted plasma residues. An acidic solution was added (100 µL of the following: 100 µl of acetic acid, 50 µl of 10% sodium disulfite and 50 µl of 5% EDTA diluted to 10 ml with deionized water) to desorb the catecholamines from the alumina. 20 µl of the resulting sample was then filtered and injected onto the reverse phase C18 column. The mobile phase was pumped at 0.9 ml/min; and the electrochemical detector was set at a potential of +0.65 volts. Catecholamine concentrations were then calculated, from the chromatographic recovery of identified peaks and the recovery of the internal standard.

Bulk pulmonary norepinephrine extraction (Ext) was calculated as follows,

$$Ext = (NE_{pa} - NE_{ao})/NE_{pa} \quad \ldots(1)$$

where NE_{pa} and NE_{ao} represent norepinephrine concentrations, mixed venous upstream, in pulmonary artery, and downstream, in aorta, from the lungs.

Gravimetric measurements. At the conclusion of each experiment, the animal was sacrificed and the lungs were removed together with the trachea, by resecting it two rings below the cricoid cartilage. The trancheobronchial tree is vascularized by the bronchial artery, and its water space is consequently not accessible to tracers entering the pulmonary circulation. To allow for this, and to measure the extent of this phenomenon, we carried out *in vitro* measurements of the extravascular lung water, including and excluding the extrapulmonary bronchial tree. The extrapulmonary bronchial tree was dissected as closely as possible to the lung parenchyma and was removed. The lung parenchyma and the extrapulmonary bronchial tree were then weighed separately. The parenchyma was homogenized in a blender, with the addition of a known quantity (usually 500 ml) of water, and the total volume of the homogenate was noted. A 1 ml aliquot of homogenate was removed and retained. [^{51}Cr]erythrocytes were counted in this sample as well as in 1 ml of mixed venous blood drawn just prior to the sacrifice. A sample of 10 ml of homogenate and the removed extrapulmonary bronchial tree were dried and the dry weights were noted.

The gravimetric extravascular lung water was then estimated. The problem which presents is how to correct values obtained from the lung tissue, for the contained vascular content. At the time of removal, the labeled red cells will still be confined to the circulation, whereas some of the labeled albumin will have left the circulation and will be in the interstitial space. We therefore were able to use only the labeled red cells as a guide to the vascular volume. The vascular volume (VLV) trapped in the lung at the time of removal, approached from this point of view, is given by the following equation,

$$VLV = H_{vol}(H_{cpm}/B_{cpm}) \qquad \ldots(2)$$

where H_{cpm} and B_{cpm} represent the ^{51}Cr activity in a 1 ml aliquot of homogenate and blood, and H_{vol} is the homogenate volume, in ml. The water content of plasma is 0.94 ml/ml, and that of the red cell is 0.70 ml/ml. Thus, if we assume that the hematocrit of the pulmonary

vessels is equal to the venous hematocrit (the assumption is not quite correct, but will be used, for now), we can calculate the vascular lung water (VLW) in g from the vascular lung volume and the hematocrit (Hct) by use of the following relation,

$$VLW = VLV\,[0.70\,Hct + 0.94\,(1 - Hct)] \quad \ldots(3)$$

The dry lung weight excluding the extrapulmonary bronchial tree (Wgt_{dry}, in g) was then calculated from the total volume of the homogenate and the dry weight (Al_{dry} in g), of the 10 ml aliquot, by use of the relation,

$$Wgt_{dry} = H_{vol}\,(Al_{dry}/10\ ml) \quad \ldots(4)$$

From the wet weight of the lung without the extraparenchymal bronchial tree, Wgt, and the corresponding dry lung weight, Wgt_{dry}, the total lung water, TLW, can be estimated from the relation

$$TLW = Wgt - Wgt_{dry} \quad (5)$$

The corresponding gravimetric estimate of extravascular lung water ($EVLW_g$) is

$$EVLW_g = TLW - VLW \quad \ldots(6)$$

The dissected extraparenchymal bronchial tree was weighed and dried, but not homogenized. Its water content was estimated from the difference between its wet and dry weights. The extravascular lung water content of the specimen as a whole was approximated by adding this to the extravascular lung water determined previously. We have implicitly neglected the small vascular volume of the extrapulmonary bronchial tree, in doing this.

Oxygen consumption. The hematocrit was determined by use of a microcapillary method and was corrected for trapped plasma. Since the normal mean hemoglobin concentration of canine red blood cells is 33 g/100 ml of red cells, the hemoglobin concentration of the blood (Hgb, in g/100 ml) is,

$$Hgb = 33 \times Hct \quad \ldots(7)$$

Since the maximal oxygen content carried by hemoglobin is 1.39 ml/g, we calculated the arterial and venous oxygen content from the oxygen saturation (O_2sat) of the blood,

$$O_2 \text{ content} = 1.39 Hgb\ (O_2 sat) \quad \ldots(8)$$

where the measured values for oxygen saturation in the arterial or venous blood are utilized. We then calculated total body oxygen consumption ($\dot{V}O_2$) as the product of blood flow (F_b, in ml/min) and the difference between the arterial (CaO_2) and mixed venous (CvO_2) oxygen contents (in ml/ml),

$$\dot{V}O_2 = F_b\ (CaO_2 - CvO_2) \quad \ldots(9)$$

This was then normalized for body weight, by dividing by the individual body weights of the dogs.

Use of tracer curves to estimate flow, mean transit times, and central blood volume. In order to provide a basis for comparison among the group, the total amount of each material injected was defined as 1 unit. The outflow concentration of each tracer is then automatically defined as its outflow fractional recovery per ml of blood; the relative behaviour of the tracers can then be appraised when the fractional recovery values are plotted as a function of time. To correct for recirculation, the dilution curves were plotted on a semilogarithmic scale, and the downslopes were extrapolated in a linear extrapolation fashion, after the classical manner of Hamilton (24). Blood flow (F_b) was calculated by use of the conservation relation,

$$F_b = 1 / \int_0^\infty C(t)\, dt \quad \ldots(10)$$

where C(t) is an outflow fractional recovery-time curve, and the integral in the denominator on the right hand side of the equation is the area under the fractional recovery curve for any tracer completely recovered at the outflow. We have used the area under the fractional recovery curve of the [^{51}Cr]erythrocytes, for this calculation.

The mean transit time for each tracer was calculated by use of the relation,

$$\text{Mean transit time} = \left(\frac{\int_0^\infty t\, C(t)\, dt}{\int_0^\infty C(t)\, dt} \right) - \bar{t}_{cath} \quad \ldots(11)$$

where $\bar{t}_{cath}$ is the mean transit time through the catheters of the injection and collection system.

The central blood volume (CBV) was calculated as the sum of the spaces accessible to the two vascular tracers, labeled red cells and albumin,

$$CBV = F_b\,Hct\;\bar{t}_{RBC} + F_b(1-Hct)\;\bar{t}_{Alb} \qquad ...(12)$$

where $\bar{t}_{RBC}$ and $\bar{t}_{Alb}$ are the transit times of labeled red cells and labeled albumin.

Dilutional estimates of extravascular water space. The volume which is ordinarily measured is a water volume. The flow used to measure it must therefore be a water flow, and the vascular reference must be a vascular water reference (17). If we define

F_b, F_r, and F_p as the flows of blood, red blood cells and plasma respectively,

F_w as the flow of water, and

f_r and f_p as fractional volumes of water in red blood cells and plasma (ml water/ml red cells or plasma), then

$$F_r = Hct\,F_b \qquad ...(13)$$

$$F_p = (1-Hct)\,F_b, \text{ and} \qquad ...(14)$$

$$F_w = F_r f_r + F_p f_p \qquad ...(15)$$

The last equation provides the appropriate relation for the calculation of blood water flow.

Similarly, the reference vascular transit time appropriate for calculating a water volume is the weighted transit time which the water would have if it did not cross the capillary barrier, $\bar{t}_{w\,ref}$. It is calculated by use of the expression

$$\bar{t}_{w\,ref} = \frac{F_r f_r \bar{t}_{RBC}}{F_w} + \frac{F_p f_p \bar{t}_{alb}}{F_w} \qquad ...(16)$$

The extravascular lung water, calculated from the indicator dilutional data, then becomes,

$$EVLW = F_w\,(\bar{t}_{oct} - \bar{t}_{w\,ref}) \qquad ...(17)$$

where $\bar{t}_{oct}$ is the mean transit time of octanediol, and this is being used as the guide for space of distribution of tissue water. This is the value which usually has been calculated

from indicator dilution data (17-19), and it is the value which corresponds to the accessible extravascular lung water.

In the present study, a part of the object of the study is to compare the tissue water accessible to tracer to that determined gravimetrically, in the same animals, and to both gain insight into the manner in which tissue space becomes accessible as the pulmonary blood flow increases, and the proportion of the gravimetric space which is accessible to tracer at maximal flows. In order to carry out the comparison, the calculated basis for the comparison needs to be the same. Since, in developing the methodology for the gravimetric estimates of lung water, we were able to use only the labeled red cell component of the vascular space as the basis for the calculation of the included vascular volume, we need, for the purposes of comparing the dilutional estimate to this, to correct the calculated gravimetric extravascular lung water estimate by adding to it the water content of the extra plasma space not seen by the red blood cell tracer. Red blood cell-albumin label separation occurs in the small vessels, especially the capillaries (2), rather than in the large vessels, and results in different transit times for labeled red cells and albumin. These were used previously by Goresky et al (17) to quantitate the extra plasma space (EPS) accessible to labeled albumin, in excess of that available to the labeled red blood cells, as follows

$$EPS = F_b\,(1-Hct)\,(\bar{t}_{alb} - \bar{t}_{RBC}) \qquad ...(18)$$

The extra plasma space was found (17) to increase linearly with blood flow, and to have an ordinate intercept, EPS_{int}, on least squares linear regression. This value represents the zero flow extra plasma space. Its water content, 0.94 EPS_{int}, represents the probable error in our calculation of the gravimetric extravascular lung water content, attributable to plasma trapped in the lungs in excess of the labeled red cells. We have therefore corrected our gravimetric extravascular lung water estimate, $EVLW_g$, by substracting from it 0.94 EPS_{int}.

Permeability surface product (PS) for tracer norepinephrine. Assuming that, early in time, the outflow profile for norepinephrine consists only of throughput material that has not been extracted by the vascular endothelium, we can say that the fraction of plasma norepinephrine reaching the outflow as a throughput (1) will be exp ($-PS/F_p$) times what would have reached the outflow if it had not been extracted (the simultaneously injected vascular reference provides the expected outflow pattern); F_p is plasma flow (the tracer norepinephrine is confined to the plasma phase of blood, in the injectate, and during the experiment). The approach represents an application of the Crone approximation, developed for the quantitation of the behaviour of diffusible tracers (10), to the extractable tracer, norepinephrine; it is ordinarily best used to quantitate the behaviour of poorly to moderately extracted materials, for which return of tracer to the circulation is much diminished. With this definition in hand, the permeability surface (PS) product for norepinephrine was calculated by the use of the expression,

$$PS = -F_p \ln(Surv) \qquad ...(19)$$

where ln is the natural logarithm, and Surv is the cumulative relative survival of tracer norepinephrine up to the peak of the dilution curve, in relation to its appropriate reference, labeled albumin. The definition for Surv is, then,

$$Surv = \int_0^{peak} NE(t)\,dt / \int_0^{peak} Alb(t)\,dt \qquad ...(20)$$

where NE(t) and Alb(t) represent the fractional recoveries of labeled norepinephrine and labeled albumin, as a function of time.

Statistical and modeling analysis. Values are reported as means ± standard deviations, unless indicated otherwise. Plasma catecholamine levels at rest and at the two levels of exercise were compared by a two tailed Student's t-test. Bulk and tracer dilutional norepinephrine extractions were also compared by a two tailed Student's t-test. Statistical significance was accepted at the $p < 0.05$ level. The pattern of change of the dilutional

estimates of the extravascular lung water with flow was fitted to a set of saturating profiles by the simplex algorithm method.

RESULTS

Form of the dilution data. A typical set of dilution curves, obtained from the three tracer dilution studies in one of the animals (exp #4) is shown in Figure 1. To demonstrate clearly the impact of increasing blood flow on the areas under the curves and on recirculation, a rectilinear ordinate is utilized, together with an identical linear abscissal time scale, for the three panels. With the change from rest to first level, and then second level exercise, the appearance time of the tracers is seen to decrease, the areas under the reference dilution curves become smaller, and recirculation occurs earlier. The primary recirculation profiles are also evident in the lower two panels. As expected, the recirculation peak for the [^{14}C]1,8-octanediol is much reduced, since this water space tracer distributes into tissue from the systemic capillaries fairly freely. The much lower recirculation of labeled norepinephrine in comparison to labeled albumin reflects the expected systemic extraction of this tracer (27). The experiment carried out at rest exemplifies the relationship between the tracers in a set of outflow curves. The outflow fraction/ml for red cells is highest in the first samples; it reaches the highest and earliest peak, and decays most quickly. The values for the albumin label are slightly lower on the upslope; its peak is slightly lower and later, and its downslope decays slightly less quickly. The values for the labeled octanediol are most displaced from those for the red blood cells; the upstroke of the curve rises least quickly, the peak is delayed and located approximately on the downslope of the red cell label curve, and the downslope of the curve falls least precipitously. The labeled norepinephrine curve needs to be examined in comparison with the labeled albumin curve, which serves as the vascular reference for the estimation of cumulative norepinephrine survival. The difference between the area of these two tracers represents the extraction of norepinephrine, that is, (1–Surv). On the downslope of the curves, on a semilogarithmic

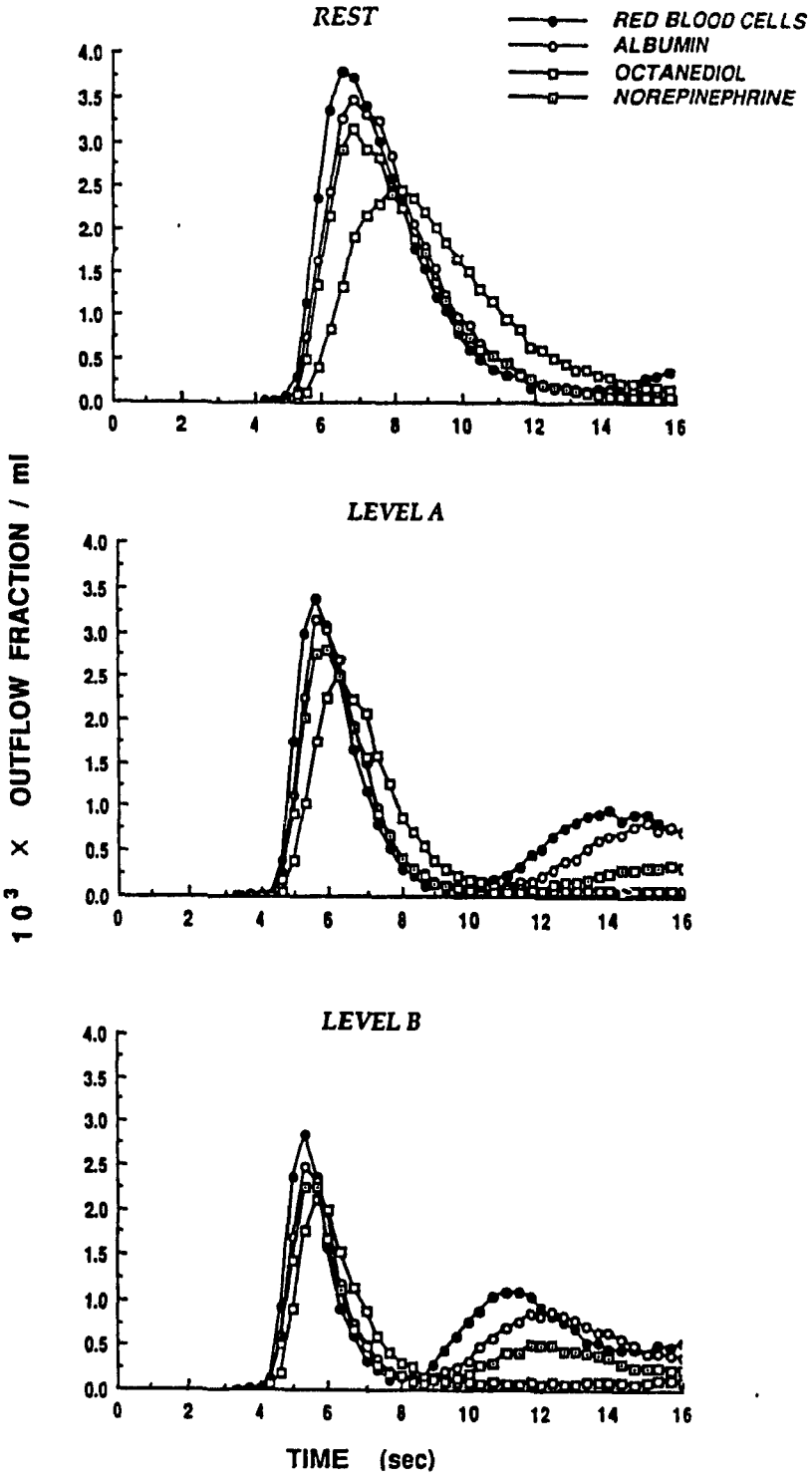

FIGURE 1. Typical set of dilution curves obtained from an awake dog at rest, and at two successive levels of exercise (levels A and B). The abscissal time scales were kept identical for the three graphs, to show the effect of increasing blood flow on the general appearance of the curves.

representation, the descending limb of the tracer norepinephrine curve approaches the albumin curve, suggesting late return of tracer to the circulation. The overall tracer norepinephrine extraction was low, however, and, at the same time, plots of extraction as a function of time (figure 2) and plots of the logarithm of norepinephrine survival as a function of time were less smooth than usually expected (the dose of labeled norepinephrine was deliberately kept low, to avoid pharmacologic effects). There were no detectable deaminated or O-methylated norepinephrine products in the lung effluent of any of the animals studied over the period of sample collection, suggesting that, early in time, there was no liberation of norepinephrine metabolites from the vascular endothelium to the circulation. With these problems, we elected to treat the data relatively simply, to quantitate norepinephrine extraction from appearance to peak, and to use these data, for permeability surface area product estimates, over a region where we can confidently say that the conditions for its application (10) are met. Mean tracer norepinephrine extraction, calculated over this region for the whole group, did not change significantly from rest to first and second levels of exercise; values (mean ± SD) were 17.4 ± 6.8%, 13.9 ± 4.1% and 15.5 ± 4.0% respectively. The numerical parameters derived from the individual multiple indicator dilution experiments for this and other characteristic experimental parameters are assembled in Table 1.

Mixed venous and aortic plasma norepinephrine levels increased significantly with exercise (Table 2). Aortic norepinephrine levels were significantly lower than mixed venous levels at rest, and tended to be lower through two successive levels of exercise. Bulk norepinephrine extractions did not vary with exercise and were not different from dilutional extractions. There was no significant variation in the extraction of norepinephrine between runs even though levels increased with exercise.

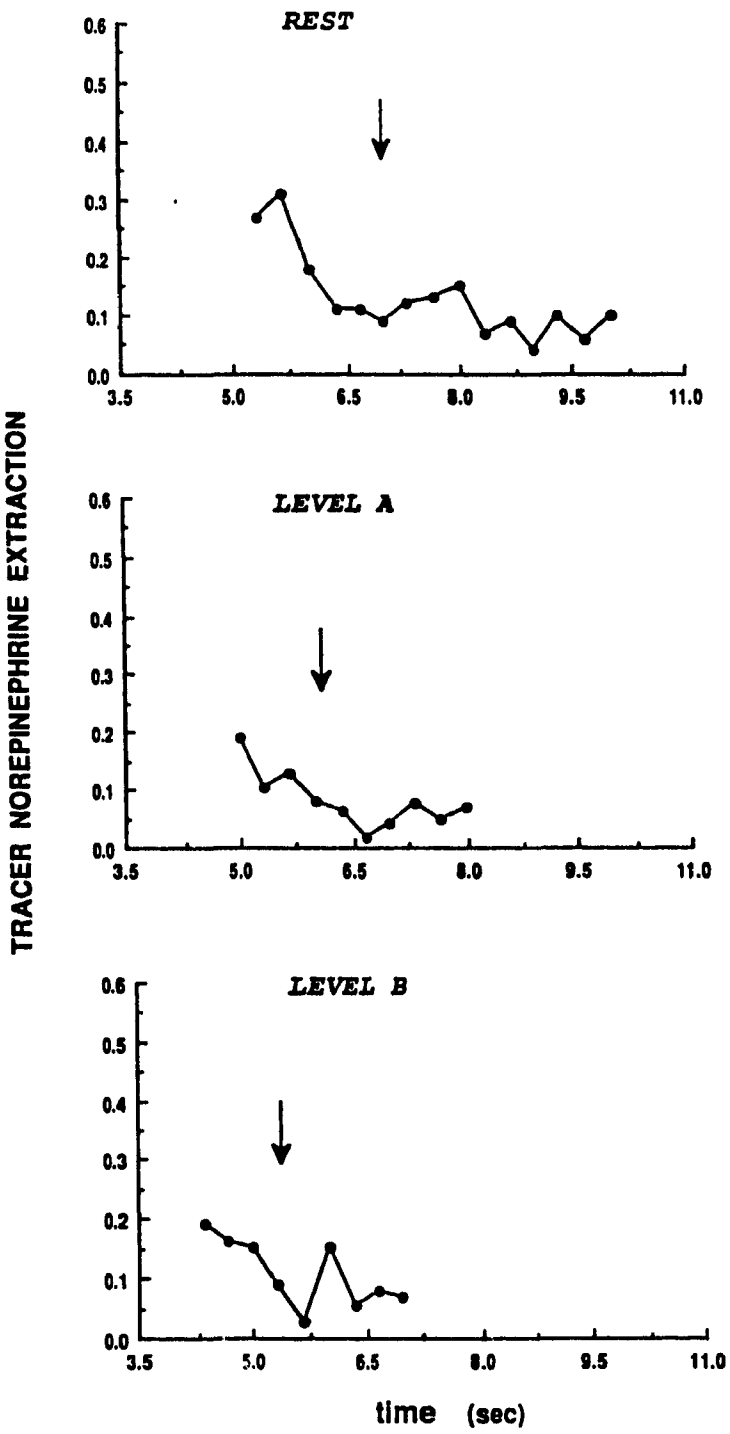

FIGURE 2. Tracer norepinephrine extraction at rest and at two successive levels of exercise (levels A and B). The origin of the abscissal time scale (3.5 sec) corresponds to the catheter mean transit times. The arrows indicate the times corresponding to the peak of the norepinephrine dilution curves in Figure 1.

TABLE 1. *Numerical values of individual parameters calculated from the indicator dilution curves in awake dogs, at rest, and at two increasing levels of exercise.*

Exp. no.	Exercise level	Body weight kg	Lung weight g	Blood flow ml/sec	$\bar{t}_{rbc}$ sec	$\bar{t}_{alb}$ sec	$\bar{t}_{oct}$ sec	$\bar{t}_{ne}$ sec	$\bar{t}_{wref}$ sec	Tracer norepi-nephrine extraction	Norepi-nephrine PS ml/sec
1	rest	33	287	92	5.01	5.83	7.33	6.15	5.51	0.31	33
	A			236	3.35	3.65	4.39	3.72	3.53	0.15	37
	B			457	1.17	1.59	1.86	1.63	1.43	0.16	80
2	rest	33	264	126	2.41	2.54	3.60	2.56	2.48	0.24	35
	A			263	1.57	1.77	2.38	1.79	1.68	0.19	54
	B			378	1.50	1.70	2.11	1.70	1.61	0.18	76
3	rest	30	262	100	3.76	4.20	5.33	4.25	4.03	0.17	19
	A			196	1.79	2.14	2.79	2.19	2.00	0.15	31
	B			372	1.15	1.45	1.90	1.56	1.33	0.19	77
4	rest	29	196	81	4.45	4.72	5.41	4.70	4.61	0.14	12
	A			144	2.47	2.73	3.40	2.74	2.71	0.15	23
	B			269	1.51	1.92	2.18	1.96	1.75	0.18	55
5	rest	26	172	64	4.11	4.48	5.61	4.54	4.31	0.18	13
	A			158	2.37	2.62	3.20	2.64	2.51	0.17	29
	B			241	1.90	2.15	2.50	2.09	2.03	0.15	39
6	rest	25	170	59	5.52	5.71	6.39	5.74	5.64	0.08	5
	A			166	2.48	2.73	3.30	2.72	2.64	0.08	13
	B			143	2.90	3.15	3.70	3.23	3.06	0.17	26

(contd)

(Table 1, contd.)

7	rest	24	227	38	6.02	6.54	8.04	6.53	6.40	0.16	7
	A			107	3.61	4.01	4.90	4.07	3.90	0.10	11
	B			95	3.26	3.72	4.76	3.80	3.60	0.18	19
8	rest	28	253	86	6.21	6.67	7.90	6.72	6.53	0.10	9
	A			173	2.90	3.18	3.90	3.20	3.10	0.10	17
	B			307	1.82	2.05	2.45	2.06	1.98	0.09	30
9	rest	32	206	79	4.36	4.87	5.82	4.92	4.69	0.18	16
	A			184	3.45	3.78	4.40	3.82	3.68	0.19	38
	B			272	2.84	3.12	3.45	3.14	3.01	0.08	23

$\bar{t}_{rbc}$, $\bar{t}_{alb}$, $\bar{t}_{oct}$, $\bar{t}_{ne}$ and $\bar{t}_{wref}$ represent the mean transit times of the red blood cells. albumin, octanediol, norepinephrine and the intravascular water reference respectively. PS = permeability surface area product for tracer norepinephrine. Lung weight = total wet lung weight including the extrapulmonary bronchial tree.

TABLE 2. *Plasma levels of mixed venous and aortic catecholamines, and comparison of bulk and dilutional lung norepinephrine extraction.*

	Rest	Level A	Level B
Norepinephrine (nM)			
mixed venous	2.45 ± 0.46	4.05 ± 0.58	8.74 ± 1.15**
aortic	2.10 ± 0.44	3.54 ± 0.48*	7.98 ± 1.08**
p =	0.023	0.065	0.053
Norepinephrine extraction (%)			
bulk	13.7 ± 2.31	10.3 ± 3.08	8.8 ± 2.31
dilutional	17.3 ± 1.15	14.2 ± 0.77	15.3 ± 0.77
p =	0.472	0.492	0.124
Epinephrine (nM)			
mixed venous	0.90 ± 0.08	1.19 ± 0.12	3.95 ± 0.98
aortic	0.96 ± 0.10	1.41 ± 0.19	4.25 ± 1.04
p =	0.152	0.214	0.167

* = $p<0.05$ and ** = $p<0.01$ vs rest. p values for differences between mixed venous and aortic norepinephrine and epinephrine levels, and between bulk and dilutional extractions are indicated. Values presented are mean ± SE.

Oxygen consumption. The oxygen consumption ($\dot{V}O_2$), expressed in proportion to body weight, is shown in Figure 3 The $\dot{V}O_2$ increases linearly as blood flow increases; the least mean squares regression line fitted through the data is

$$\dot{V}O_2 = 50.2\ F_b - 9.56;\ r = 0.956$$

where F_b is the cardiac output, or pulmonary blood flow. Note that the points assemble themselves into three groups, corresponding to the three regions of study.

Vascular label separation and the extra plasma space. When mean transit times of labeled albumin and red blood cells are plotted (Figure 4), a linear relation is found,

$$\bar{t}_{Alb} = 1.047\ \bar{t}_{RBC} + 0.193;\ R = 0.996.$$

Values deviate from the regression line only at the highest flows. The deviation suggests that, in the high flow regime, red cells become shaped into profiles more closely centered on capillary center lines, allowing proportionately higher plasma bypass. The relation between $\bar{t}_{Alb}/\bar{t}_{RBC}$ and $\bar{t}_{RBC}$ is shown in the lower panel; this demonstrates the relative increase in the red cell-plasma label separation at the highest flows (low $\bar{t}_{RBC}$). The line through this plot was the image of the linear regression fitted to the upper panel.

The extra plasma space, calculated with equation (18), was found to increase linearly with blood flow (Figure 5). The least mean squares regression line through the data is

$$EPS = 0.125\ F_b + 0.0364;\ r = 0.81.$$

The product of the ordinate intercept value (0.036 ml plasma/g lung) and the water content of plasma (0.94 ml/ml), is 0.034 ml water /g lung. This is the water content of the intercept or zero flow value for the extra plasma space, and it is the value which we have inferred is needed to correct the gravimetric estimates of extravascular lung water obtained by using the labeled red blood cells as a vascular tracer. This value was subtracted from the value obtained from the difference between total and vascular (based on red cell transit time) space water, to yield a corrected value for gravimetric extravascular lung water.

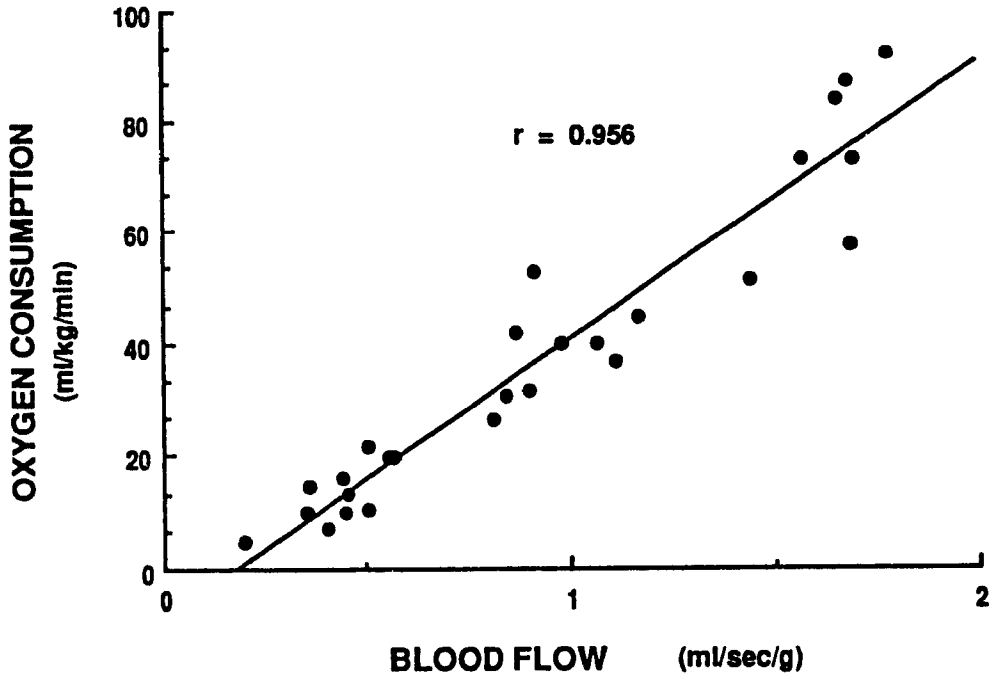

FIGURE 3. Variation of oxygen consumption as a function of blood flow in the awake dogs, at rest, and at two increasing levels of exercise. Note that the points separate into three groups, corresponding to the three parts of the experiment.

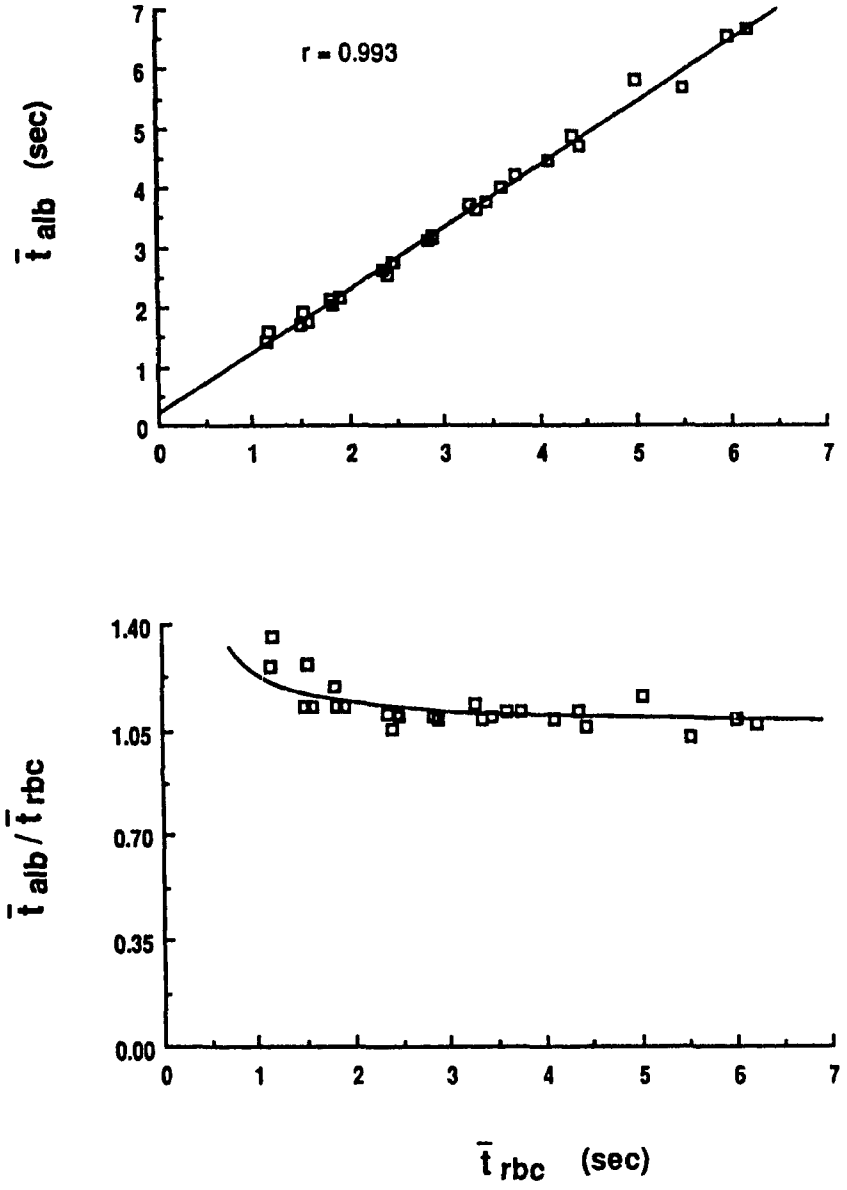

FIGURE 4. Vascular label separation. The relation between the mean transit time of labeled albumin and the mean transit time of labeled red blood cells is shown in the upper graph. When the ratio of the two is plotted (lower graph), a relatively increasing label separation becomes evident at high flows (low mean transit times). The line placed on the lower graph was constructed to correspond to the linear regression equation fitted to the data in the upper panel.

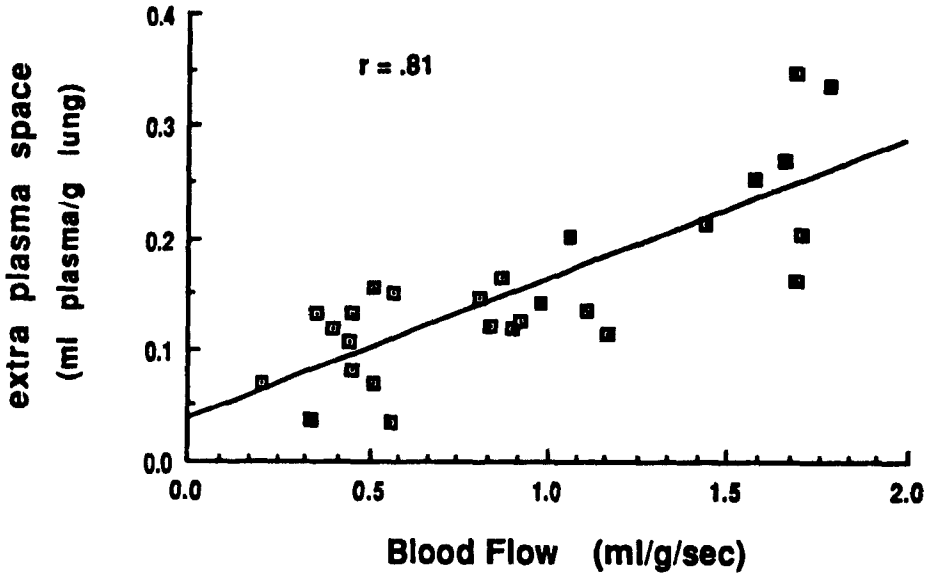

FIGURE 5. The extra plasma space (ml of plasma per gram wet lung weight), plotted as a function of blood flow.

Extravascular lung water*. In Figure 6, dilutional tracer estimates of extravascular lung water are expressed as a proportion of the extravascular wet lung weight (P), and are plotted as a function of blood flow, the latter being expressed in terms of wet lung weight. In the upper panel of the figure, the extrapulmonary bronchial tree is included in the two estimates, whereas in the lower panel, it is excluded. In both cases, the estimated extravascular lung water increases with blood flow and rapidly approaches a maximal asymptotic value. The data points were fitted by use of a simplex method to a rising exponential (solid line) and rectangular hyperbola (dotted line) and the least squares method was used to provide a criterion for goodness of fit. Both curves gave a similar quality of fit and the loci corresponded closely, over the range of the data. The maximal asymptotic value for the proportional water space was higher with the hyperbolic than the exponential fit (Table 3). This occurred because the hyperbolic fit extrapolated, above the range of the observations, to maximal values higher than any of those recorded in the upper experimental range of cardiac outputs.

The expression that provided the best fit to the data, when the extrapulmonary bronchial tree was included, was, in the rising exponential case,

$$EVLW = 0.639\ (1-\exp^{-3.12F_b})$$

In this expression, the first numerical parameter is an asymptotic maximal or $EVLW_{max}$ value, and the second, an exponential constant with dimensions reciprocal to those of F_b. In the case of the rectangular hyperbola, the best fit expression was

$$EVLW = \frac{0.769\ F_b}{F_b + 0.274}$$

where the numerical parameter in the numerator is an asymptotic $EVLW_{max}$, and that in the denominator is the value for F_b which corresponds to an EVLW value which is half the asymptote.

* Reference is often made to the extravascular lung water. Unless specified otherwise, the author is referring to the dilutional tracer accessible extravascular lung water.

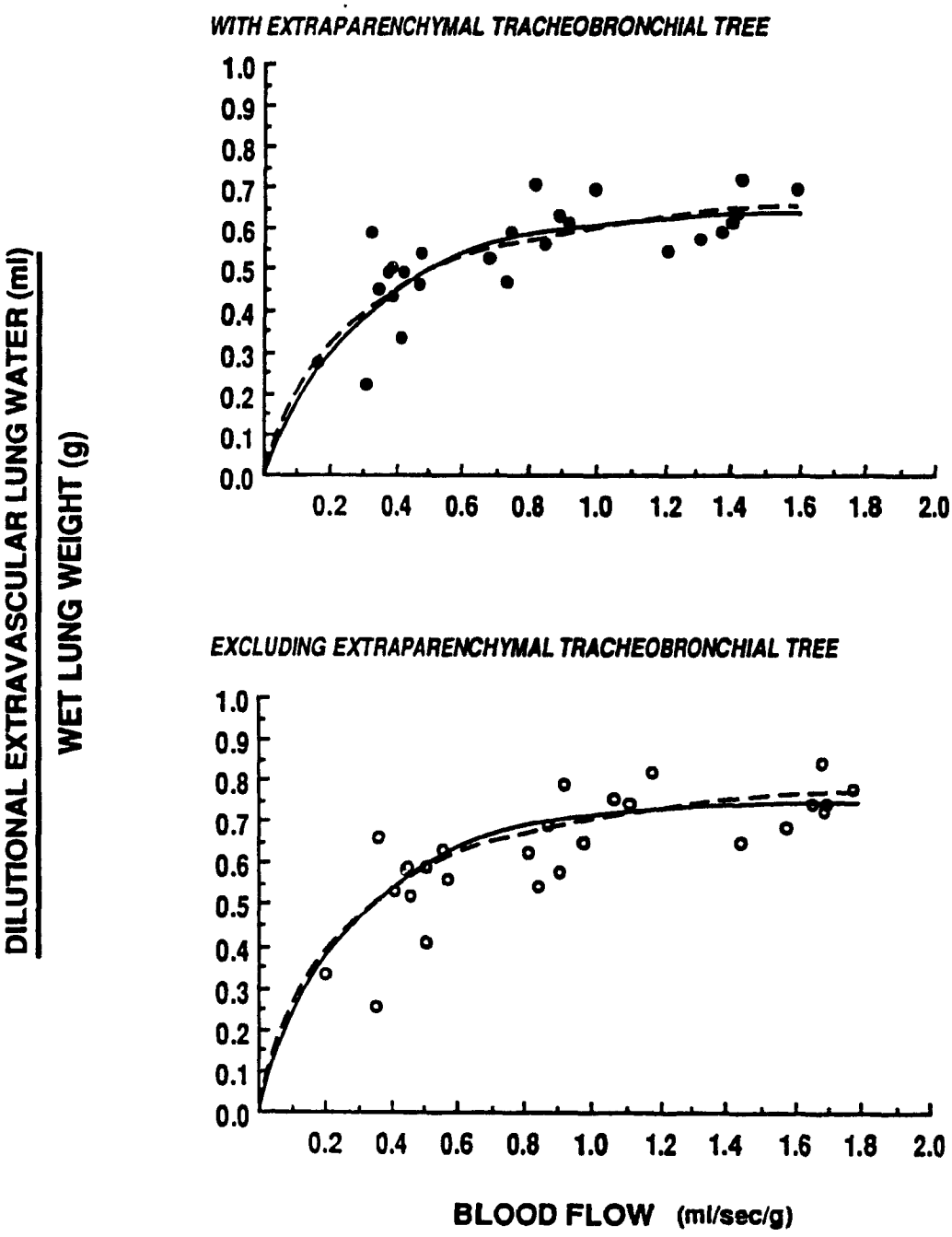

FIGURE 6. Amount of extravascular lung water. The dilutional estimates of the extravascular lung water divided by wet lung weight (ml of water per gram of lung) are plotted as a function of blood flow. The extraparenchymal tracheobronchial tree was either included (upper graph, filled circles), or excluded (lower graph, open circles) in the calculations of the wet lung weight. The data points were fitted by a rising exponential (solid line), or a rectangular hyperbola (dashed line). Notice the upward shift in the data when the tracheobronchial tree is excluded.

TABLE 3. *Parameters of the best fitting equations for the measurement of the extravascular lung water.*

	Extrapulmonary bronchial tree			
	Included		Excluded	
	Exp	Hyp	Exp	Hyp
$EVLW_{max}$	0.639	0.769	0.750	0.899
SSr	0.159	0.157	0.194	0.192
SD	0.276	0.276	0.317	0.316
R_{max}	0.871	1.042	1.0*	1.0*
SSr	0.293	0.290	0.335	0.419
SD	0.373	0.372	0.409	0.370

Exp = rising exponential; Hyp = rectanguler hyperbola; P_{max} = maximal asymptotic value for the extravascular lung water expressed as a proportion of the extravascular weight lung weight; R_{max} = maximal asymptotic proportion of the extravascular lung water that is accessible from the vascular space; SSr = sum of the squared residuals providing the best fit; SD = standard deviation of the experimental points from the fitted function. *R_{max} value was set to 1 and a one parameter fit was performed.

When the gravimetric estimate excluded the extrapulmonary bronchial tree, the least squares best fit to the rising exponential pattern was

$$EVLW = 0.750\ (1-\exp^{-2.69F_b})$$

and that to the rectangular hyperbola was

$$EVLW = \frac{0.889\ F_b}{F_b + 0.314}$$

The measured gravimetric water content of the lungs was 0.76 g/g when the extrapulmonary bronchial tree was included, and 0.80 g/g when this was excluded. The apparent maximal asymptotic water content $EVLW_{max}$ estimated with the rectangular hyperbolic pattern appears too high (the asymptotic values were higher than any of the observed values); the rising exponential, on the other hand, extrapolates through the upper range of the data to a maximal value corresponding reasonably closely to the data. Of the two exponential fit maximal values for the water content (0.639 with, and 0.750 without the extrapulmonary bronchial tree), the latter approaches the lung water content more closely.

The data demonstrate that, over the range of cardiac outputs observed, the dilutional estimates of the extravascular lung water underestimate the gravimetric water content, when the extrapulmonary bronchial tree is included in the gravimetric data. The findings also indicate that dilutional estimates of extravascular lung water approach the gravimetric water content, at high flow values.

To carry the data analysis further, to measure the proportion of the extravascular lung water accessible from the vascular space, we calculated the ratio R of dilutional to gravimetric extravascular lung water (the latter corrected for the zero flow extra plasma water space) and plotted the ratio as a function of blood flow (Figure 7). The proportion of the lung water accessible increases with flow and rapidly approaches a maximal asymptotic value. The best fit through the data points, when the extrapulmonary bronchial tree was included in the gravimetric estimate, was, with the rising exponential pattern

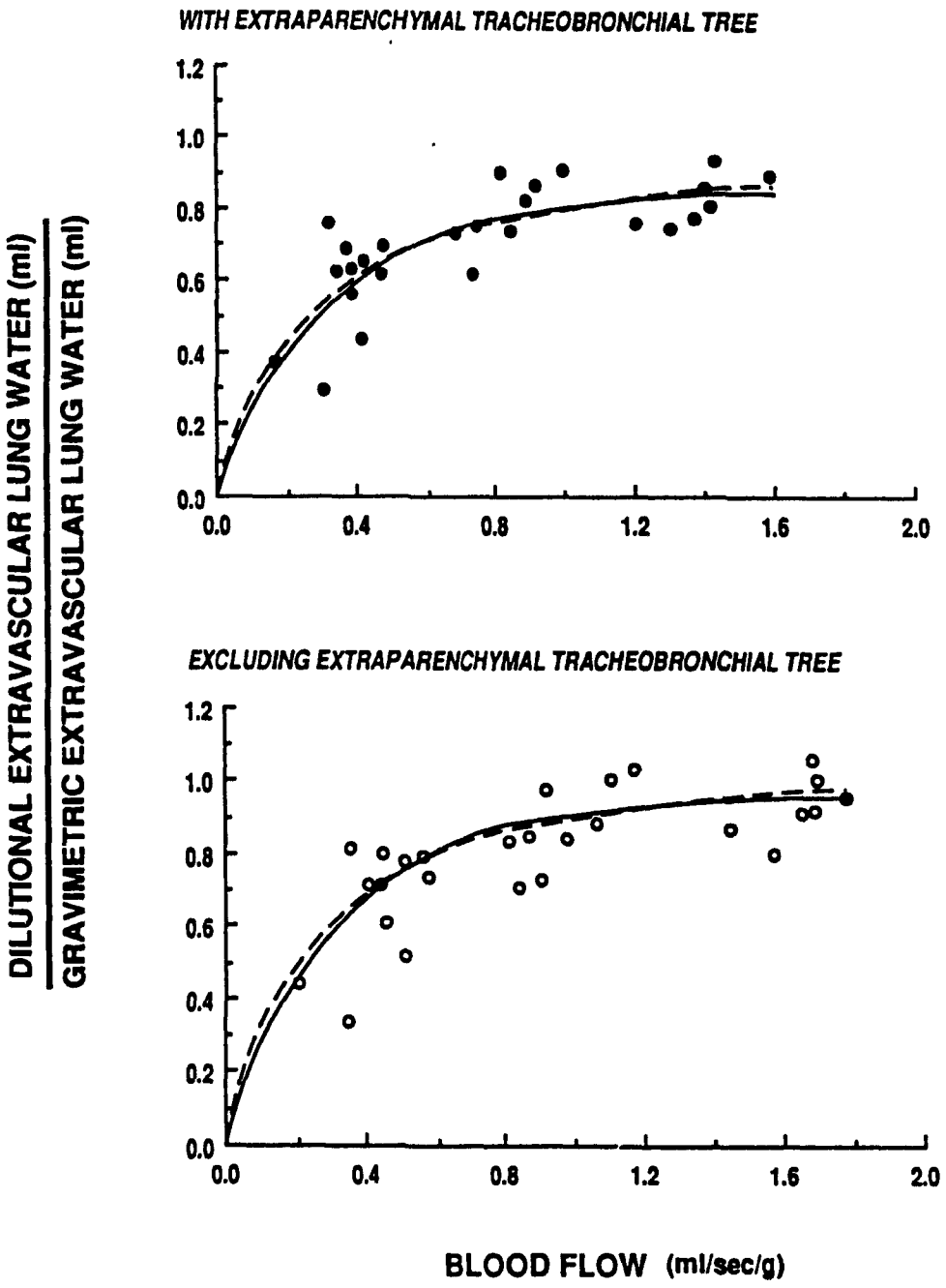

FIGURE 7. Accessible lung water. The ratio of dilutional to gravimetric estimates of the extravascular lung water (proportion of the lung water accessible from the vascular space) is plotted in relation to blood flow (see legend for Figure 5 for an explanation of the graphs).

$$R = 0.871\ (1-\exp^{-3.17F_b}),$$

and with the rectangular hyperbola pattern,

$$R = \frac{1.042\ F_b}{F_b + 0.310}$$

None of the experimental values approached the value of unity, they were all substantially lower.

When the extrapulmonary bronchial tree was excluded, the ratio data points were found to increase with flow and rapidly approach values around 1 at high flows. We consequently set the maximal value in the fitted patterns to 1 and carried out a one parameter fit. The best fit rising exponential pattern was

$$R = 1-\exp^{-2.70F_b}$$

and the best fit rectangular hyperbola was

$$R = \frac{F_b}{F_b + 0.155}$$

The one parameter fit demonstrates that the rising exponential provides a more systematic fit to the sense of the data than does the rising hyperbola. The exponential fit conforms to the data in the lower flow range, whereas the other does not. The data demonstrate that high flow tracer estimates of lung water correspond closely to the gravimetric estimates of lung water when the extrapulmonary bronchial tree is excluded from consideration (for the exponential fit, the asymptotic maximum would have been 0.99) and it may be inferred that the appropriate gravimetric frame of reference for this kind of study is the parenchymal lung tissue, with the extrapulmonary bronchial tree excluded.

A different way of visualizing the changes in the extravascular lung water is shown in Figure 8. The difference between the mean transit time of octanediol and the intravascular water reference (Table 1) is plotted as a function of blood water flow. The data points shift from a lower to a higher isovolumetric line as blood water flow increases. The change provides another way of seeing the recruitment of tissue water space at intermediate flows, and the approach to an asymptotic maximum, at higher flows.

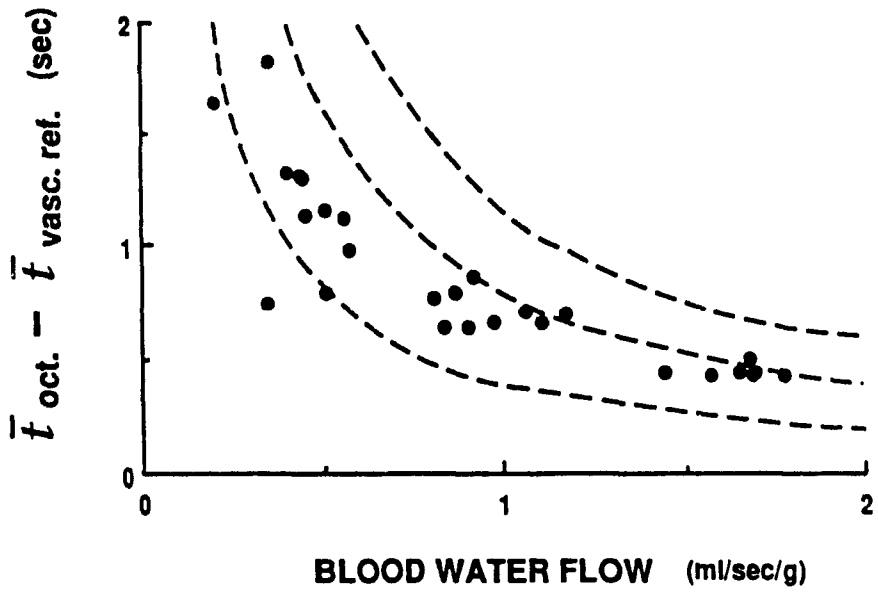

FIGURE 8. Extravascular lung water-transit time relations. The difference between the mean transit time of octanediol (a water reference) and the composite intravascular water reference is plotted as a function of blood water flow. The dashed lines represent isovolumetric lines of 0.4, 0.8, and 1.2 ml of water per gram of extravascular lung weight. The data points shift from a lower to a higher isovolume line as blood flow increases.

Central blood volume. The central blood volume (CBV), calculated by use of equation (12), increases as blood flow (F_b) increases (Figure 9), according to the following fitted mean squares regression,

$$CBV = 0.895\ F_b + 1.508;\ r = 0.621$$

The central blood volume continues to increase across the whole range of flows. The variations in central blood volume with exercise can also be visualized by plotting the mean transit time corresponding to the central blood volume against blood flow. In contrast to the plot corresponding to the tracer accessible extravascular lung water, which rapidly approaches an isovolume line corresponding to a maximal value at moderate levels of exercise, the plot corresponding to the central blood volume continues to cross isovolume lines, over the whole range of blood flows, including the higher values.

The permeability surface product for tracer norepinephrine. The permeability surface (PS) product for tracer norepinephrine increases with blood flow (Figure 10) according to the regression line,

$$PS = 0.166\ F_b + 0.002;\ r = 0.729$$

The permeability surface product for norepinephrine and consequently the pulmonary capillary surface, if the norepinephrine permeability remains constant, can be inferred to increase with the increase in blood flow with exercise, and the increase continues not only over the range of flows across which lung tissue is recruited but also over the range of flows across which the accessible lung water has increased to its asymptotic maximum.

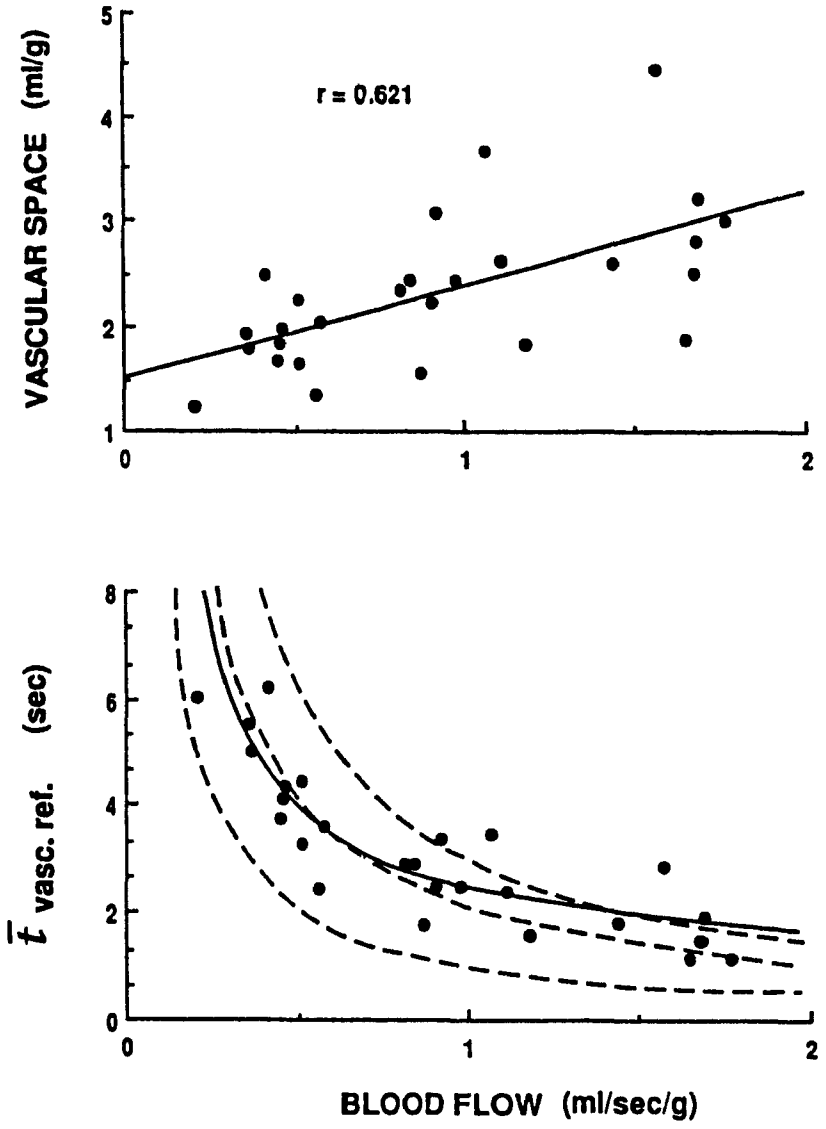

FIGURE 9. Central blood volume. The vascular space increases linearly with blood flow. The mean transit time of the vacular reference is seen to shift continuously from lower to higher isovolumetric lines as blood flow is increased. The isovolumetric lines are represented by the dashed lines at 1, 2, and 3 ml of blood/g lung weight.

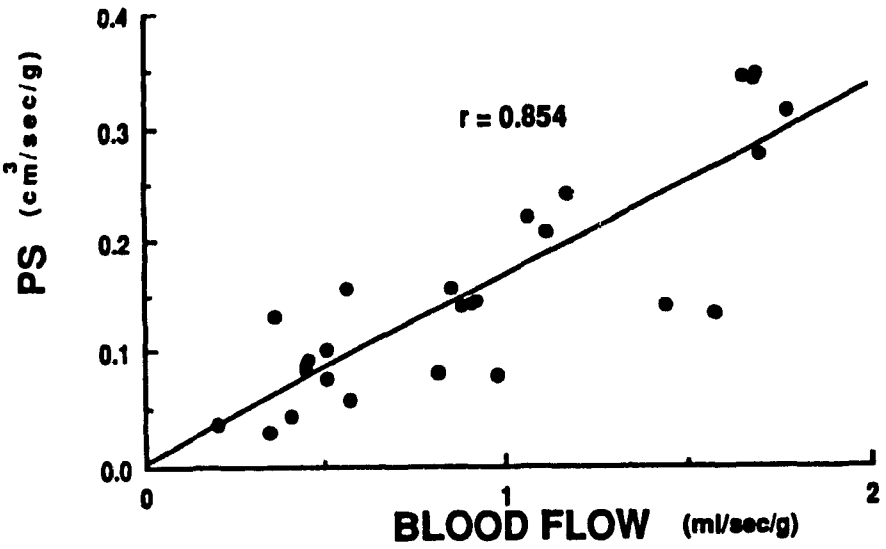

FIGURE 10. Norepinephrine permeability surface area product (PS) versus flow relation. The PS product increases linearly with blood flow.

DISCUSSION

In the present work, we have examined the effect of exercise on tracer accessible extravascular lung water, the central blood volume and the pulmonary permeability surface area product for tracer norepinephrine in awake mongrel dogs.

Extravascular lung water. The extravascular lung water is constituted by the water contained in the endothelial cells, the interstitial space, and the alveolar septal cells. A water space tracer (labeled octanediol) having access to the above structures will therefore serve as an indicator of the amount of lung tissue being perfused. With exercise the extravascular lung water measured by the indicator dilution technique increased nonlinearly and rapidly approached a maximal asymptotic value representing 0.75 of the wet lung weight. The ratio of dilutional to gravimetric estimates of lung water, which corresponds to the proportion of the lung parenchyma perfused, also increased in a similar manner and rapidly approached an asymptotic value of close to 1, when the extrapulmonary bronchial tree was not included in the specimen.

The overall pattern of variation of the tracer accessible lung water with flow was previously well documented by Goresky et al (17-18) in exercising dogs. In these studies a discrepancy of 0.15 was found between the ratio of asymptotic tracer and gravimetric estimates of extravascular lung water over the observed range of cardiac outputs, the tracer studies providing an estimate which was too low. The gap was attributed to the water space in large airways, perfused by the bronchial artery, and consequently not accessible to tracer injected into the pulmonary circulation. Our measurements of $EVLW_{max}$ by the rising exponential, with and without the extrapulmonary bronchial tree, show a change of the order of 0.11; virtually all of the difference originally found by Goresky et al can therefore be attributed to the extrapulmonary bronchial tree. When the extrapulmonary bronchial tree is excluded, there is no longer any clear difference between the dilutional and gravimetric values. The results also indicate that virtually all of the lung water (or lung

tissue) is accessible from the vascular space at moderate blood flows (0.80 ml/sec/g) and that no further tissue recruitment occurs, with higher levels of blood flow.

Central blood volume. The central blood volume measured in this study is the cardiopulmonary blood volume from the right atrium to the root of the aorta. The pulmonary circulation is unique in that with increasing blood flow there is relatively small change in the pulmonary artery pressure with a concomitant dramatic fall in vascular resistance. This could be the result of vascular distension or opening of new vascular channels (recruitment), or a combination of both. One would therefore expect an increase in central blood volume with exercise. In our study, there was a linear increase in central blood volume with exercise. By substitution in the least squares fitted linear regression equation from Figure 9, we can estimate that there was a 46% increase in central blood volume when the blood flow is tripled from 0.5 to 1.5 ml/sec/g. This increase occurs despite the demonstrated decrease in the left ventricular component of the volume which occurs in dogs during treadmill exercise (29). No data are available on the behaviour of the right heart chambers with exercise, but since these chambers share a common space in the pericardial sac, there is probably no net increase in the total cardiac blood volume with exercise, so that the increase in central blood volume can mostly be attributed to an increase in the pulmonary vascular volume. Previous pulmonary artery-aorta indicator dilution estimates of central blood volume in exercising dogs gave similar results (17). A concomitant increase in carbon monoxide diffusing capacity (DL_{CO}) with oxygen consumption has been well described (8). Investigators, dissecting the elements underlying the DL_{CO}, have inferred that there is an increase in capillary volume with increasing blood flow in healthy human subjects (23,25). Expectations are thus that pulmonary capillary volume will increase concomitantly with the increase in central blood volume. Of particular importance is the observation that the central blood volume continues to increase beyond that blood flow at which all of the lung parenchyma had become perfused, and the previous observation that the single breath carbon monoxide diffusing

capacity also continues to increase in the exercising human after estimates of dilutional water space have maximized (19).

Vascular tracer separation in the pulmonary circulation. This study sheds more light on the red cell label-plasma label separation in the pulmonary circulation. The very high flows achieved in this study resulted in a substantial number of observations of very short red blood cell and albumin mean transit times (between 1 and 2 seconds), when separation is most evident (Figure 4). The separation is of a nature such that the extra plasma space increases with flow (Figure 5). As previously suggested (17), this finding likely depends on a flow dependent deformability of red blood cells, making their capillary transit times shorter than those of the labeled albumin.

Permeability surface area product for tracer norepinephrine. This is the first time that an extractable tracer has been used to study changes in capillary surface area in awake exercising animals. Norepinephrine is extracted by the capillary endothelium by means of a specific carrier mediated process and is then rapidly metabolized (22,26). There is no apparent neuronal uptake and there are no storage granules for norepinephrine in the endothelial cells of the lung capillaries. Appropriate precautions were taken to prevent red blood cell uptake of norepinephrine (3), which would have falsely elevated measured lung extractions. The amount of labeled norepinephrine injected had no detectable hemodynamic effects on the animals studied.

It was not surprising to find an absence of detectable norepinephrine metabolites in the lung effluent, over the times of a single transit. In the *in vivo* rabbit lung, where perfusion is less and transit times are much larger, Catravas et al (7) found negligible norepinephrine metabolism over the times of a single passage, despite norepinephrine extractions averaging close to 50%. With a steady state perfusion approach in isolated perfused rabbit lungs, Gillis et al (14) found a 23% norepinephrine extraction, and found that 7% of this appeared as labeled metabolites over the following 10 minutes In the present study, the mean norepinephrine extraction was found not to change significantly in

the progression from rest over two levels of exercise but values were slightly less than those obtained with the steady state infusion approach in dogs *in vivo*, where the values were 19% and 20% (22). Our results indicate that, in a single passage through the lungs, between 14% and 17% of tracer norepinephrine is extracted and no detectable metabolites are released into circulation during the time of a single passage. Because the tracer norepinephrine extraction was low, the random error in extraction ratio plots became more important and extraction ratio plots were somewhat variable (figure 2), and although the data suggested later return of tracer, they did not appear of a quality justifying extensive rather than simple modeling.

The average bulk norepinephrine extraction did not differ significantly from the dilutional norepinephrine extraction, suggesting that there was no net norepinephrine production by the lungs. Péronnet et al (27) previously did not find a significant norepinephrine extraction across the lungs of exercising dogs (by radioimmunoassay), which suggested that the lungs did not contribute to norepinephrine clearance. We found a dilutional extraction of the order of 15%, which was maintained with exercise. This suggests that the lungs are one of the major sites of norepinephrine clearance, and that this clearance increases with exercise. The importance of this is amplified by the accompanying physiologic events. The lungs receive the whole cardiac output, the cardiac output triples or quadruples with exercise (Table 1), and mixed venous norepinephrine values nearly quadruple with exercise (Table 2). Differences between bulk mixed venous and aortic norepinephrine levels were, however, only significant at rest; and Péronnet et al (27) were previously not able to demonstrate any difference at rest or exercise. The sequence of findings suggests that the ability of the bulk norepinephrine assays to provide recovery estimates, while improving and much better than in the past, with the shift from the radioenzymatic assay to the high performance liquid chromatography, may still be somewhat less than that of the tracer approach.

In the present study, the permeability surface area product for tracer norepinephrine was found to increase linearly with flow. The mean regression line on Figure 10 indicates that the permeability surface area product approximately tripled when blood flow tripled. Assuming that there is no variation in norepinephrine permeability coefficient with variation in blood flow, changes in the permeability surface area product can be attributed to changes in the lung capillary surface area. This assumption seems reasonable since there is no present evidence that endothelial permeability to small solutes varies with lung flow. In other words, the tripling of the blood flow can be inferred to result in a tripling of the capillary surface area available for norepinephrine extraction. Since capillary distension is unlikely to result in any important change in the number of capillary endothelial transporters for norepinephrine, we suggest that the inferred capillary recruitment results from exposure of capillary endothelial cell surfaces not previously in contact with blood. This conclusion supports the work of Rickaby et al (28), who showed, in an isolated lobe preparation with variable alveolar pressure, that the accessible extravascular lung water space from a zone 3 to a zone 2 regime remained unchanged, while the rate of serotonin uptake decreased; they inferred that the underlying change was due to a collapse of capillaries, as opposed to a simple narrowing. In a recent publication, Fung and Yen (13) have modeled blood flow in an alveolar sheet and have described conditions under which portions of the alveolar sheet become unstable as the venous pressure falls below that of the pulmonary artery, with resultant local regions of collapse. As with the data of Rickaby, Fung's model is consistent with our observations, if the size of the collapsed areas is sufficiently small to allow access of [^{14}C]1,8-octanediol from adjacent perfused areas during a single passage. Studies of the endothelial metabolism of angiotensin converting enzyme substrates during a single passage (31) and morphometric examinations (15) also support the concept that lung capillaries can be recruited.

In the past, passive markers of endothelial transfer have been utilized to explore microcirculatory changes during imposed pathologic conditions (4,34). Interpretation of

changes in permeability surface area product values has then demanded an assessment of whether surface area, permeability, or both have changed. The use of a marker chiefly removed by an endothelial cell membrane carrier transport system should be helpful, under the circumstances. The recent findings by Harris et al. (21) that the ratio of pulmonary capillary permeability surface area values for labeled urea (a passively permeating marker) to labeled norepinephrine is unchanged during phase 1 of E, coli endotoxemia, but is increased during phase 2, when permeability is increased, exemplifies this kind of use.

Mechanism of recruitment. The mechanism by which recruitment occurs remains speculative, but likely results from the interaction of various mechanical forces. Opponents of the recruitment theory argue that the presence of collapsed capillaries that would "pop open" as a critical opening pressure is reached is too simplistic a representation of the problem, and they even question the presence of collapsed capillaries under normal physiologic conditions. It has appeared that some additional feature is needed, to provide understanding of the observed behavior. Such an additional feature is found in the transit of leucocytes through the lung. We would propose that recruitment could result not only from the complex interplay between vascular and alveolar pressures, but also from the distribution within and obstruction of capillaries by leucocytes, during their passage through the lung. The leucocytes have a larger diameter than some of the lung capillaries and are relatively nondeformable. Recent studies have shown that there is a 70% first pass extraction of leucocytes by the lungs, and that regional differences in leucocyte retention vary inversely with regional differences in blood flow (13,25,29). The retained pool of leucocytes in the lung is 2.5 times larger than the total circulating pool and has a turnover of 1.3%/sec (29); and the capillary leucocyte concentration is, relative to red cells, 50-100 times that in peripheral blood, at normal resting levels of flow. The major force controlling leucocyte retention in the lung seems to be the blood velocity, and with decreasing blood flow there is an increasing lung leucocytic uptake (14,37); increased leucocyte burden will result. In anesthetized dogs, microscopic studies estimated that one out of thirteen

capillaries is occupied by a leucocyte (25). It is plausible that such capillaries are temporarily blocked by the leucocytes and they may or may not be collapsed, depending on the intracapillary pressure distal to the leucocytes. With increasing blood velocity (as with exercise) the dispersion forces pushing the leucocytes will overcome the retention forces and "unplug" or recruit the capillaries, thus increasing the pulmonary vascular space. Thus the leucocytes may, in fact, be the missing and necessary link to vascular recruitment.

Conclusions. The data indicate that, in the transition from rest to low level exercise, water space and hence lung tissue are recruited, and that, at moderate levels of exercise, the totality of lung tissue becomes perfused. With increasing levels of flow above this, there is a further linear increase in the vascular volume without further tissue recruitment. This change is accompanied by increases in the endothelial norepinephrine permeability surface area product over the whole range of flows, and this increase can be inferred to reflect capillary recruitment.

The use of endothelial uptake processes to discern the nature of the in vivo physiological functioning of the lung during exercise represents a new approach to this area. The extension of this approach to other vascular surface markers, known to have greater pulmonary extractions, should yield more precision to estimates of permeability surface area products, for these materials. Labeled serotonin or labeled angiotensin converting enzyme substrates, which have higher pulmonary extractions than norepinephrine, seem appropriate candidates for this role, and it appears likely that further studies with substances such as these will cast more light on the physiological functioning of the lung during exercise.

ACKNOWLEDGEMENTS

This work was supported by grants from the Medical Research Council of Canada, the Quebec Heart Foundation, Les Fonds de la Recherche en Santé du Québec, and the Fast Foundation.

The authors thank Dr. C. Norman Gillis for his interest and help in planning these studies.

The authors also thank Hugues Gosselin and Nicole Poitras for their expert technical assistance, and Elizabeth Capon for typing the manuscript.

REFERENCES

1. BASSINGTHWAIGHTE, J. B., AND C. A. GORESKY. Modeling in the analysis of solute and water exchange in the microvasculature. In, *Handbook of Physiology - The Cardiovascular System:Microcirculation.* eds. E. M. Renkin and C. C. Michel, Amer. Physiol. Soc., Washington, DC, pp. 549-626, 1984.

2. BERGENTZ, S. E., L. LEANDOER, AND D. H. LEWIS. Induced red cell aggregation and the transit time of red cells and albumin through the lung. *Bibl. Anat.* 9: 304, 1967.

3. BOUVIER, M., L. FARLEY, AND J. DE CHAMPLAIN. Red cell catecholamine levels in normotensive and DOCA-salt hypertensive rats. *Am. J. Physiol.* 253 (Heart Circ. Physiol. 22): H270-H275, 1987.

4. Bradley, J. D., R. J. Roselli, R. E. Parker, and T. R. Harris. Effects of endotoxemia on the sheep lung microvascular membrane: a two-pore theory. *J. Appl. Physiol.* 64: 2675-2683, 1988.

5. BROWER, R., R. A. WISE, C. HASSAPOYANNES, B. BROMBERGER-BARNEA, AND S. PERMUTT. Effect of lung inflation on lung blood volume and pulmonary venous flow. *J. Appl. Physiol.* 58: 954-963, 1985.

6. BROWER, R., R. A. WISE, C. HASSAPOYANNES, M. HAUSKNECHT, AND S. PERMUTT. Longitudinal distribution of vascular compliance in the canine lung. *J. Appl. Physiol.* 61: 240-247, 1986.

7. J. D. CATRAVAS, AND C. N. GILLIS. Pulmonary clearance of [^{14}C]-5-hydroxytryptamine and [^{3}H]norepinephrine *in vivo*: effects of pretreatment with imipramine or cocaine. *J. Pharmacol. Exp. Ther.* 213: 120-127, 1980.

8. CERRETELLI, P., AND P. E. DI PRAMPERO. Gas exchange in exercise. In, *Handbook of Physiology - The Respiratory System IV*, eds. A. P. Fishman, L. E. Farhi, S. M. Tenney, and S. R. Geiger, Am. Physiol. Soc., Bethesda, Maryland, ch. 16, pp. 297-339, 1987.

9. CUA, W. O., R. A. GARR'CK, V. BOWER, AND F. P. CHINARD. Octanediol and $^{3}H^{1}HO$ as tracers for liquid water in the pulmonary circulation: blood flow effects. *FASEB Journal* 3: A1382, 1989.

10. CRONE, C. Permeability of capillaries in various organs as determined by the indicator diffusion method. *Acta Physiol. Scand.* 58: 292-305, 1963.

11. DAWSON, C. A., D. A. RICKABY, and J. H. Linehan. Location and mechanisms of pulmonary vascular volume changes. *J. Appl. Physiol.* 60: 402-409, 1986.

12. DOERSCHUK, C. M., M. F. ALLARD, B. A. MARTIN, A. MACKENZIE, A. P. AUTOR, AND J. C. HOGG. Marginated pool of neutrophils in rabbit lungs. *J. Appl. Physiol.* 63: 1806-1815, 1987.

13. FUNG, Y. C., AND R. T. YEN. A new theory of pulmonary blood flow in zone 2 condition. *J. Appl. Physiol.* 60: 1638-1650, 1986.

14. GILLIS, C. N., AND J. A. ROTH. The fate of biogenic monoamines in perfused rabbit lung. *Br. J. Pharmac.* 59: 585-590, 1977.

15. GLAZIER, J. B., J. M. B. HUGHES, J. E. MALONEY, AND J. B. WEST. Measurements of capillary dimensions and blood volume in rapidly frozen lungs. *J. Appl. Physiol.* 26:
65-76, 1969.

16. GOLDSTEIN, D. S., G. FEUERSTEIN, J. L. IZZO JR., I. J. KOPIN, AND H. R. KEISER. Validity and reliability of liquid chromatography with electrochemical detection for measuring plasma levels of norepinephrine and epinephrine in man. *Life Sci.* 28: 467-475, 1981.

17. GORESKY, C. A., R. F. P. CRONIN, AND B. E. WANGEL. Indicator dilution measurements of extravascular water in the lungs. *J. Clin. Invest.* 48: 487-501, 1969.

18. GORESKY, C. A., J. W. WARNICA, J. H. BURGESS, AND R. F. P. CRONIN. Measurement of the extravascular water space in the lungs: its dependence on alveolar blood flow. *Microvasc. Res.* 15: 149-167, 1978.

19. GORESKY, C. A., J. W. WARNICA, J. H. BURGESS, AND B. E. NADEAU. Effect of exercise on dilution estimates of extravascular lung water and on the carbon monoxide diffusing capacity in normal adults. *Circ. Res.* 37: 379-389, 1975.

20. HAMILTON, W. F., J. W. MOORE, J. M. KINSMAN, AND R. G. SPURLING. Simultaneous determination of the pulmonary and systemic circulation umes in man and of a figure related to cardiac output. *Am. J. Physiol.* 84: 338-344, 1928.

21. Harris, T. N., N. A. Pou, P. E. Wright, and G. R. Bernard. Norepinephrine uptake measures changes in lung capillary surface during E. coli endotoxemia in sheep. (abstract). *Fed. Proc.* 46: 1099, 1987.

22. JUNOD, A. F. 5-Hydroxytryptamine and other amines in the lungs. In, *Handbook of Physiology - The Respiratory System I*, eds. A. F. Fishman, and A. B. Fisher, Amer. Physiol. Soc., ch. 9, pp. 337-349, 1985.

23. LAWSON, W. H. Effect of drugs, hypoxia, and ventilatory maneuvers on lung diffusion for CO in man. *J. Appl. Physiol.* 32: 788-794, 1972.

24. MARTYN, B. A., B. R. WIGGS, S. LEE, AND J. C. HOGG. Regional differences in neutrophil margination in dog lungs. *J. Appl. Physiol.* 63: 1253-1261, 1987.

25. MILLER, J. M., AND R. L. JOHNSON JR. Effect of lung inflation on pulmonary diffusing capacity at rest and exercise. *J. Clin. Invest.* 45: 493-500, 1966.

26. NICHOLAS, T. E., J. M. STRUM, L. S. ANGELO, AND A. F. JUNOD. Site and mechanism of uptake of ^{3}H-/-norepinephrine by isolated perfused rat lungs. *Circ. Res.* 35: 670-680, 1974.

27. PERONNET, L. BELIVEAU, G. BOUDREAU, F. TRUDEAU, G. BRISSON, AND R. NADEAU. Regional plasma catecholamine removal and release at rest and exercise in dogs. *Am. J. Physiol.* 254 (Regulatory Integrative Comp. Physiol. 23): R663-R672, 1988.

28. RICKABY, D. A., C. A. DAWSON, J. H. LINEHAN, AND T. A. BRONIKOWSKI. Alveolar vessel behavior in the zone 2 lung inferred from indicator-dilution data. *J. Appl. Physiol.* 63: 778-784, 1987.

29. RUSHMER, R. F., O. SMITH, AND D. FRANKLIN. Mechanism of cardiac control in exercise. *Circ. Res.* 7: 602-627, 1959.

30. THOMMASEN, H. V., B. A. MARTYN, B. R. WIGGS, M. QUIROCA, E. M. BAILE, AND J. C. HOGG. Effect of pulmonary blood flow on leucocyte uptake and release by dog lung. *J. Appl Physiol.*(Respirat. Environ. and Exercise Physiol.) 56: 966-974, 1984.

31. TOIVONEN, H. J., AND J. D. CATRAVAS. Effects of alveolar pressure on lung antiotensin-converting enzyme function in vivo. *J. Appl. Physiol.* 61: 1041-1050, 1986.

32. WARRELL, D. A., J. W. EVANS, R. O. CLARKE, G. P. KINGABY, AND J. B. WEST. Pattern of filling in the pulmonary capillary bed. *J. Appl. Physiol.* 32: 346-356, 1972.

33. WEST, J. B., AND C. T. DOLLERY. Distribution of blood flow and ventilation-perfusion ratio in the lung measured with radioactive CO_2. *J. Appl. Physiol.* 15: 405-410, 1960.

34. Zelter, M., A. Lipavsky, J. M. hoeffel, and J. F. Murray. Effect of lung injuries on [^{14}C]urea permeability-surface area product in dogs. *J. Appl. Physiol.: resp. Environ. Exercise Physiol.* 56: 1512-1520, 1984.

CHAPTER 3

Pulmonary angiotensin-converting enzyme substrate hydrolysis during exercise

ABSTRACT

We examined exercise-induced changes in indicator-dilution estimates of the angiotensin-converting enzyme first order kinetic parameter A_{max}/K_m, which under stable enzymatic conditions will vary with the pulmonary vascular surface area accessible to vascular substrate, the extravascular lung water (an index of the proportion of lung tissue perfused), and the central blood volume (from pulmonary trunk to aorta). Experiments were performed in 10 mongrel dogs at rest and through two increasing levels of treadmill exercise, with the use of two vascular space tracers (labeled erythrocytes and albumin), a water space tracer ([14C]1,8-octanediol), and a vascular endothelium surface area marker, Benzoyl-Phe-Gly-Pro ([^{3}H]BPGP), which is a pharmacologically inactive angiotensin-converting enzyme substrate. The exercise-induced increase in cardiac output was accompanied by a linear increase in central blood volume; and dilutional extravascular lung water rapidly increased to an asymptotic proportion close to 100% of post-mortem vascular lung water. There was an average 55% [^{3}H]BPGP hydrolysis, which did not vary with flow; and the computed A_{max}/K_m increased linearly with exercise. We conclude that exercise results in complete lung tissue recruitment and increases the pulmonary vascular surface area available for BPGP hydrolysis linearly with flow, so that pulmonary vascular recruitment continues after full tissue recruitment.

INTRODUCTION

An area of continuous exploration in pulmonary physiology is the appraisal of the relative roles of vascular distensibility and vascular recruitment in the increase in pulmonary vascular volume which occurs with increase in blood flow, particularly with exercise (25). A complex interplay between pulmonary vascular pressures, alveolar pressure and other factors likely not yet defined results in both gravity-dependent (42,43) and independent (20) heterogeneities in pulmonary blood flow. With increase in blood flow, there is a reduction in the gravity-dependent heterogeneity of perfusion, the upper parts of the lung becoming better perfused (20). This could be the result of either vascular distension (increase in the diameter of already perfused vessels) or recruitment (perfusion of new vessels) or a combination of both.

Accumulating evidence indicates that capillary recruitment, at least in part, must contribute to the process. Morphometric studies of zone 2 conditions have shown local areas of capillary collapse as the alveolar pressure-venous pressure difference is increased (13,41). Increase in the surface area of the blood-gas interface by capillary recruitment has been adduced from the increase in carbon monoxide diffusing capacity with exercise, when tissue space has been completely recruited (6). In vivo microscopic observation of subpleural vessels under zone 2 conditions (21) has shown capillary recruitment with hypoxia and fluid loading, maneuvers which, like exercise, result in increase in pulmonary arterial pressure. When the labeled microsphere technique is used to explore changes in flow distribution with changes in cardiac output, blood flow appears to change regionally in proportion to cardiac output except in the upper regions of the lung (zone 1) where there is an evident recruitment-derecruitment phenomenon (20).

Angiotensin-converting enzyme (ACE) is located on the luminal surface of the pulmonary vascular endothelium (38). ACE activity therefore will reflect the interaction between plasma and the endothelial surface in the capillaries perfused, and the total activity will be expected to be closely influenced by the vascular surface area available for

interaction with vascular substrate. A close correlation between total activity available for processing plasma substrate, calculated capillary endothelial cell surface area, and carbon monoxide diffusing capacity has been demonstrated by Pitt et al. during postnatal development in lambs (29,30); and the changes in ACE activity with lung injury (27) and increases in alveolar pressure (39) have been inferred to reflect changes in perfused microvascular surface area. The foregoing suggest that an *in vivo* appraisal of pulmonary ACE activity during exercise could be used to assess change in the perfused pulmonary capillary surface area with exercise.

In the present study we have therefore used the multiple indicator dilution studies with tritiated benzoyl-phenylalanyl-glycyl-proline ([^{3}H]BPGP), a pharmacologically inactive ACE substrate, to probe pulmonary ACE activity and provide information concerning changes in the perfused pulmonary microvascular surface with exercise. We conducted experiments in 10 mongrel dogs, at rest and through two successive levels of exercise, and measured the first order kinetic parameter corresponding to the ratio of a normalized maximal enzymic conversion rate and the K_m or Michaelis constant for the activity of angiotensin converting enzyme on [^{3}H]BPGP. This ratio is the equivalent of a unidirectional permeability surface area product for a diffusible tracer and is thus expected to be proportional to the perfused endothelial luminal surface area (39). We have, simultaneously, estimated the extravascular lung water accessible from the vascular space, to provide an index of the amount of tissue perfused, and have compared these dilution estimates with postmortem gravimetric measurements of the extravascular lung water. The water space tracer used was [^{14}C]1,8-octanediol, which has an identical transit time to that of labeled water (7). In addition, vascular space tracers for the cellular and plasma phases of blood, [^{51}Cr]erythrocytes and [^{125}I]albumin, were injected simultaneously with the other tracers. With this approach, it became possible to measure simultaneously the effect of the increase in cardiac output with exercise on the central blood volume (measured from the pulmonary artery to the root of the aorta), the proportion of extravascular lung water that is

accessible from the pulmonary vascular space (which reflects the proportion of lung tissue being perfused), and the fractional hydrolysis and calculated kinetic rate constant for [^{3}H]BPGP (which should be related to the perfused pulmonary capillary surface area). The theoretical basis for the analysis of the surface-mediated hydrolytic process was examined, as part of the process underlying the analysis of the data.

MATERIALS AND METHODS

Animal preparation. Eight healthy mongrel dogs (mean weight 23.5 ± 5.5 [SD] kg) were studied in the awake state. After being trained to perform on the treadmill, they were prepared under general anesthesia for later studies. Induction was carried out by the use of 6 mg/kg pentobarbital (Abbott Laboratories, Montreal, Canada), and anesthesia was maintained with halothane (Ayerst Laboratories, Montreal, Canada) while the animal was mechanically ventilated by use of a respiratory pump (Harvard Apparatus, Milis, MS, U.S.A.) with a gas mixture containing oxygen and nitrous oxide. A right paramedial cervical incision was performed and the right internal jugular vein as well as the right internal carotid artery were dissected and isolate Permanent cannulas (modified stomach tubes, Argyle, St. Louis, MO, U.S.A.) were then erted through a small incision in both vessels and, under fluoroscopic guidance with the help of vascular contrast medium (MD-76, Mallinckrodt, Pointe Claire, QC, Canada), the tip of the arterial cannula was positioned 2 cm above the aortic valve, while the venous cannula was secured in the right atrium. Subcutaneous tunnels were then constructed from the incision to the back of the neck, where two small incisions permitted the exit of the cannulae. The dogs were allowed a minimum of one week to recover from surgery, while patency of the cannulae was assessed every day. To prevent clotting and thromboembolism, the animals received subcutaneous injections of heparin (Leo Laboratories, Pickering, Ontario, Canada), 8000 units twice a day, and the cannulae were flushed with heparin every day.

On the day of the experiment, the animal was positioned on the treadmill and a balloon tipped catheter (Edwards Laboratories, Santa Anna, CA, U.S.A.) was introduced through the venous cannula and advanced to the main pulmonary artery, its final position being guided by pressure tracings (Gould Recorder 2400S, Cleveland, OH, U.S.A.) and fluoroscopic guidance. The arterial cannula was connected to a peristaltic pump (Cole Palmer, Chicago, IL, U.S.A.), which in turn led to a sample collector containing borosilicate tubes. A first multiple indicator dilution study was then carried out. With the dog at rest, a radioactive bolus containing the tracers to be studied was introduced into the pulmonary artery catheter and rapidly flushed into the circulation with 5 ml of blood. Simultaneously, the sampling pump (2 ml/s) and collecting rack (2 tubes/s) were started, and samples were collected over a period of 2ɔ seconds. The procedure was then repeated, for each of the two studies carried out during exercise. The treadmill was started, with the dog moving at a speed of two miles per hour and every 3 minutes the slope was increased by 10°. The experimental run was repeated at the completion of six minutes (Level A), and again at 15 minutes (Level B) of exercise. Two pilot studies were performed using anesthetized animals and the data from these were included in the analysis of this study. In these, two healthy mongrel dogs were studied and one dilution experiment was carried out in each animal. Anesthesia was induced with pentobarbital (30 mg/kg). Temporary catheters were inserted as for the awake animals and the experiment was performed with the animal in the supine position. The animal was manually ventilated for 30 seconds every 5 minutes in order to prevent pulmonary atelectasis. The data from these experiments were included in the illustrations, but were not analyzed with the runs done in the resting state.

Injection mixture. Since there is a small amount of angiotensin converting enzyme activity in plasma and, potentially, associated with platelets, it was necessary to make up an injection mixture lacking these. The following procedure was devised. From each animal, 15 ml of blood was withdrawn from the arterial cannula and layered on top of 35 ml of Percoll in a centrifuge tube. The isotonic Percoll had previously been adjusted to a specific

gravity (S.G.) of 1.07 g/L. The tube was then centrifuged at 3000 g for 20 minutes. This procedure resulted in separation of the erythrocytes (SG 1.09 g/L) from the other components of whole blood (plasma, white cells, and platelets) which have a lower specific gravity than Percoll. The plasma and platelets were discarded and the erythrocytes were labeled as previously described (18). The Percoll separation did not result in any damage to the erythrocytes as assessed by light microscopy. The Percoll separation and the subsequent washings of the erythrocytes (on three occasions) during the labeling procedure resulted in a 'plasma free' injection mixture. We prepared 8 ml of injection mixture for each animal. It contained approximately 20 μCi of [^{51}Cr]-labeled erythrocytes and 60 μCi of [^{125}I]albumin (NEN, Boston, MA, U.S.A.), two tracers that remain in the intravascular space and do not cross the capillary barrier significantly during a single passage time. Additionally, 100 μCi of [^{14}C]1,8-octanediol (2.94 mCi/mmol, NEN, Boston, MA, U.S.A.) was added to serve as a water space tracer (its mean transit time is identical to that of labeled water [7]). The octanediol, because of its essentially nonvolatile nature, is virtually excluded from the alveolar space. Cua et al (7) have interpreted differences in the outflow curves for labeled water and octanediol to indicate the presence of a diffusional shunt for labeled water through the vapor phase in the alveolar space (the mass of the vapor phase is, of course, tiny in comparison with tissue water), leading to a small early precession and delayed downslope of the labeled water with respect to the octanediol. The labeled erythrocytes, the [^{125}I]-albumin, and the [^{14}C]1,8-octanediol were then added to a beaker containing 25 nmol of dried [^{3}H]BPGP (500 μCi; 20 Ci/mmol) and the injection mixture was adjusted to match the venous hematocrit of the dog, and was separated into three parts, for later injection. Aliquots of 50 μl of the injection mixture were diluted with 950 μl of blood, to be counted later and serve as a standard of reference for the determination of the quantity of tracers injected. The radioactivity retained in the input venous cannula was determined after each bolus injection by aspirating the cannula and assaying an aliquot, and this was subtracted from the total injected.

Sample collection and preparation. The sample collector was filled with ice, to cool the collecting tubes and samples, and each collecting tube contained 1 ml of stop solution (0.15 M NaCl, 3 x 10^{-3} M Na_2EDTA, 1 x 10^{-3} M 1,10-phenanthroline and pH adjusted to 6.8-8 by 1.0 N NaOH) which blocked the minor amount of plasma angiotensin-converting enzyme activity present in the outflow samples. Immediately after each experiment, a 200 µl aliquot was taken from each sample and placed in a new tube for processing; 300 µl of normal NaCl and 300µl of 25% TCA were added, and the tubes were centrifuged at 1000g for 10 minutes. The tubes with the precipitated pellets were then assayed for gamma activity. The remaining sample (blood + stop solution) was then centrifuged (1000 g x 15 min). A 200 µl aliquot of the supernatant from each sample was then added to a 20 ml scintillation vial to which 1 ml of 0.1 N HCl and 1 ml of toluene-Omnifluor (4 g Omnifluor [Dupont-New England Nuclear, Boston, Mass.] per litre reagent grade toluene) were added. The vials were capped and inverted 20 times before being assayed for beta activity. The contents resolve themselves into two phases, the toluene phase floating on top of the water phase. At the acid pH, the organophilic radioactive product is extracted into the counting phase, the organic solvent containing the scintillants, while the unhydrolyzed substrate remains in the aqueous or "non-counting" phase. The vials were then reopened and 17 ml of aqueous scintillation cocktail was added (Ready Safe, Beckman); they were then vigorously shaken by hand before being counted for a second time. A single phase results. The tritium activity assayed is now that corresponding to the total.

Gravimetric measurements. At the conclusion of each experiment, the animal was sacrificed and the lungs were removed together with the trachea, by resecting it two rings below the cricoid cartilage. The tracheobronchial tree is vascularized by the bronchial artery, and its water space is consequently not accessible to tracers entering the pulmonary circulation. To allow for this, we carried out *in vitro* measurements of the extravascular lung water, excluding the extrapulmonary bronchial tree. The extrapulmonary bronchial tree was dissected as closely as possible to the lung parenchyma and was removed. The

lung parenchyma and the extrapulmonary bronchial tree were then weighed separately. The parenchyma was homogenized in a blender, with the addition of a known quantity (usually 500 ml) of water, and the total volume of the homogenate was noted. A 1 ml aliquot of homogenate was removed and retained. [^{51}Cr]Erythrocytes were counted in this sample as well as in 1 ml of mixed venous blood drawn just prior to the sacrifice. A sample of 10 ml of homogenate and the removed extrapulmonary bronchial tree were weighed and dried separately and the dry weights were determined.

The gravimetric extravascular lung water was then estimated. The problem which presents is how to correct values obtained from the lung tissue, for their contained vascular content. At the time of removal, after three experimental runs, the labeled red cells will still be confined to the circulation, whereas some of the labeled albumin will have left the circulation and will be in the interstitial space. We therefore were able to use only the labeled red cells as a guide to the vascular volume. The vascular volume (VLV) trapped in the lung at the time of removal, approached from this point of view, is given by the following equation,

$$VLV = H_{vol}(H_{cpm}/B_{cpm}) \quad \ldots(1)$$

where H_{cpm} and B_{cpm} represent the ^{51}Cr activity in a 1 ml aliquot of homogenate and blood, and H_{vol} is the homogenate volume, in ml. The water content of plasma is 0.94 ml/ml, and that of red cells is 0.70 ml/ml. Thus, if we assume that the hematocrit of the pulmonary vessels is equal to the venous hematocrit (the assumption is not quite correct, but will be used, for now), we can calculate the trapped vascular lung water (VLW) in ml from the trapped vascular volume and the hematocrit (Hct) by use of the following relation,

$$VLW = VLV\,[0.70\,Hct + 0.94\,(1 - Hct)] \quad \ldots(2)$$

The weight of the trapped blood can also be calculated from the specific gravity of plasma (1.027 g/ml) and that of erythrocytes (1.090 g/ml).

The dry lung weight excluding the extrapulmonary bronchial tree (Wt_{dry}, in g) was then calculated from the total volume of the homogenate and the dry weight (Al_{dry} in g), of the 10 ml aliquot, by use of the relation,

$$Wt_{dry} = H_{vol} (Al_{dry}/10\,ml) \quad ...(3)$$

From the wet weight of the lung without the extraparenchymal bronchial tree, Wt, and the corresponding dry lung weight, Wt_{dry}, the total lung water, TLW, can be estimated from the relation

$$TLW = Wt - Wt_{dry} \quad ...(4)$$

The corresponding gravimetric estimate of extravascular lung water ($EVLW_g$) is

$$EVLW_g = TLW - VLW \quad ...(5)$$

Use of tracer curves to estimate flow, mean transit times, and central blood volume.

In order to provide a basis for comparison among the groups, the total amount of each material injected was defined as 1 unit. The outflow concentration of each tracer is then automatically defined as its outflow fractional recovery per ml of blood; the relative behaviour of the tracers can then be appraised when the fractional recovery values are plotted as a function of time. To correct for recirculation, the dilution curves were plotted on a semilogarithmic scale, and the downslopes were extrapolated linearly, after the classical manner of Hamilton (11). Blood flow (F_b) was then calculated by use of the conservation relation,

$$F_b = 1 / \int_0^{\infty} C(t)\, dt \quad ...(6)$$

where C(t) is an outflow fractional recovery-time curve, and the integral in the denominator on the right hand side of the equation is the area under the fractional recovery curve for any tracer completely recovered at the outflow. We used the area under the fractional recovery curve of the [^{51}Cr]erythrocytes, for this calculation.

The mean transit time for each tracer was calculated by use of the relation,

$$\text{Mean transit time} = \left(\frac{\int_0^\infty t\, C(t)\, dt}{\int_0^\infty C(t)\, dt} \right) - \bar{t}_{cath} \qquad ...(7)$$

where $\bar{t}_{cath}$ is the mean transit time through the catheters of the injection and collection system.

The central blood volume (CBV) was calculated as the sum of the spaces accessible to the two vascular tracers, labeled red cells and albumin,

$$CBV = F_b\, Hct\, \bar{t}_{RBC} + F_b(1-Hct)\, \bar{t}_{Alb} \qquad . (8)$$

where $\bar{t}_{RBC}$ and $\bar{t}_{Alb}$ are the transit times of labeled red cells and labeled albumin.

Dilutional estimates of extravascular water space. The volume which is ordinarily measured is a water volume. The flow used to measure it must therefore be a water flow, and the vascular reference must be a vascular water reference (11,18). If we define F_b, F_r, and F_p as the flows of blood, red blood cells and plasma respectively, F_w as the flow of water, and f_r and f_p as fractional volumes of water in red blood cells and plasma (ml water/ml red cells or plasma), then

$$F_r = Hct\, F_b \qquad ...(9)$$

$$F_p = (1-Hct)\, F_b, \text{ and} \qquad ...(10)$$

$$F_w = F_r f_r + F_p f_p \qquad ...(11)$$

The last equation provides the appropriate relation for the calculation of blood water flow.

Similarly, the reference vascular transit time appropriate for calculating a water volume is the weighted transit time which the water would have if it did not cross the capillary barrier, $\bar{t}_{w\,ref}$. It is calculated by use of the expression,

$$\bar{t}_{w\,ref} = \frac{F_r f_r \bar{t}_{RBC}}{F_w} + \frac{F_p f_p \bar{t}_{alb}}{F_w} \qquad ...(12)$$

The extravascular lung water, calculated from the indicator dilutional data, then becomes,

$$EVLW = F_w\, (\bar{t}_{oct} - \bar{t}_{w\,ref}) \qquad ...(13)$$

where $\bar{t}_{oct}$ is the mean transit time of octanediol, and this is being used as a guide for the space of distribution of tissue water. The calculated EVLW value is that which usually has been calculated from indicator dilution data (11,18,19); it provides a quantitative value for the accessible extravascular lung water volume.

In the present study, a part of the object of the study is to compare the tissue water accessible to tracer to that determined gravimetrically, in the same animals, and to both gain insight into the manner in which tissue space becomes accessible as the pulmonary blood flow increases, and the proportion of the gravimetric space which is accessible to tracer at maximal flows. In order to carry out the comparison, the calculated basis for the comparison needs to be the same. Since, in developing the methodology for the gravimetric estimates of lung water, we were able to use only the labeled red cell component of the vascular space as the basis for the calculation of the included vascular volume, we need, for the purposes of comparing the dilutional estimate to this, to correct the calculated gravimetric extravascular lung water estimate by adding to it the water content of the extra plasma space not seen by the red blood cell tracer. Red blood cell-albumin label separation is expected to occur primarily in the small vessels, especially the capillaries (1), rather than in the large vessels, and to result in different transit times for the labeled red cells and albumin. This separation was used previously by Goresky et al (18) to quantitate the extra plasma space (EPS) accessible to labeled albumin, in excess of that available to the labeled red blood cells, as follows,

$$EPS = F_b\,(1-Hct)\,(\bar{t}_{alb} - \bar{t}_{RBC}) \qquad ...(14)$$

The extra plasma space was found (18) to increase linearly with blood flow, and to have a small ordinate intercept, EPS_{int}, on least squares linear regression. This value represents the zero flow extra plasma space. Its water content, 0.94 EPS_{int}, represents the probable error in our calculation of the gravimetric extravascular lung water content, attributable to plasma trapped in the lungs in excess of the labeled red cells. We have

therefore corrected our gravimetric extravascular lung water estimate, $EVLW_g$, by subtracting from it 0.94 EPS_{int}.

Angiotensin-converting enzyme kinetics. Samples were analyzed for [^{3}H]BPGP and the labeled hydrolysis product [^{3}H]BP by use of the toluene extraction procedure outlined above, as originally described by Ryan (37). The amount of metabolite ([^{3}H]BP) in each sample was determined by use of the relation,

$$[^3H]BP = [DPM_E - (fr_s \cdot DPM_T)]/(fr_p - fr_s) \quad ...(15)$$

where DPM represents calculated [^{3}H]dpm values, E represents values from the toluene extraction while T represents the total values, fr_p represents the fractional extraction of pure product ([^{3}H]BP) into the counting phase (toluene) of the cocktail during the differential extraction procedure, and fr_s represents the fractional extraction of pure substrate ([^{3}H]BPGP) into the toluene phase. The parameters fr_p and fr_s were determined from two separate *in vitro* experiments, on the stock solution of [^{3}H]BPGP used for the experiments in this study, and on hydrolyzed [^{3}H]BP derived from this. Average values of 0.61 ± 0.016 (SD) for fr_p and 0.068 ± 0.004 (SD) for fr_s were obtained. At the end of each experiment, the quality of the injection mixture (that is the lack of angiotensin converting enzyme activity in the prepared mixture) was assessed by taking an aliquot of the remaining injectate and measuring the ratio of the [^{3}H] DPM extracted into the toluene phase to the total [^{3}H] DPM. The mean value was 0.057 ± 0.01. This value was not different from the average value for fr_s (0.068), proving that no detectable hydrolysis of [^{3}H]BPGP had occurred in the injection mixture, prior to its use in the experiment.

The instantaneous proportional BPGP metabolism (M_i) in each sample was calculated by use of the relation,

$$M_i = [^3H]BP/([^3H]BPGP + [^3H]BP) \quad ...(16)$$

Note that the denominator represents the total [^{3}H] DPM counted in the cocktail. The cumulative fraction of BPGP metabolized by the lung during passage of the bolus was calculated as

$$M = \int_0^T [^3H]BP(t)\,dt \Big/ \int_0^T \{[^3H]BP(t) + [^3H]BPGP(t)\}\,dt \qquad ...(17)$$

where T represents the time at which recirculation occurs.

In Appendix I, we have developed, at a theoretical level, the expected description for the kinetics of enzyme catalyzed formation of [^{3}H]BP from [^{3}H]BPGP by the lung, in a form corresponding to the experimental observations. The relation derived in Appendix I (equation [A27]) to fit the data is

$$\ln\left[\frac{C_{ref}(t)}{C_{BPGP}(t)}\right] = \frac{A_{max}}{K_m F_p} \qquad ...(18)$$

where A_{max} is the product of the total enzymic activity in the part of the capillary bed which is perfused, and the rate constant for product formation k_{cat} (5), K_m is the Michaelis constant for the angiotensin converting enzyme, and F_p is the plasma flow rate.

This equation can, alternatively, be expressed as

$$\frac{A_{max}}{K_m F_p} = \ln\left[\frac{1}{1-M}\right] \qquad ...(19)$$

This is the most convenient form for calculating the parameter on the left hand side of the equation. It corresponds to that utilized by Toivonin and Catravas (39).

Now since, experimentally, F_p is independently determined, from the data, we can separate the ratio A_{max}/K_m, and calculate it by use of the expression

$$\frac{A_{max}}{K_m} = F_p \ln\left[\frac{1}{1-M}\right]$$
$$= -F_p \ln(1-E) \qquad ...(20)$$

where E corresponds to an instantaneous extraction, but in this case is the fractional formation of product within the vascular space. The parameter A_{max}/K_m provides a measure of the ratio of the reacting enzymic mass to the K_m for the substrate. With the data at hand, it is not separable into its components. Equation (20) indicates that it is, in form, analogous to a permeability surface area product. Its changes can therefore be regarded in this sense.

RESULTS

Dilution curves. Typical sets of dilution curves obtained from the three dilution studies carried out in one of the animals (exp. 9) are shown in Figures 1, 2 and 3. To demonstrate clearly the impact of increasing blood flow on the areas under the curves and their transit times, and on recirculation of the tracers, a rectilinear ordinate is utilized, together with an identical abscissal time scale for all three studies. Figure 1 depicts the relationship between the vascular tracers, [^{51}Cr]erythrocytes and [^{125}I]albumin, and the water space tracer [^{14}C]1,8-octanediol. With the change from rest to first level and then second level of exercise, the appearance time of the tracers is seen to decrease, the areas under the reference dilution curves become smaller, and recirculation occurs earlier. The recirculation profiles of the vascular tracers are more evident in the lower two panels. As expected, there is reduced recirculation of [^{14}C]1,8-octanediol, since this water space tracer freely diffuses into peripheral tissue from systemic capillaries. The experiment carried out at rest exemplifies the relationship between the tracer outflow curves. The outflow fraction per ml for the erythrocytes is highest in the first samples; it reaches the highest and earliest peak, and decays most quickly. The values for albumin are slightly lower on the upslope; its peak is slightly lower and later, and its downslope decays slightly less quickly. The values for the labeled octanediol are most displaced from those for the red blood cells; the upslope of the curve rises less quickly, the peak is delayed and located approximately on the downslope of the red blood cell curve, and the downslope of the curve falls less precipitously.

The relationship between the plasma reference [^{125}I]albumin, the total [^{3}H] in the lung effluent ([^{3}H]BPGP + [^{3}H]BP) and unmodified [^{3}H]BPGP is shown in Figure 2. The average recovery of total [^{3}H]BPGP + [^{3}H]BP with respect to the vascular plasma [^{125}I]albumin reference, 0.994 ± 0.049 (SD), was complete, and there was no systematic difference between the mean transit times of [^{125}I]albumin and total [^{3}H] at any of the three levels of cardiac output (Table 2). The cumulative fractional hydrolysis fraction (M) for

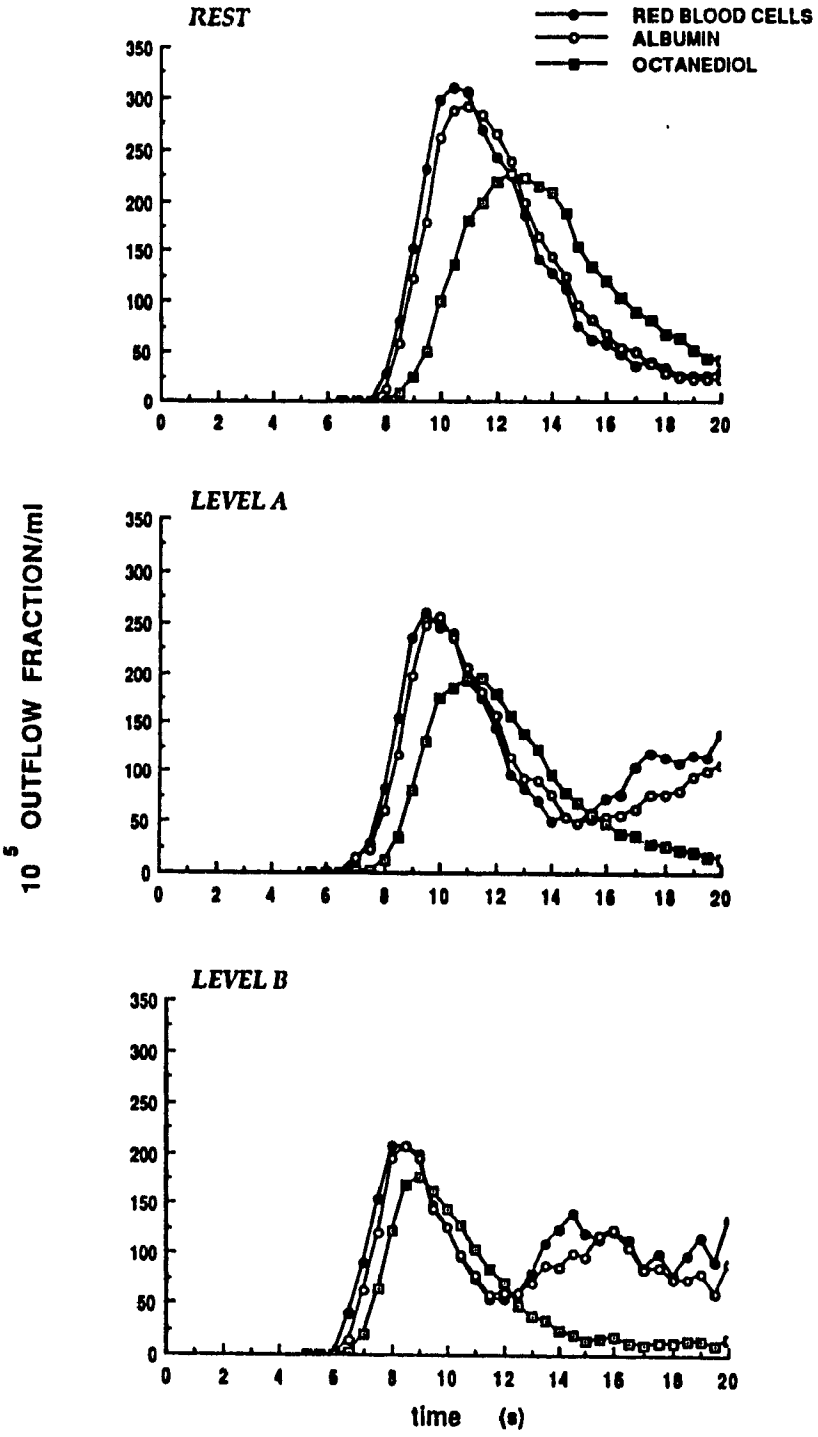

FIG. 1. Typical set of dilution curves obtained from a dog at rest and at two successive levels of exercise (levels A and B). The time scale on the abscissa was kept identical for 3 graphs to show the effect of increasing blood flow on the general appearance of the curves.

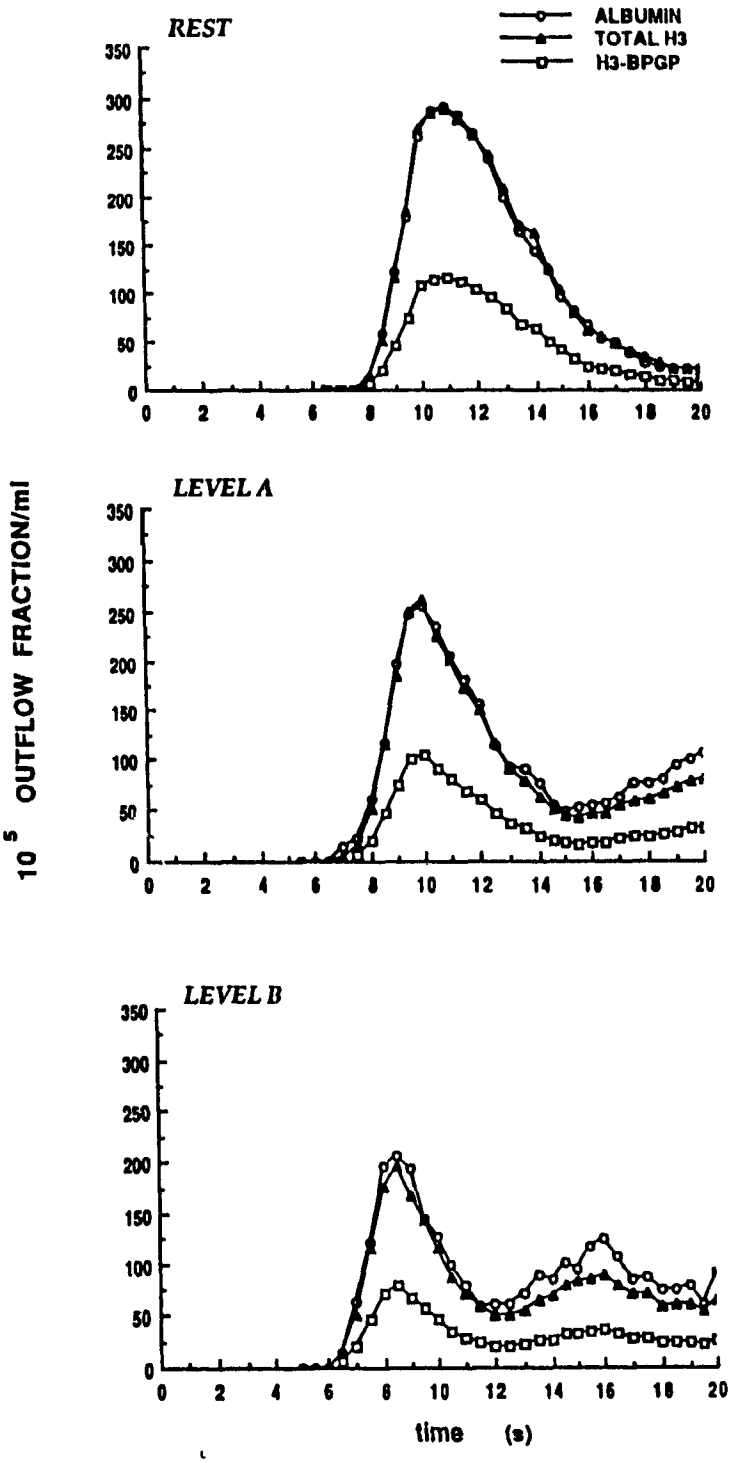

FIG. 2 Relationship between the outflow profile of the plasma reference [^{125}I]albumin, the total [^{3}H] in the lung effluent ([^{3}H]BPGP) and unmodified [^{3}H]BPGP, from the data set shown in Fig. 1. Total [^{3}H] recovery was complete and the proportional [^{3}H]BPGP hydrolysis averaged 55% and did not vary from rest to level A or B of exercise.

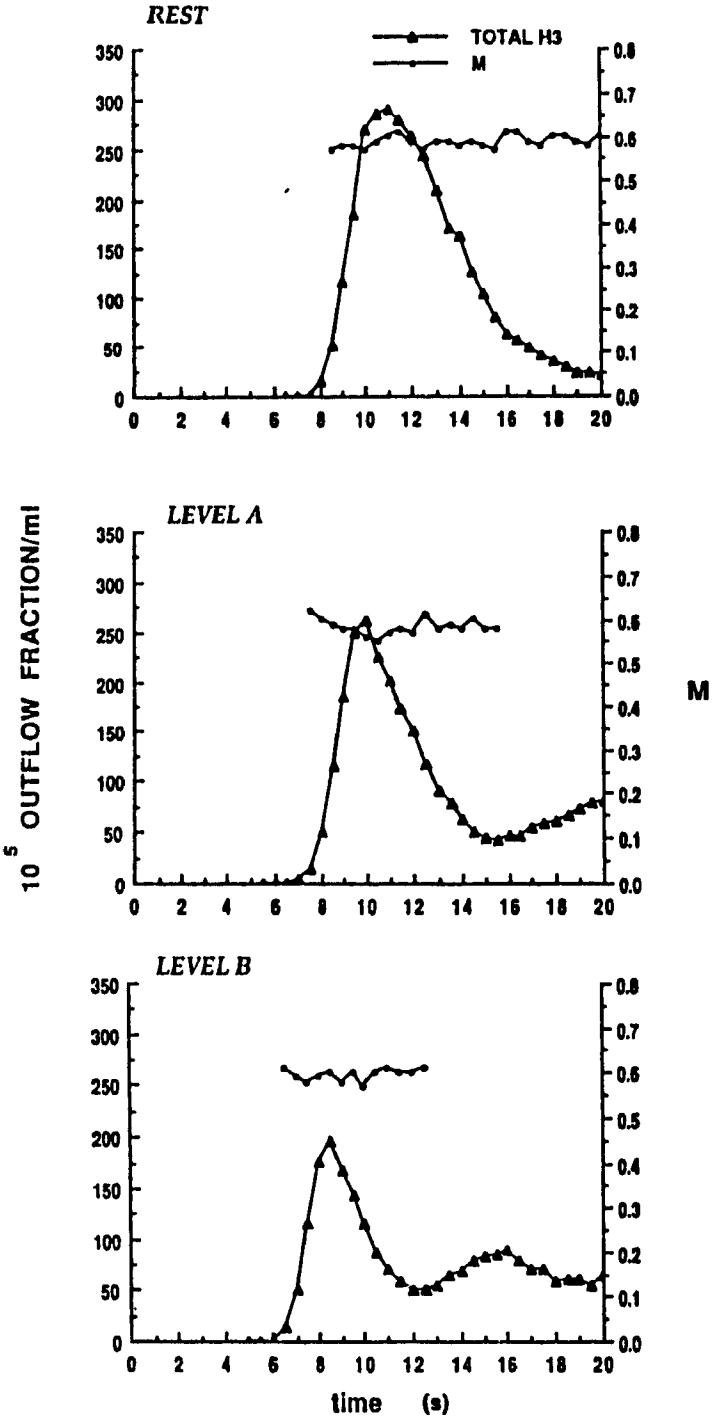

FIG. 3 Outflow profile for instantaneous [^{3}H]BPGP metabolism from one set of experiments at rest, and at two successive levels of exercise (level A and B). Total [^{3}H] recovery curves are shown for purposes of reference. The instantaneous metabolism curve, as a function of time, did not show systematic variation. Percentage hydrolysis did not vary with exercise (cf. Table 2).

TABLE 1. *Numerical values of individual parameters calculated from the indicator dilution curves in awake dogs, at rest, and at two increasing levels of exercise.*

Exp. no.	Exercise level	Body weight kg	Lung weight g	Blood flow ml/s	$\bar{t}_{rbc}$ s	$\bar{t}_{alb}$ s	$\bar{t}_{oct}$ s	$\bar{t}_{^3H}$ s	EVLW ml	M	$\ln\left(\frac{1}{1-M}\right)$	A_{max}/K_m ml/s
1-A*	anesth.	34	262	79	7.19	7.36	8.56	7.46	99	0.55	0.80	39
2-A*	anesth.	24	227	47	7.10	7.74	9.00	7.65	70	0.49	0.67	18
3-A	rest	24	217	61	6.45	6.97	8.21	6.92	87	0.50	0.69	23
3-B	A			134	3.39	3.70	4.41	3.73	110	0.59	0.89	66
3-C	B			210	3.51	3.80	4.30	4.11	127	0.59	0.89	104
4-A	rest	32	219	72	3.58	3.90	4.68	3.97	63	0.58	0.87	39
4-B	A			121	3.16	3.48	4.24	3.43	103	0.55	0.80	31
4-C	B			173	3.06	3.50	4.00	3.24	109	0.55	0.80	87
5-A	rest	24	217	41	5.42	5.86	7.78	5.86	84	0.56	0.82	20
5-B	A			67	4.89	5.18	6.59	5.22	100	0.52	0.73	29
5-C	B			63	4.89	5.40	6.70	6.20	92	0.54	0.78	29
6-A	rest	23	179	83	4.19	4.55	5.09	4.59	56	0.54	0.78	35
6-B	A			104	3.66	3.94	4.60	3.71	79	0.50	0.69	40
6-C	B			153	3.37	3.60	4.00	3.70	74	0.46	0.62	52
7-A	rest	16	124	54	4.61	4.84	5.60	4.82	45	0.55	0.80	25
7-B	A			66	3.21	3.48	4.09	3.47	46	0.59	0.89	34
7-C	B			109	2.87	3.10	3.50	3.05	52	0.60	0.92	58

Table 1 (contd.)

8-A	rest	19	154	63	4.93	5.13	6.18	5.27	71	0.59	0.89	29
8-B	A			92	3.15	3.41	4.13	3.43	75	0.58	0.87	41
8-C	B			160	2.69	2.75	3.20	2.56	76	0.56	0.82	68
9-A	rest	19	175	60	4.26	4.40	5.06	4.53	42	0.48	0.65	23
9-B	A			77	4.18	4.29	4.80	4.24	42	0.51	0.71	33
9-C	B			119	3.38	3.75	4.46	3.89	98	0.46	0.62	44
10-A	rest	20	233	62	7.05	7.47	8.57	7.43	76	0.58	0.87	33
	A			82	6.09	6.42	7.57	6.40	102	0.58	0.87	44
	B			128	3.93	4.39	5.19	4.60	120	0.61	0.94	75

$\bar{t}_{rbc}$, $\bar{t}_{alb}$, $\bar{t}_{oct}$, $\bar{t}_{^3H}$ and $\bar{t}_{wref}$ represent the mean transit times of the red blood cells, albumin, octanediol, total ^3H activity, and the intravascular water reference respectively. M = Fractional hydrolysis of BPGP. Lung weight = total wet lung weight including the extrapulmonary bronchial tree. *Experiments 1 and 2 were done in anesthetized animals.

[^{3}H]BPGP did not vary significantly from resting conditions through the two successive levels of exercise (Table 2). The outflow profile for instantaneous metabolism of [^{3}H]BPGP in the example data set is shown in Figure 3. The outflow curve of total [^{3}H] is included, to provide a time reference. At all three levels of cardiac output, M_i appears to be remarkably constant during the passage time of the bolus, and we observe that there is no substantial change in M_i between the resting state and the two successive levels of exercise. The numerical parameters derived from the individual multiple indicator dilution experiments are assembled in Table 1. The relationship between the mean transit times of the total [^{3}H] (here $\bar{t}_{3H} = \bar{t}_{3HBP+3HBPGP}$) and those of albumin ($\bar{t}_{Alb}$) is presented in Figure 4, for the rest and exercise data (data from the two anesthetized animals were excluded). There is a nice linear relation between the two, following the best fit mean squares regression line,

$$\bar{t}_{3H} = 1.03\bar{t}_{Alb} - 0.003 \; (r = 0.99).$$

In the lower panel the relation is simplified by plotting $\bar{t}_{3H} / \bar{t}_{Alb}$ vs. $\bar{t}_{Alb}$. Again, we do not find any systematic label separation between the two tracers and it thus seems appropriate to use the total [^{3}H] count as the reference for the calculation of the fractional hydrolysis of [^{3}H]BPGP. Since there was no delay, this finding confirms that the majority of the angiotensin converting enzyme interacting with vascular substrate must be located at the luminal surface of the pulmonary vascular endothelium.

Vascular label separation and the extra plasma space. When the mean transit times of labeled albumin and erythrocytes are plotted, a linear relation is found (Figure 5),

$$\bar{t}_{Alb} = 1.040\bar{t}_{RBC} + 0.140; \; r = 0.996$$

Values deviate from the regression line only at the lowest transit times (highest flows) as is clearly demonstrated in the lower panel, where a red blood cell-albumin label separation occurs with the highest flows. As we described before, this vascular red blood cell-plasma label separation suggests that at the highest flows, the erythrocytes shape into profiles which preferentially adopt the central vascular streamlines, thus obtaining lower transit

TABLE 2. *Mean transit times of albumin and total ^3H activity and fractional hydrolysis of BPGP at rest and through two successive levels of exercise.*

	$\bar{t}_{alb}$ (s)	$\bar{t}_H$ (s)	P value	M
Rest*	5.39 ± 1.27	5.42 ± 1.22	0.238	0.54 ± .04
Level A	4.24 ± 1.06	4.20 ± 1.07	0.305	0.55 ± .04
Level B	3.79 ± 0.81	3.85 ± 0.98	0.390	0.55 ± .05

$\bar{t}_{alb}$, $\bar{t}_H$ represent the average of the mean transit times for albumin and total ^3H activity, respectively. The P values for the paired t tests between $\bar{t}_{alb}$ and $\bar{t}_H$ are represented. The fractional hydrolysis of BPGP (M) did not vary with exercise. *Values from anesthetized animals are excluded from the calculated averages.

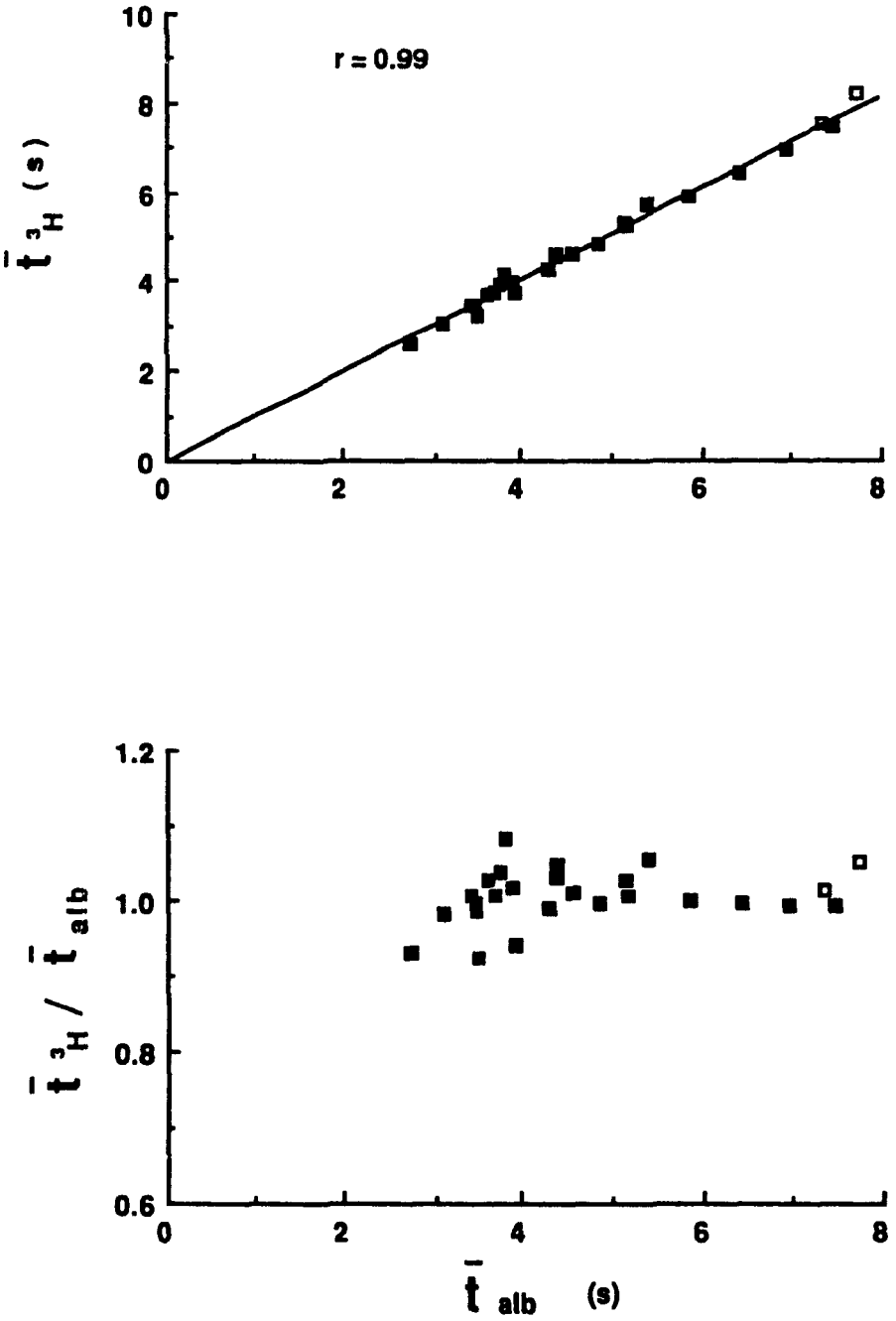

FIG. 4 Relationship between the mean transit time of total [^{3}H] ([^{3}H]BPGP + [^{3}H]BP) and mean transit time of labeled albumin. There was a linear relation between the two (top panel). When the ratio of the two is plotted (bottom panel), the identity in transit times becomes evident; the data points scatter around 1.

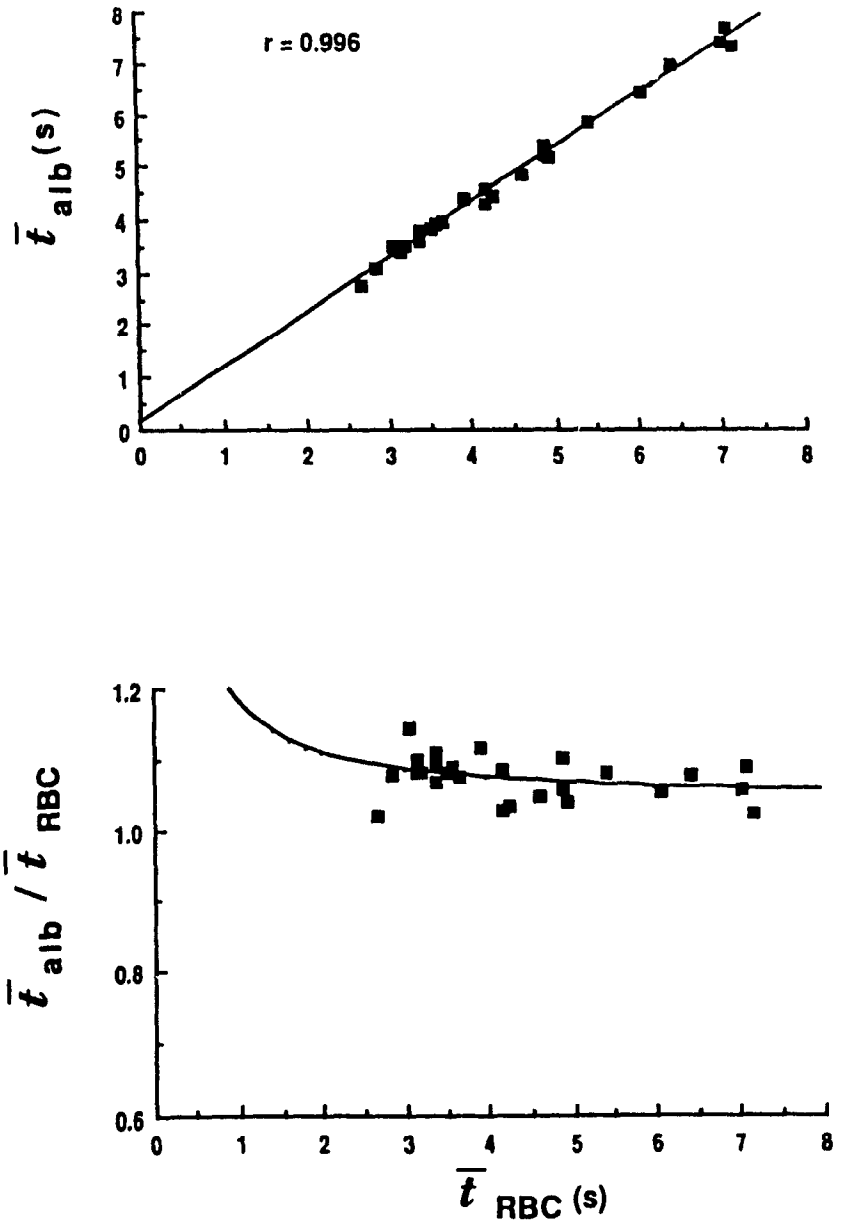

FIG. 5 Vascular label separation. Relationship between mean transit time of labeled albumin ($\bar{t}_{alb}$) and mean transit time of labeled erythrocytes ($\bar{t}_{RBC}$) is shown in the top panel. When the ratio of the two is plotted (bottom panel), a relatively increasing label separation becomes evident at high flows (low mean transit times). The line on the bottom panel is the locus predicted from the best fit linear regression equation illustrated in the top panel.

times than plasma (1,11). The extra plasma space (EPS, Figure 6), was found to increase linearly with blood flow. The least mean squares regression through the data was,

$$EPS = 0.101F_b + 0.029; r = 0.637$$

The product of the ordinate value (0.029 ml plasma/g lung) and the water content of plasma (0.94 ml/ml), is 0.027 ml water/g lung. This is the water content of the intercept or zero flow value for the extra plasma space, and it is the value which we have inferred is needed to correct the gravimetric estimates of the extravascular lung water obtained by using the labeled erythrocytes as a vascular tracer. This value was thus subtracted from the calculated gravimetric extravascular lung water to yield corrected values.

Extravascular lung water. The tracheobronchial tree receives its blood supply from the bronchial circulation. A water space tracer injected into the pulmonary circulation will consequently not have access to these structures. We have shown in a previous study that exclusion of the extraparenchymal tracheobronchial tree results in gravimetric estimates which correlate closely with dilution estimates of the extravascular lung water at high flows (11). We therefore subtracted the contribution of the extraparenchymal tracheobronchial tree from the gravimetric estimates in our calculations, to provide a base for comparison with the dilutional estimates of the extravascular lung water. The dilutional EVLW, expressed as a proportion of the wet lung, weight is shown in the upper panel of Figure 7. The filled circles represent the data from the present study, while the open circles represent data obtained from 9 dogs in a previous study (11). The dilutional EVLW increased nonlinearly and rapidly approached a maximal asymptotic value at moderate levels of blood flow. The least squares best fit rising exponential fitted through the data, was,

$$EVLW = 0.726\ (1 - \exp^{-2.47F_b})$$

where the first numerical parameter is an asymptotic maximal or $EVLW_{max}$ value, and the second, an exponential rate constant with dimensions reciprocal to those of F_b. Alternatively, the best fit expression using a rectangular hyperbola was,

$$EVLW = 0.899F_b/(F_b + 0.378)$$

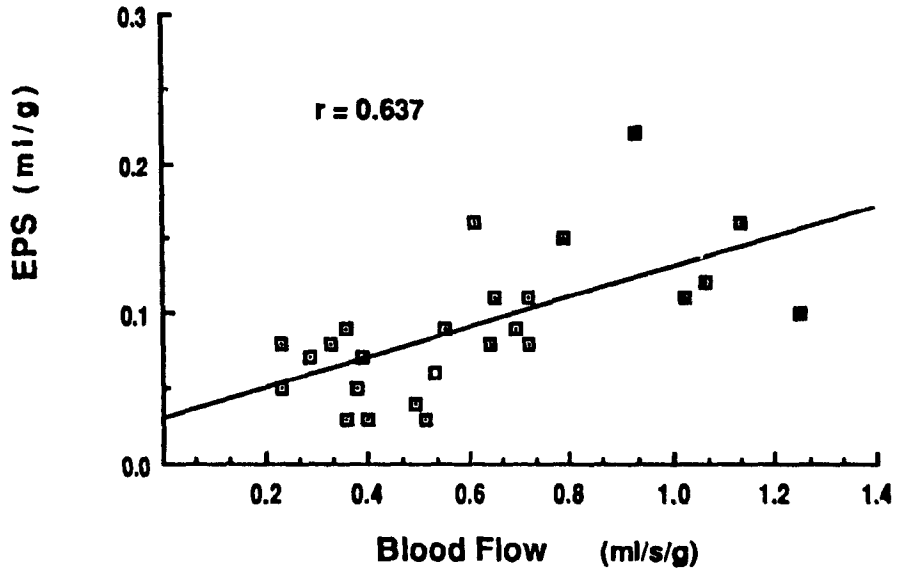

FIG. 6 Extra plasma space (EPS), in ml plasma/g wet lung wt, plotted as a function of blood flow. An increase in the extra plasma space with blood flow is evident. The intercept (0.029 ml plasma/g lung) was used to correct the gravimetric estimates of extravascular lung water.

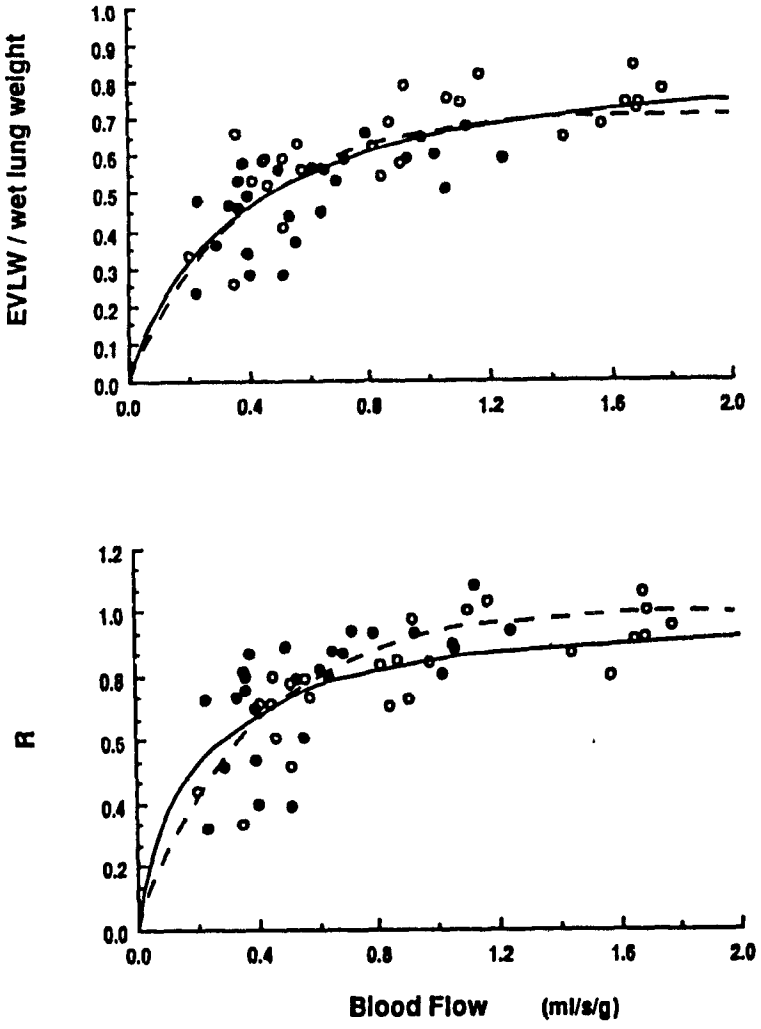

FIG. 7 Dilutional lung water. The dilutional extravascular lung water (EVLW), expressed as a proportion of wet lung weight, is plotted in the top panel. The EVLW increases with exercise, and rapidly approaches a maximal asymptotic value representing approximately 80% of the wet lung weight. The ratio (R) of the dilutional over the gravimetric estimates of the extravascular lung water is depicted in the lower panel. The ratio increases rapidly with blood flow, to reach an asymptotic value of close to 1, indicating that all of the lung tissue is then perfused. The filled circles represent data from the present study, while the open circles were taken from a previous study (10). The data were fitted using a rectangular hyperbola (solid line) or a rising exponential (solid line).

where the numerical parameter in the numerator is an $EVLW_{max}$, while the one in the denominator corresponds to an EVLW value which is half the asymptote. Both patterns provided a similar quality of fit through the range of the data, but the maximal value from the hyperbolic fit, which was not reached within the observed range of flows, was substantially larger than any of the measured values. The apparent lack of change of the dilutional estimate at higher flows suggests that all of the lung water had become accessible to the octanediol probe, in the moderate and high ranges of blood flow.

To amplify this potential relation, the ratio (R) of tracer accessible EVLW to gravimetrically determined EVLW is plotted as a function of blood flow, in the lower panel of Figure 7. Again, a similarly rising pattern is found for R, and we obtained R_{max} values of 0.94 and 1.11 using an exponential and hyperbolic fit, respectively. At moderate levels of blood flow, the observed R values approach unity and all of the lung water has become accessible from the vascular space. If we therefore set R_{max} equal to 1 and obtain a one parameter fit, the best fit rising exponential is,

$$R = 1 - \exp^{-2.67F_b}$$

and the best fit rectangular hyperbola,

$$R = F_b/(F_b + 0.175)$$

The latter does not correspond to the sense of the data in the low flow region. The rising exponential seems to provide a systematically better fit through the data points.

Central blood volume. The central blood volume (CBV), as calculated by use of equation (8), increases linearly with blood flow (Figure 8), according to the following fitted least mean squares regression line,

$$CBV = 1.62F_b + 1.10; r = 0.841$$

The image of the increase in central blood volume with increase in blood flow is also portrayed in a different fashion in the lower panel, where the mean transit time of the vascular reference is plotted against blood flow and compared with isovolume lines. In contrast to the tracer accessible extravascular lung water, which rapidly approaches a value

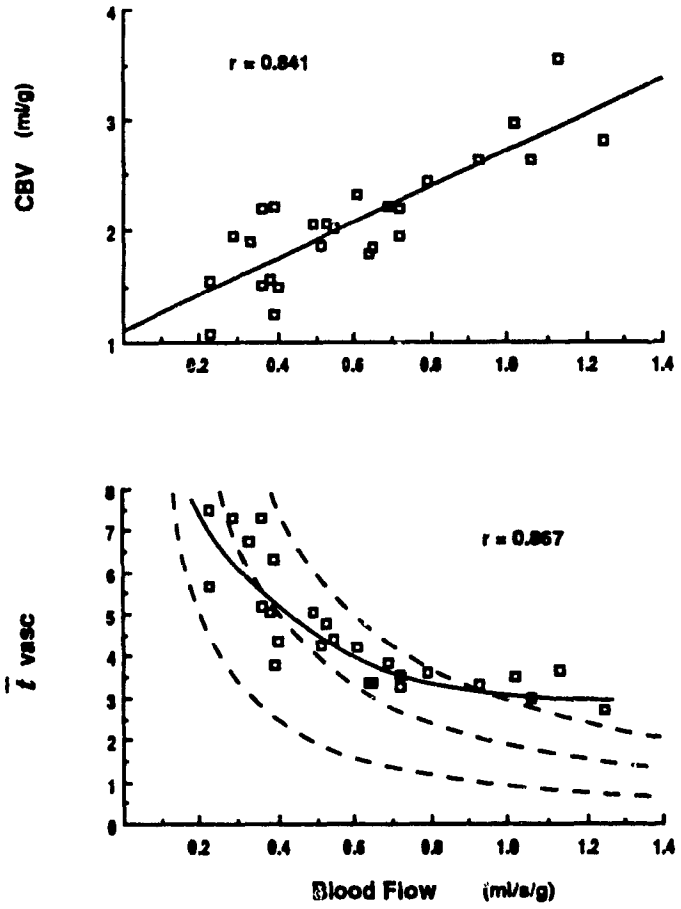

FIG. 8 Upper panel: Central blood volume, CBV, versus blood flow. The vascular space increases linearly with exercise. Lower panel: Mean transit time of the vascular reference ($\bar{t}_{vasc}$) is seen to shift from lower to higher isovolumetric lines as blood flow is increased. Isovolumetric lines are represented by dashed lines at 1, 2, and 3 ml of blood/g lung weight.

corresponding to a maximal asymptotic proportion at moderate levels of exercise (Figure 7), the plot corresponding to the central blood volume continues to cross higher isovolume lines even at the highest flows, reflecting the continuing increase in central blood volume across the higher flow range.

Angiotensin-converting enzyme kinetics. The cumulative fractional [^{3}H]BPGP hydrolysis fraction (M) did not vary as a function of blood flow, but took the shape of a flat line when fitted by least mean squares linear regression (Figure 9, top panel),

$$M = 0.017F_b + 0.54;\ r = 0.109$$

The lumped parameter A_{max}/K_mF_p was calculated by use of equation (19). It did not vary significantly with blood flow and also gave a flat line relationship versus F_b (Figure 9, middle panel), similar to that for M,

$$A_{max}/(K_mF_p) = 0.029F_b + 0.415;\ r = 0.137$$

The parameter A_{max}/K_m, calculated by use of equation (20), shows an entirely different relation to blood flow. A_{max}/K_m, which is an index of enzymic mass and, presumably, capillary surface area, increases linearly over the blood flow range, according to the relation (Figure 9,lower panel),

$$A_{max}/K_m = 0.371F_b + 0.014;\ r = 0.937$$

Capillary surface area appears to be recruited essentially in proportion to the change in blood flow.

This conclusion would be buttressed if other parameters relating to the capacity of the pulmonary circulation correlate with A_{max}/K_m. We therefore also examined the relation between A_{max}/K_m and central blood volume, and the extra plasma space. When A_{max}/K_m is plotted against the central blood volume we find a significant correlation according to the relation

$$A_{max}/K_m = 0.167CBV - 0.11;\ r = 0.81$$

where the central blood volume is expressed in ml/g of wet lung weight.

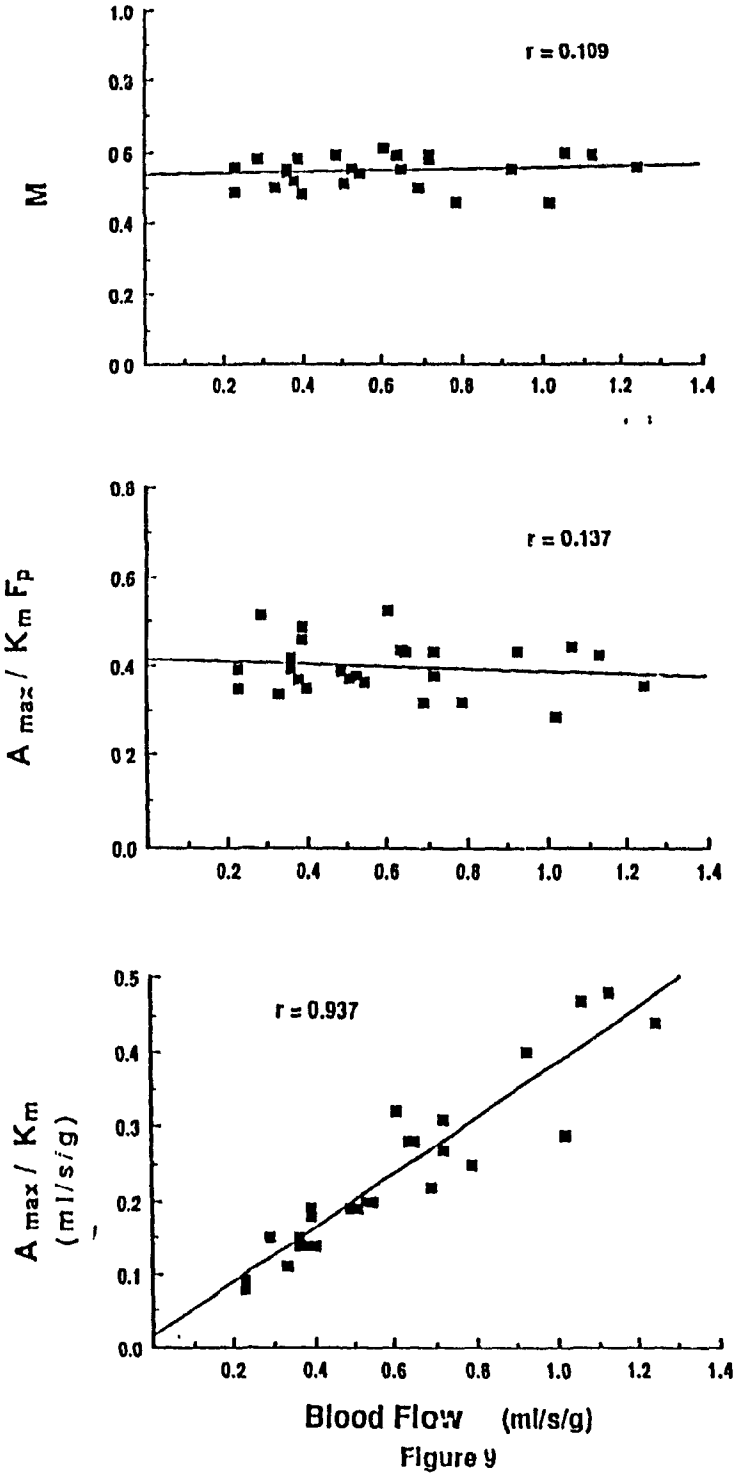

Figure 9

FIG. 9 Aggregate values for angiotensin-converting enzyme conversion of substrate, as a function of blood flow. The proportional [^{3}H]BPGP hydrolysis, M, did not change with increase in flow with exercise (top panel). The parameter A_{max}/K_mF_p also did not change with increasing blood flow (middle panel). The first order kinetic parameter A_{max}/K_m, on the other hand, increased linearly with flow (bottom panel).

The extra plasma space is thought to reside mostly within the microcirculation, where the hematocrit is lower than in the great vessels. A positive and significant correlation was also found between A_{max}/K_m and EPS with

$$A_{max}/K_m = 1.75\ EPS + 0.08;\ r = 0.70$$

The EPS is expressed in ml/g of wet lung weight.

DISCUSSION

We studied the effect of graded exercise on the central blood volume, the tracer accessible extravascular lung water, and the first order kinetic parameter A_{max}/K_m for the angiotensin converting enzyme substrate BPGP in awake mongrel dogs.

Central blood volume. The central blood volume measured in the present work is that from the base of the main pulmonary artery to the root of the aorta. This volume is that comprised by the pulmonary circulation plus the left heart chambers. Variations in the volume of the left atrium, because of its small capacity compared to the pulmonary circulation, probably do not contribute significantly to change to the central blood volume with exercise. The left ventricular end diastolic volume increases with exercise while the end systolic volume decreases (40). The increase in the left ventricular ejection fraction is accompanied by an increase in heart rate resulting mainly from a decrease in the diastolic period of the cardiac cycle. The left ventricular contribution to the central blood volume is thus a complex and dynamic one which will vary with the different periods of the cardiac cycle, with the heart rate, and with the inotropic state of the myocardium. We can, however, analyze the static extremes in which the left ventricle is regarded to be a simple reservoir, and examine the impact of the change in relation to the whole. Suppose we have a situation in which the left ventricle has an end diastolic volume of 60 ml and an ejection fraction of 60%. If all time were spent at end diastolic volume, there would be a 60 ml contribution to the central blood volume, while if all time were spent in end systole there would be a 24 ml contribution, a difference of 36 ml. During the recording of an indicator

dilution curve, the volume will cycle, and the volume calculated will represent a time-averaged value. The change around the average is of the order of 5% of the central blood volume at rest, and thus, by comparison, can be regarded as small. Since the average left ventricular volume is not expected to increase perceptibly with exercise, it will not contribute substantially to the observed much larger central blood volume observed with exercise. Change in the pulmonary vascular volume can therefore be considered to be the major contributor to the change in the central blood volume with exercise. Since the central blood volume continued to increase over the complete range of flows encountered with exercise, the pulmonary vascular volume also can be considered to increase over this range. The increase could be the result of distension of pulmonary vasculature, recruitment, or a combination of both. Insight into the latter must come from the tissue space and capillary surface tracers.

Extravascular lung water. The tracer accessible extravascular lung water is the water contained in tissue structures which are perfused at the time of the experiment. The dilutional extravascular lung water can consequently serve as an index of the amount of lung tissue being perfused from the pulmonary artery and any increase in this parameter must be the result of lung tissue recruitment. The tracer accessible extravascular lung water (Figure 7) increased with increasing blood flow approximately over the interval from rest to first level exercise, and thereafter remained close to an apparent maximal value representing approximately 75% of the wet lung weight. The ratio of the dilutional over the gravimetric estimates of the extravascular lung water also increased in a similar nonlinear fashion, to asymptote close to the value of unity. The saturating behavior of extravascular lung water with exercise had previously been described by Goresky et al. (18,19), the asymptotic estimates, expressed as a ratio of wet weight, being somewhat lower, however, since the extraparenchymal tracheobronchial tree had been included in the gravimetric measurements (11).

Thus, in the transition from low to moderate levels of blood flow with exercise, there must be pulmonary vascular recruitment, underlying the observed lung tissue recruitment. The results correspond, in a sense, to experiments with isolated lung lobes in which the effects of increasing size embolic beads on dilutional estimates of the vascular and the extravascular lung water volumes have been examined: the investigators found a linear relationship between the estimated vascular and extravascular volumes (9). Exclusion of part of the microvascular bed led to exclusion of part of the extravascular lung water, in this instance.

It may seem paradoxical that, in the present work, the central blood volume increased over the whole range of blood flows and kept on increasing despite the fact that all of the lung tissue was being perfused. The additional increase in central blood volume in the transition from moderate to high levels of blood flow did not result in further lung tissue recruitment and so might easily be attributed to vascular distension rather than microvascular recruitment without further tissue recruitment. We would, however, suggest that this is not the case and that vascular recruitment still takes part in the phenomena observed even when the tissue space is fully recruited. Demonstration that this is the case demands the use of a capillary surface marker in the analysis of the data. Previous observation, utilizing this kind of approach, has indicated that recruitment likely occurs. Thus, we found that pulmonary capillary endothelial cell tracer norepinephrine uptake by the lungs at rest and at two levels of exercise increased in proportion to the increase in blood flow (11). Also, in the transition from a zone 3 to a zone 2 situation in the isolated lung lobe (33), obtained by increase in alveolar pressure, there is no change in the measured accessible extravascular lung water, but there is a reduction in the rate of uptake of serotonin (its endothelial uptake is limited by the capillary permeability surface product). These data, like ours, are consistent with vascular recruitment if the size of the collapsed areas is sufficiently small to allow diffusional equilibration of water tracer from adjacent perfused capillaries. A realistic three-dimensional sheet flow model of the pulmonary

circulation supports this concept and predicts that local small areas of the alveolar sheet will become unstable and collapse as the alveolar pressure-venous pressure difference increases (12). The mechanism of vascular recruitment at higher levels of exercise is likely different, and may include the dislodging of white cell plugs (11).

Angiotensin-converting enzyme kinetics. The angiotensin converting enzyme (ACE) is located at the luminal surface of the pulmonary vascular endothelium, predominantly in the capillaries. The determinable parameter A_{max}/K_m is a function of the available ACE mass, which in turn is predominantly a function of the pulmonary capillary surface area that is perfused (5,39). With increasing blood flow, an increase in vascular surface area caused by recruitment (perfusion of more vessels) will cause an increase in the measured A_{max}/K_m. Vessel distension can also increase the vascular surface area, but it should not add to the number of ACE sites which can interact with the vascular substrate and should theoretically not change A_{max}. We were not able to measure A_{max} and K_m independently since it was technically impossible to do more than one substrate injection for each level of exercise. However, numerous studies in the rabbit have described the stability of the K_m of the angiotensin converting enzyme for an analogous substrate, benzoyl-phenylalanyl-alanyl-proline (BPAP), in physiologic as well as pathologic conditions. In fact, K_m was unaffected by variations in pulmonary blood flow and surface area (27,39), in blood pH (31) (between 7.1 and 7.9) or pO_2 (from 10 to 110 Torr). In the developing lamb, lung vascular growth is not associated with any changes in K_m and the latter is also not affected by hypoxia (29). It thus seems reasonable to assume that there likely was no dysfunction of the enzyme for BPGP during the 15 minutes of exercise in this study and that the K_m was unaffected, so that the ratio A_{max}/K_m becomes a valid index of the perfused microvascular surface area. On the other hand, in the presence of significant endothelial injury, the K_m may (2, 26) or may not (34) be affected.

As pulmonary blood flow increased with exercise there was a simultaneous and quantitatively similar increase in A_{max}/K_m (a threefold increase in blood flow with a

threefold increase in A_{max}/K_m, Figure 9). Assuming no variation in angiotensin converting enzyme function, the data indicate that exercise under the experimental conditions triples the pulmonary vascular surface area that is able to provide ACE activity, by recruiting or perfusing new vascular channels. Further supporting this argument are the significant correlations between A_{max}/K_m and the central blood volume, and A_{max}/K_m and the extra plasma space. The extra plasma space is thought to reflect the lower microvascular hematocrit and consequently to increase more or less in proportion with the microvascular volume. This is the first time that the ACE substrate BPGP has been used in *in vivo* awake animals. Previous studies have validated the use of ACE substrates as indices of the perfused vascular surface area. In the developing lamb, with BPAP as the capillary surface marker, a linear relationship was found between the observed A_{max} and both the morphometrically determined pulmonary vascular surface area and the carbon monoxide diffusing capacity (29,30), the latter being expected to be related to and determined by the tissue interface between gas and blood, and the lung capillary volume. Endothelial cell damage by PMA or bleomycin in the rabbit also decreases A_{max} activity (3,34). In isolated lung lobes, Moalli et al. varied airway and vascular pressures in a manner which reproduced the various physiologic lung zones and found that the measured A_{max} increased and decreased with corresponding recruitment or derecruitment of pulmonary capillaries (27). High static intra-alveolar pressure (PEEP) is found to reduce the fraction of microvessels perfused (that is, to produce derecruitment), as reflected by changes in the A_{max}/K_m ratio (39).

Increases in the pulmonary vascular surface area in awake subjects during exercise have been inferred to occur, with the observed increase in the carbon monoxide diffusing capacity with exercise (6); and the increase in sheep thoracic lymph flow with exercise has been estimated to result from a tripling in the perfused lung microvascular surface area (8). In the present work, there was a linear increase in central blood volume, accompanied by a similar increase in A_{max}/K_m, which suggests that the increase in pulmonary blood volume

with exercise is partly accounted for by capillary recruitment. We cannot readily distinguish between large vessel distension and capillary distension and recruitment but the magnitude of the changes in A_{max}/K_m indicates that there must be substantial capillary recruitment with exercise. The parameter A_{max}/K_mF_p does not vary with recruitment, which suggests that the ACE activity within individual capillaries remains the same. This confirms the findings of Toivonen et al. (39) and, interestingly and surprisingly, suggests that recruitment occurs in such a fashion that the small vessel or capillary transit time (t_c, Appendix 1) remains more or less constant throughout the lungs, independent of cardiac output or pulmonary blood flow.

We have preferred BPGP to the more commonly used BPAP mainly because of its smaller percent hydrolysis in a single pass (55% versus 80% for BPAP), since estimates of A_{max}/K_m become very sensitive to small analytical error when percent hydrolysis is high (39). BPAP has been hypothesized to bind slowly to, and then unbind slowly from serum albumin in a fashion which affects its pulmonary hydrolysis (23). In the introduction of the tracer BPGP, we took special care in preparing a "plasma free" injection mixture to prevent hydrolysis. No albumin was added. Within the transit times found in these experiments, there would not appear to have been sufficient time for similar slow equilibrating protein binding sites to have had any impact on BPGP hydrolysis, since the absence of variation in BPGP hydrolysis as a function of the time of passage of the bolus in these experiments (Figure 3) indicates that there was not likely such an effect. More rapid binding and unbinding is possible. Plasma binding has not been explored, because of the difficulty imposed by ongoing hydrolysis. The "plasma free" injection mixture avoided hydrolysis of the BPGP in the injection mixture by plasma ACE. The Percoll separation of the erythrocytes and the subsequent washings resulted in disappearance of detectable ACE activity from the injection mixture, the fractional toluene extraction of the injection mixture at the end of the procedure being similar to fr_s (the fractional toluene extraction of pure unhydrolyzed substrate).

We measured *in vitro* dog serum ACE activity using [^{3}H]BPGP as substrate (Appendix 2, Figure 10). Serum hydrolysis of BPGP proceeds in an exponential fashion with a single rate constant of 0.0167 sec^{-1}. If we extrapolate to *in vivo* conditions, within the mean transit time of our experiments (less than 10 sec, including collecting times), we would expect to have seen around 5% hydrolysis of BPGP by plasma ACE, if the activity in the bolus had been acted on by plasma ACE, at normal levels of activity. Thus, if the first pass hydrolysis is of the order of 55%, the plasma hydrolysis will be expected to contribute, on average, perhaps an additional 5% or less, and thus perhaps 10% of the total. Thus the plasma ACE contribution to BPGP hydrolysis is expected to have been relatively small. The idea is supported by the flat aspect of the fractional hydrolysis plot (Figure 3). If plasma ACE had played a substantial role, we would have expected the hydrolysis to increase substantially at larger transit times.

A potential source of error in the computation of ACE kinetics with the toluene extraction procedure would occur if an erroneous fr_p (fractional extraction of product) had been utilized (4). To prevent this, we utilized the same stock solution of [^{3}H]BP for all experiments and measured fr_p recurrently through the study. We found no systematic variation in fr_p with time; the mean value was 0.61 ± 0.016(SD).

Conclusions arising from this study. The increase in pulmonary blood flow induced by exercise is accompanied by a simultaneous increase in the central blood volume. In the transition from low to moderate levels of blood flow, there is a recruitment of lung vasculature which is accompanied by lung tissue recruitment. With further increase in blood flow, despite the fact that all of the accessible lung tissue is being perfused, there is nevertheless further pulmonary microvascular recruitment. The manner in which the increase in pulmonary volume is accommodated with increase in blood flow with exercise is not completely resolved by this study. It does indicate, however, that capillary recruitment takes place across the whole range of flows, and that, because of the magnitude of the change in the first order kinetic parameter A_{max}/K_m with exercise, a substantial

proportion of the vascular volume change with exercise must be microvascular rather than macrovascular. The exact mechanism of recruitment remains to be defined. The phenomenon appears to result from a complex interplay between alveolar pressure, vascular pressures and forces retaining and/or driving leucocytes through the lung microcirculation (22).

Are there alternative explanations? The present studies need to be compared to the set of studies carried out with BPAP by Dawson et al. (10) and Linehan et al. (23). They have also observed, with BPAP, that the fractional utilization is relatively stable, and have inferred that there is a mixture of two interconvertible forms of BPAP, one of which is immediately highly metabolizable, and the other only after a prolonged interconversion time. They have therefore argued that A_{max}/K_mF_p is large enough that almost all of the metabolizable form of BPAP is used up in a single passage, and that the unconverted remainder is initially unmetabolizable. These investigators have bolstered their hypothesis by presenting an *in vitro* study of hydrolysis of BPAP by commercially prepared ACE, which exhibits both a larger early rapid and a smaller late slow component to the hydrolysis (10).

It was therefore of interest to examine, in the present instance, the hydrolysis of BPGP by ACE, prepared from dog lung. Dog lung acetone powder, 1 g (Sigma Chemical Corp.), was mixed with 35 ml of 0.15 M NaCl containing 0.1% Nonidet P-40. The mixture was incubated at 37°C for 1 h and then centrifuged at 10,000 g for 30 min. The pellet was discarded. The supernatant was dialyzed in 5 mM potassium phosphate buffer, pH 6.8 for 16 h. The precipitate that formed during dialysis was removed by centrifugation at 2000 g for 10 min. The resulting supernatant was applied to a 3 ml column of DE-52 cellulose (Whatman) equilibrated and developed with the potassium phosphate buffer. After unretained proteins were eluted, ACE was eluted using 0.25 M potassium phosphate buffer, pH 6.8, containing 0.5 M NaCl. The ACE-containing fractions were pooled, and the resulting solution (about 12 ml) was dialyzed in 20 mM

Hepes buffer, pH 7.0, containing 0.5 M NaCl. The dialyzed solution was applied to a 6 ml column of N-[1-carboxy-2-phenylethyl]-L-Lys-L-Pro coupled via its epsilon amino group to Sepharose CL-4B as described by Pantoliano et al. (28). The column was equilibrated and washed with the dialysis buffer. After unretained proteins were eluted, the column was developed with 0.1 M sodium borate buffer, pH 8.9, and ACE was eluted in a volume of 9.5 ml. The ACE pool was concentrated to 1 ml by centrifugal ultrafiltration (Centricell, Millipore Corp.). ACE was recovered in a yield of about 17 μg. A 2 μg sample behaved as a single substance on SDS PAGE, M_r 150,000.

The reaction of dog lung ACE with ^{3}H-BPGP was then studied. ^{3}H-BPGP, 7 μCi at 20 Ci/mmol, was added to a 20 ml liquid scintillation vial containing 4 ml of 50 mM Hepes buffer, pH 7.5, with 0.15 M NaCl. To a separate 20 ml vial, 200 μl of dog lung ACE was added. Both vials were heated at 37°C for 10 min. At time zero, the contents of the first vial were poured into the second, and the resulting mixture was poured back into the first vial. The latter was incubated at 37°C. As quickly thereafter as possible, a 200 μl sample of the reaction mixture was transferred to the first of a series of 20 ml vials, each of which contained 1.0 ml of 0.1 M HCl. Subsequent timed samples (200 μl) were collected and transferred to their respective HCl-containing vials over the next 140 seconds. At the end of 10 min of incubation, each of the HCl-containing vials received 1.0 ml of toluene containing Omnifluor, 4 g/l. The vials were capped, inverted twenty-times and then submitted for liquid scintillation counting. The toluene-extractable ^{3}H of each vial was counted for 10 min in each of eight counting cycles performed over a 60 h period. The vials were then uncapped, and 15 ml of the aqueous-miscible scintillation cocktail Scint A (Packard Instruments) was added to each. The vials were recapped and inverted until a single phase mixture was obtained. Liquid scintillation counting was repeated (four cycles of 10 min per vial) to quantify total ^{3}H in each vial. A separate incubation was performed in which 200 μl of the assay buffer was substituted for dog ACE. This 'blank' incubation enabled an evaluation of the behavior of unhydrolyzed ^{3}H-BPGP in the above-described

extraction and counting procedures and provided a value for fractional extraction of substrate, fr_s. In a third experiment in which dog ACE was reacted with ^{3}H-BPGP for 18 h at 37°C, the toluene-extractable ^{3}H was taken as the fractional extraction of product (fr_p). Timed results from the dog lung ACE experiment were computed via the integrated form of the first order rate equation, modified to take into account fr_p and fr_s:

$$\left[\frac{V_{max}}{K_m}\right] t = \ln\left(\frac{u_{tot}}{u}\right)$$

$$= \ln\left[\frac{((fr_p - fr_s)\, u_{tot})}{((fr_p\, u_{tot}) - E)}\right]$$

where V_{max} is the maximal in vitro rate of conversion by the enzyme, in this case, u_{tot} is total ^{3}H in a given vial, E is toluene-extractable ^{3}H, u/u_{tot} is the fraction of substrate remaining at a given sample collection time, and t is the time.

Results are shown in Fig. 10. In this case, the reaction of ^{3}H-BPGP with dog lung ACE proceeds to completion, and the reaction obeys a single first order rate constant throughout its course. There is no evidence for a late slower component to the hydrolysis reaction, over a time course similar to that explored by Dawson et al. (10) for BPAP, particularly for one with a magnitude corresponding to the fraction of BPGP not hydrolyzed during a single pass. The *in vivo* analysis of our ^{3}H-BPGP experiments has therefore been carried forward in a direct fashion. It is reassuring that the conclusions of the present study and the examination of tracer norepinephrine uptake during exercise (11) are consonant, that both indicate that pulmonary vascular recruitment not only occurs with tissue recruitment during exercise but also continues after pulmonary tissue recruitment is complete.

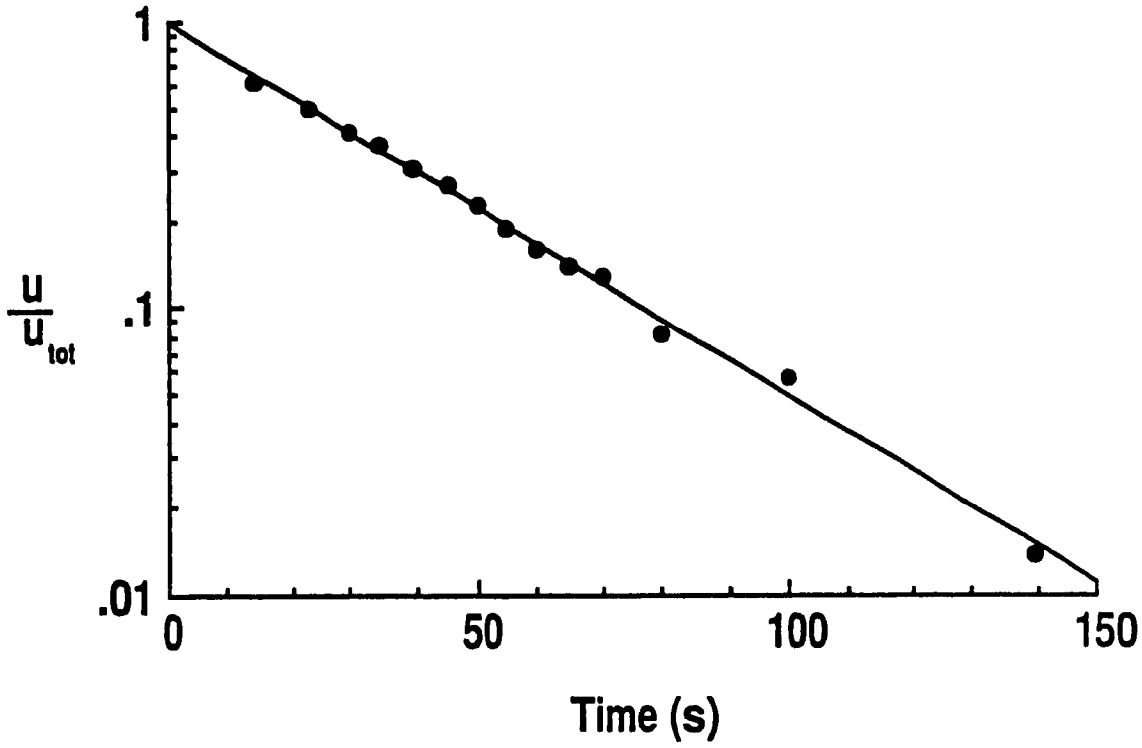

FIG. 10. The reaction of [^{3}H]BPGP with dog lung ACE. The time course proceeds in an exponential fashion, with a single rate constant, V_{max}/K_m, 0.031 s^{-1}.

APPENDIX I

KINETICS OF THE ENZYME-CATALYZED CONVERSION OF TRACER SUBSTRATE TO PRODUCT, AT THE INNER SURFACE OF THE CAPILLARY ENDOTHELIAL CELLS (THAT IS, AT THE WALL OF THE MICROVASCULAR LUMEN), IN THE ABSENCE OF AN ENZYMIC SPACE EFFECT.

Description of events along a single microvascular channel. Consider that, at the margin of a capillary (the ACE activity is associated with the endothelial cell glycocalyx), substrate u combines with free enzyme e to form an enzyme-substrate complex eu with the rate constant k_a, and that the complex either dissociates to form e and u with the rate constant k_d or proceeds to form product p in an irreversible manner, with the rate constant k_{cat}, viz.,

$$e + u \underset{k_d}{\overset{k_a}{\rightleftarrows}} eu \xrightarrow{k_{cat}} e + p \qquad \text{...(A1)}$$

In the reaction case being considered, the enzyme e and the enzyme complex eu are attached to the inner surface of the vessel, whereas precursor u and product p move along with plasma flow F_p at the velocity W, in a capillary with cross sectional area for plasma A_r, constant circumference D_c, and with the ratio of capillary surface area to contained plasma volume $D_c/A_r = \mu$. The capillary is of such small dimensions that diffusional cross sectional equilibration is expected to be so rapid that all of u is available to e, at each point along the length.

In the following development, for a capillary surface removal process, concentrations (in square brackets) are therefore of two kinds. For precursor u and product p, which are free in plasma, they are of the usual dimension (moles/unit plasma volume), whereas for the surface-bound enzymes and enzyme-substrate combinations, they are of the dimensions (moles/unit surface area). The latter, when multiplied by μ, will be expressed in equivalent moles/unit plasma volume.

Now define the Michaelis constant K_m of the reaction from either the rate constants of the reactions or the concentrations of the species under consideration,

$$K_m = \frac{k_d + k_{cat}}{k_a} = \frac{[e][u]}{[eu]} \qquad (A2)$$

and the total enzyme concentration $[e_t]$ as,

$$[e_t] = [e] + [eu] \qquad (A3)$$

from which,

$$\frac{[eu]}{[u]} = \frac{[e_t]}{[u] + K_m} \qquad (A4)$$

The association of substrate with enzyme results, kinetically, in a space effect, like that imposed by exchange with a parallel additional compartment, whereas for product, which is released but does not recombine, no such effect will be present. The effect has been termed an enzymic space effect (16,17). Its incremental magnitude above the vascular space is expected to be dictated, in this instance, by the ratio $\mu[eu]/[u]$. It varies between two extremes:

(a) When $[u] \rightarrow 0$

$$\frac{\mu[eu]}{[u]} \rightarrow \frac{\mu[e_t]}{[K_m]} \qquad (A4A)$$

and

(b) When $[u] \rightarrow \infty$

$$\frac{\mu[eu]}{[u]} \rightarrow 0 \qquad (A4B)$$

In the present investigation a radiochemical (that is, very low) concentration of substrate was utilized, yet the experimental finding is that the mean transit times of labeled albumin and of total labeled substrate plus product activity do not differ in any detectable fashion, and the mean transit times for labeled albumin and labeled substrate also do not differ. There is, then, no measurable enzymic space effect in the system and there is, concomitantly, no perceptible additional delay attributable to the creation and release of product. The lack of an observable enzymic space at radiochemical concentrations indicates that either the concentration of enzyme is small or the K_m for BPGP is quite large. With

reference to the latter possibility, it is of interest that the K_m for BPGP hydrolysis by rabbit lung homogenate ACE is approximately two orders of magnitude higher (36) than that for benzoyl-phenylalanyl-alanyl-proline (BPAP), for which an enzymic space effect has been reported (24).

To gain insight into this problem, we will examine what is expected in the steady state (this case is what has usually been treated in the past), how tracer is expected to behave within this steady state, and what the expected asymptotic form of this behavior is, in the low concentration extreme.

Steady state behavior. First consider the long time response to a steady infusion of concentration $[u_0]$ at the inflow, when a steady state has been established. Then,

$$k_a \mu [e][u] - (k_d + k_{cat})[eu] = 0 \qquad \text{...(A5)}$$

$$W \frac{d[u]}{dx} = - k_a \mu [e][u] + k_d \mu [eu] \qquad \text{...(A6)}$$

and

$$W \frac{d[p]}{dx} = k_{cat} \mu [eu] \qquad \text{...(A7)}$$

From equations (A5) to (A7), we find,

$$\frac{d}{dx}([u] + [p]) = 0$$

or $[u] + [p] =$ constant.

Hence, since $[u(0)] = [u_0]$, and $[p(0)] = 0$,

$$[u] + [p] = [u_0] \qquad \text{...(A8)}$$

The total of bulk precursor and product concentrations in the plasma space is expected to be constant along the length.

From the foregoing, we find that

$$\left[\frac{[u] + K_m}{[u]}\right] d[u] = - \frac{\mu k_{cat}}{W} [e_t] dx \qquad \text{...(A9)}$$

Integration indicates that the expected underlying concentration of precursor [u], at any point along the length, will be defined by the relation,

$$[u] - [u_0] + K_m (\ln [u] - \ln [u_0]) = - \frac{\mu k_{cat}}{W} \int_0^x [e_t] \, dx \qquad ...(A10)$$

which may be recast into the highly implicit form,

$$[u] = [u_0] \, e^{- \frac{\mu k_{cat}}{W[\hat{u}] + K_m} \int_0^x [e_t] \, dx} \qquad ...(A11)$$

where $[\hat{u}] = \dfrac{[u_0] - [u]}{\ln [u_0] - \ln [u]}$

is a logarithmic average. And from equation (A8),

$$[p] = [u_0] \left(1 - e^{- \frac{\mu k_{cat}}{W[\hat{u}] + K_m} \int_0^x [e_t] \, dx} \right) \qquad ...(A12)$$

The integral on the right hand side of the two foregoing equations indicates that, for the nonuniform enzyme distribution case, the outflow concentration depends only on the total amount of enzyme in the system, not on its longitudinal distribution, whereas the lengthwise spatial concentration gradients will depend on the distribution of enzyme. In the uniform enzyme distribution case, where $[e_t]$ is constant along the length, the expression $\mu k_{cat}[e_t]$ can be set equal to V_{max}, the maximal conversion rate for substrate, which will now be constant along the length.

Tracer behaviour. The general set of equations governing the conversion of tracer substrate u* to tracer product p* along a capillary of length L ($0 < x < L$) are,

$$\frac{\partial [u^*]}{\partial t} + W \frac{\partial [u^*]}{\partial x} = - k_a \mu [e][u^*] + k_d \mu [eu^*] \qquad ...(A13)$$

$$\frac{\partial [e]}{\partial t} = - k_a \mu [e][u^*] + (k_d + k_{cat}) \mu [eu^*] \qquad ...(A14)$$

$$\frac{\mu \partial [eu^*]}{\partial t} = k_a \mu [e][u^*] - (k_d + k_{cat}) \mu [eu^*] \qquad ...(A15)$$

$$\frac{\partial [p^*]}{\partial t} + W \frac{\partial [p^*]}{\partial x} = k_{cat} \mu [eu^*] \qquad ...(A16)$$

In this instance we will examine the tracer within a steady state situation, the behaviour of tracer within the system when it is in steady state with respect to bulk, as outlined earlier. The tracer input to which the system response needs to be found is that of an impulse input at time zero, that is,

$$[u^*(x,0)] = \frac{q_0^*}{A_r}\delta(x) = \frac{q_0^*}{F_p}\delta\left(\frac{x}{W}\right) \qquad \ldots(A17)$$

where q_0^* is the amount of tracer introduced, A_r is the mean plasma cross sectional area of the capillary, W is the velocity of flow, and $A_rW = F_p$, the plasma flow rate along the capillary.

The general solution to the system has been explored elsewhere, together with the behavior of various limiting solutions (15). In the extreme where the enzyme concentration is so small that it cannot be perceived, in terms of a space effect, and where the dispersion of neither substrate nor product increases as a result of the enzymic mechanism (this occurs when k_a and k_d are very large, and when, simultaneously, there is no perceptible enzymic space effect), neither tracer substrate nor tracer product will be expected to be delayed with respect to a simultaneously introduced vascular tracer, propagating with the velocity W. The expected outflow profiles at the exit (x = L) are, then,

$$[u^*(L,t)] = \frac{q_0^*}{F_p} e^{-\frac{1}{W}\left\{\frac{\mu k_{cat}}{[\hat{u}]+K_m}\right\}\int_0^x [e_t]\,dx}\,\delta\left(t-\frac{L}{W}\right) \qquad \ldots(A18)$$

and

$$[p^*(L,t)] = \frac{q_0^*}{F_p}\left[1 - e^{-\frac{1}{W}\left\{\frac{\mu k_{cat}}{[\hat{u}]+K_m}\right\}\int_0^x [e_t]\,dx}\,\delta\left(t-\frac{L}{W}\right)\right] \qquad \ldots(A19)$$

where $[\hat{u}]$ is the underlying logarithmic average space concentration, defined by the expression,

$$[\hat{u}] = \frac{[u(0)]-[u(L)]}{\ln[u(0)]-\ln[u(L)]}$$

and where again [u(0)] is the underlying steady state input concentration and u(L), the output concentration. The labeled product emerges as an impulse function propagating

with the same speed as that of substrate, and it is built up at the same rate as the substrate is consumed. The sum of labeled precursor plus substrate is equal to (q_0^*/F_p) at each point along the length, at the time it is present. It corresponds to the profile expected for a reference substance, which does not leave the capillary.

It should be noted that the outflow depends again only on the total amount of enzyme dispersed along the single channel and not on the nature of its distribution along the length. If the enzyme concentration is uniform along the length, the exponential assumes the form, $\exp[-(\mu k_{cat}[e_t]/(\{[\hat{u}] + K_m\})\,(L/W)]$, where $\mu k_{cat}[e_t]$ corresponds to V_{max}, the maximal rate of conversion which can be achieved by the enzyme, and (L/W') is the capillary transit time. With this change, the exponential has the form, $\exp[-(V_{max}/(\{[\hat{u}] + K_m\})\,(L/W)]$.

The proportional loss of tracer from the substrate impulse and gain in tracer by the product impulse is dictated by the underlying bulk substrate concentrations. The fractional loss rate saturates (that is, diminishes) with increase in the underlying concentration of substrate.

In the extreme where there is only tracer (that is, when $u \rightarrow 0$), the outflow responses become, for the uniform enzyme distribution case,

$$[u^*(L,t)] = \frac{q_0^*}{F_p} e^{-\left(\frac{V_{max}}{K_m}\right)\left(\frac{L}{W}\right)} \delta\left(t - \frac{L}{W}\right) \qquad \ldots(A20)$$

and

$$[p^*(L,t)] = \frac{q_0^*}{F_p}\left[1 - e^{-\left(\frac{V_{max}}{K_m}\right)\left(\frac{L}{W}\right)} \delta\left(t - \frac{L}{W}\right)\right] \qquad \ldots(A21)$$

This is the set of expressions which we assume applies to the conversion of radiochemical levels of substrate during its passage along the capillary. When utilizing these expressions to analyze data, we intrinsically assume that contributions to hydrolysis by plasma ACE and any conversion by the quantitatively less important ACE activity in the endothelium of the small feeding and draining vessels are minor.

The V_{max} (mol.ml^{-1}.min^{-1}) expression has also been regarded from another point of view. It has been set equal to the quotient of the total activity in the capillary, A_{max} (mol.min^{-1}) divided by the total capillary plasma volume, A_tL or V_p. The exponential then becomes $\exp\{-(A_{max}/V_pK_m)(V_p/F_p)\}$ or $\exp\{-(A_{max}/K_mF_p)\}$. The ratio (A_{max}/V_p) allows one to develop expectations concerning the effect of capillary distension. Capillary distension, if it occurs, will not be expected to affect the total enzymatic substrate change effected in the capillary plasma, although it will increase the capillary volume, and hence the ratio (A_{max}/V_p) will decrease with distension. Correspondingly, the ratio (V_p/F_p), by which it is multiplied, increases, and the expression $\exp\{-(A_{max}/K_mF_p)\}$ will remain unchanged. There will thus be no expected change in the metabolism rate with distension unless accompanied by a change in plasma flow rate. The predicted lack of change in extraction with change in microvascular volume has previously been observed in the liver (14). In the absence of change in flow, the extraction of tracer norepinephrine by the liver has been found not to change in the face of a significant reduction in sinusoidal volume, induced by sympathetic stimulation.

Whole organ modeling. The multicapillary model developed by Rose and Goresky (35) has been utilized by Rickaby et al. (32) to account for the influence of perfusion heterogeneity on indicator extraction by the lungs. The modeling was based on the finding that, on a semilogarithmic plot of outflow dilution data from the heart, there was, between the reference vascular material and a substance being lost from the capillaries, a progressive upslope divergence, which varied with the state of coronary tone (32), and that with the large dose bolus approach developed to examine metabolic changes during passage through the pulmonary vasculature (32), a similar kind of heterogeneity was required to fit the data. The underlying idea developed was that, in these organs, the sequence of average capillary transit times observed at the outflow $\tau_c(t)$ was a linear function of elapsed time. Utilizing this kind of approach, one would expect, in the present study,

$$\ln\left[\frac{C_{Ref}(t)}{C_{BPGP}(t)}\right] = \left[\frac{V_{max}}{K_m}\right]\tau_c(t) \qquad \ldots(A22)$$

where $C_{Ref}(t)$ is the labeled albumin outflow curve and $C_{BPGP}(t)$ is the labeled BPGP substrate outflow curve.

The whole organ capillary modeling as previously developed, is expected to have the general form,

$$C(t) = \frac{q^*}{F}\int_{\tau_{lm}+\tau_{cm}}^{t}\left(\frac{F_p}{q_0^*}\right)[u\{L, t-\tau_l(t)\}]\, w[\tau_c(t)+\tau_l(t)]\, dt \qquad \ldots(A23)$$

where q* is the total dose of tracer, F is the total plasma flow through the organ, τ_c and τ_l are the average of the capillary and large vessel transit times at the time t (their sum is, of course, equal to the outflow time t), τ_{cm} and τ_{lm} are the minimum capillary and large vessel transit times, respectively, and w $[\tau_c(t) + \tau_l(t)]$ represents the proportion of capillary-large vessel units with transit times between $[\tau_c(t)$ and $\tau_l(t)]$ and $[\tau_c(t) + \tau_l(t) + dt]$ (the outflow profile for the plasma reference material provides this weight function), and where

$$\tau_c(t) = \tau_{cm} + b(t - \tau_{lm} - \tau_{cm}) \qquad \ldots(A23A)$$

and

$$\tau_l(t) = \tau_{lm} + (1-b)(t - \tau_{lm} - \tau_{cm}) \qquad \ldots(A23B)$$

The dimensionless parameter b can vary between 0 and 1. It partitions each increment in transit time between the exchanging (reactive capillary) and nonexchanging larger (conduit) vessels, the latter being regarded as essentially metabolically nonreactive. When b is one, all of the increment in transit time occurs in the microvasculature, as t is increased; and when b is zero, none of the increment is found in the microvasculature (all of it occurs in the large vessels).

From the foregoing we would expect, for the vascular reference,

$$C_{Ref}(t) = \frac{q}{F}\, w(\tau_c(t) + \tau_l(t)) \qquad \ldots(A24)$$

and for the labeled substrate,

$$C_{BPGP}(t) = \frac{q}{F} e^{-\left[\frac{V_{max}}{K_m}\right]\tau_c(t)} w[\tau_c(t) + \tau_l(t)] \quad ...(A25)$$

$$= e^{-\left[\frac{V_{max}}{K_m}\right]\tau_c(t)} C_{ref}(t) \quad ...(A25A)$$

In the set of accompanying experimental data, the fractional hydrolysis M_i did not change significantly as a function of outflow time. Therefore, if the hydrolysis process is as described by the modeling, the apparent microvascular transit time $\tau_c(t)$ does not vary significantly as a function of time during the recording of a dilution curve at any of the cardiac output levels observed. The parameter b must therefore be zero, and the microvascular transit time therefore appears to be a constant value, τ_c. This, in turn, is expected to be equal to V_p / F_p, and the inference is, surprisingly, that this is a relatively unchanging parameter, along the dilution curve. If the alternate A_{max} notation is utilized in the development, equation (A25) becomes

$$C_{BPGP}(t) = e^{-\left[\frac{A_{max}}{K_m F_p}\right]} C_{ref}(t) \quad ...(25B)$$

and the expression for product

$$C_{BP}(t) = \left(1 - e^{-\left[\frac{A_{max}}{K_m F_p}\right]}\right) C_{ref}(t) \quad ...(A26)$$

Since K_m is likely to be independent of flow, the ratio A_{max}/F_p puts the problem emerging from the data squarely into view. The inference of the experimental findings is that the ratio of the total maximal enzymatic activity to plasma flow, in the microvascular vessels which are perfused, is relatively constant along the outflow dilution curve and is thus likely also to be relatively constant throughout the lungs. Extraction is dependent only on the total amount of surface related activity and the flow.

The relation resulting from equation (25) is, then

$$\ln\left[\frac{C_{ref}(t)}{C_{BPGP}(t)}\right] = \frac{A_{max}}{K_m F_p} \quad ...(A27)$$

Hence we can find $A_{max}/K_m F_p$ for each experiment. In the expression on the right hand side of equation (A27), we know F_p, for the whole lung. Therefore we will be able to

explore, over the whole group of experiments, how A_{max}/K_m varies with cardiac output and, since K_m is expected not to vary with flow, how total enzymatic activity (which we expect to reflect capillary surface area) varies with flow.

APPENDIX II

DOG SERUM HYDROLYSIS OF BPGP.

To evaluate the potential impact of hydrolysis of BPGP in blood, due to plasma ACE, we carried out an *in vitro* assessment of the process. The following procedure was carried out.

To a 20 ml liquid scintillation vial, containing 5.2 μCi of [^{3}H]BPGP (2.6×10^{-10} mols) in 5 μl of 70% ethanol, was added 500 μl of buffer (0.2 M Hepes buffer, pH 7.5, containing 0.15 M NaCl). To a second vial was added 2000 μl of dog serum. Two vials were heated in a 37°C water bath for 10 min. At time zero, the contents of the second vial were poured into the first vial, and the resulting mixture was poured back into the second vial (final serum concentration of 80%). While incubation of the second vial at 37°C was continued, 100 μl samples were collected at predetermined time intervals over 4 minutes. Each 100 μl sample was transferred to a corresponding 20 ml vial containing 1100 μl of 0.1 M HCl. To each of the latter vials was added 1000 μl of toluene containing Omnifluor, 4 g/l. The vials were capped, inverted 20 times and then submitted for liquid scintillation counting (4 cycles of 5 min per vial). The vials were then uncapped and 15 ml of Scint A was added to each. The vials were capped and inverted 20 times to obtain a single phase. The vials were again submitted for counting (4 cycles of 5 min/vial). Results were computed as usual to obtain ln ($[S_o]/[S]$), and u/u_{tot} was taken as the inverse of the antilog.

Figure 11 shows the plot of u/u_{tot} as a function of time. [^{3}H]BPGP hydrolysis proceeds in an exponential fashion with a single rate constant of 0.0167 sec^{-1}. The hydrolysis occurs very slowly compared with that occurring during a single pass through

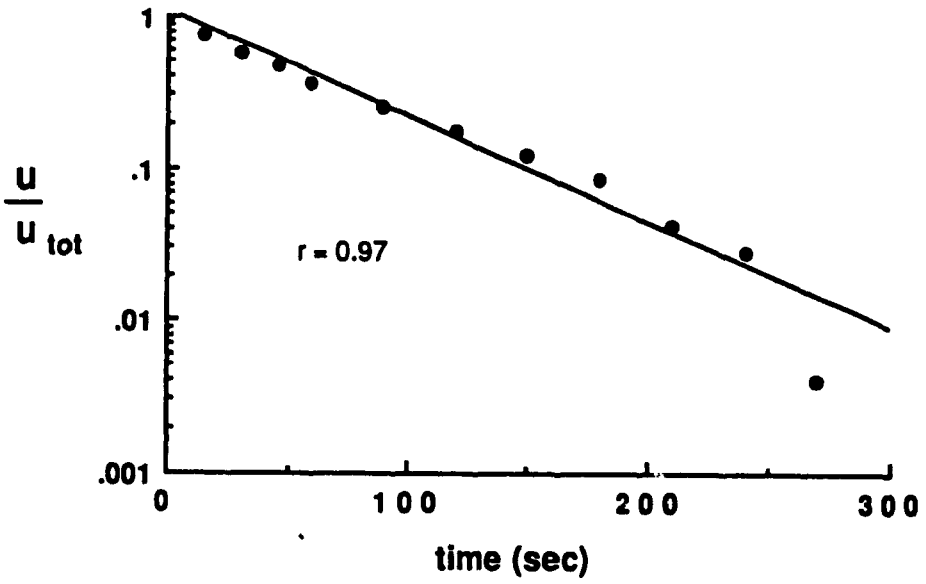

FIG. 11 In vitro angiotensin-converting enzyme kinetics in dog serum. The time course for [^{3}H]BPGP hydrolysis proceeds in an exponential fashion, with a single rate constant, $V_{max}/K_m = 0.0167\ s^{-1}$.

the lung. We can estimate from Figure 10 that there is only 5.6% BPGP hydrolysis after 10 sec of *in vitro* incubation. This is quite small when compared with the 55% *in vivo* hydrolysis occurring in a transit time of usually less than 5 seconds. We also note that there is no suggestion over the time course of the plasma hydrolytic reaction of a second slower phase, corresponding to the proportion not hydrolyzed in the pulmonary circulation during a single pass.

ACKNOWLEDGEMENTS

This work was supported by grants from the Quebec Heart Foundation, the Medical Research Council of Canada, the U.S. Public Health Service (HL 22087), Les Fonds de la Recherche en Santé du Québec, and the Fast Foundation.

The authors thank Hughes Gosselin, Eva Ibrahim, Kay Lumsden and Nicole Poitras for their expert technical assistance, and Elizabeth Capon for typing the manuscript.

REFERENCES

1. BERGENTZ, S. E., L. LEANDOER, AND D. H. LEWIS. Induced red cell aggregation and the transit time of red cells and albumin through the lung. *Bibl. Anat.* 9: 304, 1967.

2. CATRAVAS, J. D., S. E. BURCH, B. O. SPURLOCK, AND L. R. MILLS. Early effects of ionizing radiation on pulmonary endothelial angiotensin-converting enzyme and 5′-nucleotidase. *Toxicol. Appl. Pharmacol.* 94: 342-355, 1988.

3. CATRAVAS, J. D., J. S. LAZO, K. J. DOBULER, L. R. MILLS, AND C. N. GILLIS Pulmonary endothelial dysfunction in the presence or absence of interstitial injury induced by intratracheally injected bleomycin in rabbits. *Am. Rev. Resp. Dis.* 128: 740-746, 1983.

4. CATRAVAS, J. D., J. W. RYAN, X-L. CHEN, S. F. ORPHANOS, AND A. Y. K. CHUNG. Influence of erroneous fractional product extraction values on the estimation of angiotensin converting enzyme substrate utilization. (Abstract) *FASEB Journal* 4: A840, 1990 .

5. CATRAVAS, J. D., AND R. E. WHITE. Kinetics of pulmonary angiotensin converting enzyme and 5′-nucleotidase in vivo. *J. Appl. Physiol.: Respirat. Environ. Exercise Physiol.* 57: 1173-1181, 1984.

6. CERRETELLI, P., AND P. E. DI PRAMPERO. Gas exchange in exercise. In, *Handbook of Physiology - The Respiratory System IV.* Eds. A. P. Fishman, L. E. Farhi, S. M. Tenny, and S. T. Geiger, Am. Physiol. Soc., Bethesda, MD, ch. 16, pp. 297-339, 1987.

7. CUA, W. O., V. BOWER, AND F. P. CHINARD. Is 1,8-octanediol the ideal non-volatile tracer for liquid phase water in the lungs? (Abstract) *Fed. Proc.* 46: 1525, 1987.

8. COATES, G., H. O'BRODOVICH, A. L. JEFFERIES, AND G. W. GRAY. Effects of exercise on lung lymph flow in sheep and goats. *J. Clin. Invest.* 74: 133-141, 1984.

9. DAWSON, C. A., D. A. RICKABY, AND J. H. LINEHAN. Influence of size of emboli on extravascular lung water. *J. Appl. Physiol.* 67: 663-670, 1989.

10. DAWSON, C. A., R.D. BONGARD, D. A. RICKABY, J. H. LINEHAN, AND D.L. ROERIG. Effect of transit time on metabolism of a pulmonary endothelial substrate. *Am. J. Physiol.* 257 *(Heart Circ. Physiol. 26)*: H853-H865, 1989.

11. DUPUIS, J., C. A. GORESKY, C. JUNEAU, A. CALDERONE, J. L. ROULEAU, C. P. ROSE, AND S. GORESKY. Use of norepinephrine uptake to measure lung capillary recruitment with exercise. *J. Appl. Physiol.* 68: 700-713, 1990.

12. FUNG, Y. C., AND R. T. YEN. A new theory of pulmonary blood flow in zone 2 condition. *J. Appl. Physiol.* 60: 1638-1650, 1986.

13. GLAZIER, J. B., J. M. B. HUGHES, J. E. MALONEY, AND J. B. WEST. Measurement of capillary dimensions and blood volume in rapidly frozen lungs. *J. Appl. Physiol.* 26: 65-76, 1969.

14. GORESKY, C. A., G. G. BACH, D. COUSINEAU, A. J. SCHWAB, C. P. ROSE, S. LEE, AND S. GORESKY. Handling of tracer norepinephrine in dog liver. *Am. J. Physiol.* 256 (*Gastrointest. Liver Physiol. 19*): G107-123, 1989.

15. GORESKY, C. A., G. G. BACH, AND A. J. SCHWAB. Distributed-in-space product formation: nonlinear kinetics. *Am. J. Physiol.* (Manuscript submitted for consideration for publication.)

16. GORESKY, C. A., G. G. BACH, AND C. P. ROSE. Effects of saturating metabolic uptake on space profiles and tracer kinetics. *Am. J. Physiol. (Gastrointest. Liver Physiol. 7)* 244: G215-G232, 1983.

17. GORESKY, C. A., E. R. GORDON, AND G. G. BACH. Uptake of monohydric alcohols by liver: demonstration of a shared enzymic space. *Am. J. Physiol. (Gastrointest. Liver Physiol. 7)* 244: G198-G214, 1983.

18. GORESKY, C. A., R. F. P. CRONIN, AND B. E. WANGEL. Indicator dilution measurements of extravascular water in the lungs. *J. Clin. Invest.* 48: 487-501, 1969.

19. GORESKY, C. A., J. W. WARNICA, J. H. BURGESS, AND B. E. NADEAU. Effect of exercise on dilution estimates of extravascular lung water and on carbon monoxide diffusing capacity in normal adults. *Circ. Res.* 37: 379-389, 1975.

20. HAKIM, T. S. R., R. LISBONA, AND G. W. DEAN. Effect of cardiac output on gravity-dependent and nondependent inequality in pulmonary blood flow. *J. Appl. Physiol.* 66: 1570-1578, 1989.

21. HANSON, W. L., J. D. EMHARDT, J. P. BARTEK, L. P. LATHAM, L. L. CHECKLEY, R. L. CAPEN, AND W. W. WAGNER. Site of recruitment in the pulmonary microcirculation. *J Appl. Physiol.* 66: 2079-2083, 1989.

22. HOGG, J. C. Neutrophil kinetics and lung injury. *Physiol. Rev.* 64: 1249-1295, 1987.

23. LINEHAN, J. H., C. A. DAWSON, R. D. BONGARD, T. A. BRONIKOWSKI, AND D. L. ROERIG. Plasma protein binding and endothelial enzyme interactions in the lung. *J. Appl. Physiol.* 66: 2617-2628, 1989.

24. LINEHAN, J. H., C. A. DAWSON, D. A. RICKABY, AND D. A. BRONOKOWSKI. Angiotensin converting enzyme reaction rate constant in intact lung. *Fed. Proc.* 46: 66, 1987 (Abstract).

25. MASERI, A., P. CALDINI, P. HARWARD, R. C. JOSHI, S. PERMUTT, AND K. L. ZIERLER. Determinants of pulmonary vascular volume: recruitment versus distensibility. *Circ. Res.* 31: 218-228, 1972.

26. MCCORMICK, J. R., R. CHRZANOWSKI, J. ANDREANI, AND J. D. CATRAVAS. Early pulmonary endothelial enzyme dysfunction after phorbol ester in conscious rabbits. *J. Appl. Physiol.* 63: 1972-1978, 1987.

27. MOALLI, R., B. R. PITT, AND C. N. GILLIS. Effect of flow and surface area on angiotensin-converting enzyme activity in rabbit lungs. *J. Appl. Physiol.* 62: 2042-2050, 1987.

28. PANTOLIANO, M.W., B. HOLMQUIST, AND J.F. RIORDAN. Affinity chromatographic purification of angiotensin-converting enzyme. *Biochemistry* 23: 1037-1042, 1984.

29. PITT, B. R., AND G. LISTER. Kinetics of pulmonary angiotensin-converting enzyme activity in conscious developing lambs. *J. Appl. Physiol.: Respirat. Environ. Exercise Physiol.* 57: 1158-1166, 1984.

30. PITT, B. R., G. LISTER, P. DAVIES, AND L. REID. Correlation of pulmonary ACE activity and capillary surface area during postnatal development. *J. Appl. Physiol.* 62: 2031-2041, 1987.

31. RICKABY, D. A., R. D. BONGARD, M. J. TRISTANI, J. H. LINEHAN, AND C. A. DAWSON. Effect of gas composition and pH on kinetics of lung angiotensin-converting enzyme. *J. Appl. Physiol.* 62: 1216-1221, 1987.

32. RICKABY, D. A., C. A. DAWSON, AND J. H. LINEHAN. Influence of blood and plasma flow rate on the kinetics of serotonin uptake by lungs. *J. Appl. Physiol: Resp. Exercise Physiol.* 53: 677-684, 1982.

33. RICKABY, D. A., C. A. DAWSON, J. H. LINEHAN, AND T. A. BRONIKOWSKI. Alveolar vessel behavior in the zone 2 lung inferred from indicator-dilution data. *J. Appl. Physiol.* 63: 778-784, 1987.

34. RIGGS, D., A. M. HAVILL, B. R. PITT, AND C. N. GILLIS. Pulmonary angiotensin-converting enzyme kinetics after acute lung injury in the rabbit. *J. Appl. Physiol.* 64: 2508-2516, 1988.

35. ROSE, C. P., AND C. A. GORESKY. Vasomotor control of capillary transit time heterogeneity in the canine coronary circulation. *Circ. Res.* 39: 541-554, 1976.

36. RYAN, J. W. Assay of pulmonary endothelial surface enzymes in vivo. In, *Pulmonary Endothelium in Health and Disease*. Ed. C. Lenfant. Marcel Dekker, New York, pp. 161-188, 1987.

37. RYAN, J. W. Angiotensin converting enzyme, dipeptidyl carboxypeptidase I, and its inhibitors. In, *Methods in Enzymology*. Ed. G. DiSabato, Academic Press, London, Vol. 163, ch. 18, pp. 194-210, 1988.

38. RYAN, J.W., U.S. RYAN, D.R. SCHULTZ, C. WHITAKER, A. CHUNG, AND F.E. DORER. Subcellular localization of pulmonary angiotensin converting enzyme (kininase II). *Biochem. J.* 146: 497-499, 1975.

39. TOIVONEN, H. J., AND J. D. CATRAVAS. Effects of alveolar pressure on lung angiotensin-converting enzyme function in vivo. *J. Appl. Physiol.* 61: 1041-1050, 1986.

40. VATNER, S. F., D. FRANKLIN, C. B. HIGGINS, T. PATRICK, AND E. BRAUNWALD. Left ventricular response to severe exertion in untethered dogs. *J. Clin. Invest.* 51: 3052-3060, 1972.

41. WARREL, J. A., J. W. EVANS, R. O. CLARKE, G. P. KINGABY, AND J. B. WEST. Pattern of filling in the pulmonary capillary bed. *J. Appl. Physiol.* 32: 346-356, 1972.

42. WEST, J. B., AND C. T. DOLLERY. Distribution of blood flow and the pressure-flow relations of the whole lung. *J. Appl. Physiol.* 201: 175-183, 1965.

43. WEST, J. B., C. T. DOLLERY, AND A. NAIMARK. Distribution of blood flow in isolated lung; relation to vascular and alveolar pressures. *J. Appl. Physiol.* 19: 713-724, 1964.

CHAPTER 4

GENERAL CONCLUSION

We have used the metabolic properties of the pulmonary vascular endothelium to study the accommodation of increased pulmonary blood flow by the lungs with exercise. Two different probes of the vascular surface area were utilized: [^{3}H]norepinephrine, a substance extracted by the endothelium, and [^{3}H]BPGP, an angiotensin-converting enzyme substrate hydrolyzed at the luminal surface of the vascular endothelium. The estimated vascular surface area for these two different metabolic properties of the vascular endothelium behaved similarly in the exercising dog. In the transition from low to moderate and to high levels of blood flow there was a calculated linear increase of the pulmonary vascular surface area that can interact with vascular substrates. Such an increase suggests that capillary recruitment does occur in normal physiologic conditions such as exercise, and that recruitment is present over the whole range of cardiac output achieved, continuing to occur even after full lung tissue recruitment.

The use of vascular endothelial metabolic properties to assess recruitment of pulmonary vascular surface represents a novel approach to the study of the pulmonary microcirculatory physiology in awake animals. In the foreseeable future, the pulmonary surface area tracer substances may play an increasing role in fundamental as well as clinical research. There are numerous pathological situations in man, in which the integrity of the metabolically active surface area of the pulmonary vascular endothelium is compromised. The adult respiratory distress syndrome, to name only one, represents probably the most important of these diseases. The development of better surface area tracers together with the simplification of the techniques for their use will undoubtedly lead to new clinical applications in the future.

CLAIMS TO ORIGINAL RESEARCH

In the present studies we took advantage of the pulmonary vascular endothelium metabolic properties to study changes in the pulmonary vasculature with exercise. Such an approach has been used before but this is the first time that it has been used in *in vivo* awake dogs at rest and during exercise.

1. CLAIMS TO ORIGINAL RESEARCH FOR CHAPTER 2

1.1 This is the first time that norepinephrine or any other extractable tracer has been used to study changes in the pulmonary capillary surface area in awake exercising animals. This is also the first account of the behavior of the pulmonary capillary surface area (PS) product during exercise.

1.2 Because of the behaviour of the tracers in blood, very special precautions were taken to avoid any significant interaction of [^{3}H]norepinephrine with the animal's red blood cells. The labeled norepinephrine was added to the bolus mixture just prior to injection, the samples were collected on ice, and cold norepinephrine was added to each collecting tube to act as a competitive inhibitor of the red blood cell uptake of the catecholamine, prior to addition of a protein precipitant mixture.

1.3 Pulmonary norepineprine extraction can be measured by assessing labeled substrate uptake by dilution techniques and by simply measuring the arterio-venous difference in norepinephrine concentration (bulk extraction). Neither of these techniques, by itself, accounts for the possibility of norepinephrine production by the lung itself. To examine this, we measured dilutional and bulk norepinephrine extractions simultaneously; no significant differences were found between the two

estimates, indicating that unlabeled norepinephrine release by the lung, if present, proceeds at levels too low to be detected. There was net uptake, as assessed by both indices. Production would have shown up as a difference between the two.

2. CLAIMS TO ORIGINAL RESEARCH FOR CHAPTER 3

2.1 This is the first time that the angiotensin-converting enzyme substrate [^{3}H]BPGP has been utilized to study the pulmonary vascular surface area in awake exercising animals.

2.2 Special techniques had to be developed to minimize the contact of [^{3}H]BPGP with plasma angiotensin-converting enzyme and plasma proteins. The Percoll separation of the red blood cells prior to labeling ensured a plasma free injection mixture and also enabled us to utilise labeled erythrocytes as one of the vascular references.

2.3 By additional *in vitro* studies we have demonstrated that, within a single transit time through the pulmonary circulation (approximately 5 sec), it is unlikely that plasma ACE contributed significantly to the overall [^{3}H]BPGP hydrolysis observed. We have also demonstrated that *in vitro* hydrolysis of [^{3}H]BPGP by either dog serum or dog lung ACE follows a single rate constant. Consequently, and unlike BPAP, there is not evidence of two conformers of [^{3}H]BPGP, one of which is limiting, and protein binding (if it exists) does not substantially interfere with the activity of the enzyme.

3. CLAIMS TO ORIGINAL RESEARCH PERTAINING TO BOTH CHAPTER 2 AND 3

3.1 An animal model specifically suited for indicator dilution experiments in awake exercising animals was developed. This chronically instrumented dog model enabled us to obtain pulmonary indicator dilution curves at exercise and to draw simultaneous arterial and venous blood samples for catecholamines and blood gas analysis.

3.2 The water space tracer [^{14}C]1,8-octanediol was used for the first time in awake exercising animals. This tracer has been shown previously to be a better tissue water space tracer than tritiated water itself since the latter has a small diffusional shunt through the alveolar space; the mean transit time for both is the same. The calculated extravascular lung water (an index of the perfused lung tissue) increased in the transition from rest to the first level of exercise, and reached a maximal value which was maintained in the transition from the first to the second level of exercise.

3.3 Gravimetric estimates of the extravascular lung water were obtained by estimating the postmortem lung water according to dilution principles, by homogenizing the lungs, estimating the water content, and utilizing the retained [^{51}Cr] to estimate the contained vascular space.

3.4 We have shown that when comparing dilutional to gravimetric estimates of the extravascular lung water, one has to consider that the tracheobronchial tree is supplied by the bronchial circulation and is consequently not accessible to tracer injected in the pulmonary circulation. To correct for this we subtracted the weight of the extrapulmonary tracheobronchial tree from the total lung weight. *In vivo* estimates at high level exercise then corresponded closely to postmortem gravimetric estimates.

3.5 The major findings of this work are based on the utilization of pulmonary endothelial metabolic properties to study the pulmonary vasculature during exercise. This represents a novel approach to the study of pulmonary vascular physiology. The two different tracers utilized, labeled norepinephrine and BPGP, behaved similarly; the computed permeability surface area product per unit lung weight for norepinephrine and the first order kinetic parameter A_{max}/K_m per unit lung weight for BPGP both increased linearly with increasing pulmonary blood flow. The uptake of these indicators is limited by the metabolically available capillary surface area. For each, analysis of the data indicated that the capillary surface area tripled as pulmonary blood flow tripled. The findings indicate that lung capillary recruitment occurs concomitantly with lung tissue recruitment, in the change from rest to first level exercise, and that futher capillary recruitment continues to occur with the increase in flow from first to second level exercise, when lung tissue recruitment is already complete. The change in calculated capillary permeability surface area with exercise parallels the simultaneously observed change in central blood volume.